

SIMPLE EXPERIMENTS IN OPTICS

Roshan L. Aggarwal
and Kambiz Alavi

Simple Experiments in Optics

Simple Experiments in Optics

By

Roshan L. Aggarwal and Kambiz Alavi

**Cambridge
Scholars
Publishing**



Simple Experiments in Optics

By Roshan L. Aggarwal and Kambiz Alavi

This book first published 2019

Cambridge Scholars Publishing

Lady Stephenson Library, Newcastle upon Tyne, NE6 2PA, UK

British Library Cataloguing in Publication Data

A catalogue record for this book is available from the British Library

Copyright © 2019 by Roshan L. Aggarwal and Kambiz Alavi

All rights for this book reserved. No part of this book may be reproduced, stored in a retrieval system, or transmitted, in any form or by any means, electronic, mechanical, photocopying, recording or otherwise, without the prior permission of the copyright owner.

ISBN (10): 1-5275-3551-7

ISBN (13): 978-1-5275-3551-0

This book is dedicated to our parents (Chet Ram Aggarwal and Lila Vati Aggarwal, and Seyed Mohammed Kazem Alavi and Bibi Ozra Nadji Alavi), our spouses (Pushap Lata Aggarwal and Homa Rahmani-Khezri Alavi), our children (Rajesh Aggarwal and Achal Aggarwal, and Maysa Alavi, Tara Alavi and Kiana Alavi), and our grandchildren (Isha Aggarwal, Neena Aggarwal, Akash Aggarwal and Ashok Aggarwal).

CONTENTS

Preface	xi
Acknowledgments	xiii
Chapter 1	1
Lenses	
1.1 Focal length of a lens	
Experiment 1.1	
1.2 Focal length of a combination of two lenses	
Experiment 1.2	
1.3 Spherical aberration of a lens	
Experiment 1.3	
1.4 Chromatic aberration of a lens	
Experiment 1.4	
1.5 Laser beam expander	
Experiment 1.5	
1.6 Field of view of a camera	
Experiment 1.6	
1.7 Magnification of a microscope objective	
Experiment 1.7	
Chapter 2	25
Mirrors	
2.1 Angle of reflection	
Experiment 2.1	
2.2 Rotation of a mirror	
Experiment 2.2	
2.3 Longitudinal spherical aberration of a spherical mirror	
Experiment 2.3	
2.4 Off-axis concave parabolic mirror	
Experiment 2.4	
2.5 Ellipsoidal mirror	
Experiment 2.5	

Chapter 3	39
Gratings	
3.1 Grating equation	
Experiment 3.1	
Experiment 3.2	
3.2 Diffraction efficiency	
Experiment 3.3	
Experiment 3.4	
Experiment 3.5	
Experiment 3.6	
Chapter 4	59
Polarizers	
4.1 Malus' law	
Experiment 4.1	
4.2 Wollaston polarizer	
Experiment 4.2	
4.3 Rochon polarizer	
Experiment 4.3	
4.4 Brewster window polarizer	
Experiment 4.4	
4.5 Wire-grid polarizer	
Experiment 4.5	
Chapter 5	73
Optical Windows	
5.1 External transmittance	
Experiment 5.1	
5.2 Single-surface reflectance	
Experiment 5.2	
5.3 Reflection loss	
Experiment 5.3	
Experiment 5.4	
Chapter 6	83
Optical Filters	
6.1 Bandpass filters	
Experiment 6.1	
Experiment 6.2	
6.2 Longpass filters	
Experiment 6.3	

6.3 Raman filters	
Experiment 6.4	
Experiment 6.5	
Chapter 7	95
Beamsplitters	
7.1 Plate beamsplitters	
Experiment 7.1	
7.2 Polka dot beamsplitters	
Experiment 7.2	
7.3 Pellicle beamsplitters	
Experiment 7.3	
7.4 Cube beamsplitters	
Experiment 7.4	
7.5 Dichroic beamsplitters	
Experiment 7.5	
Chapter 8	109
Light sources	
8.1 Incandescent tungsten lamps	
Experiment 8.1	
8.2 Light-emitting diode (LED) lamps	
Experiment 8.2	
8.3 Lasers	
Experiment 8.3	
Experiment 8.4	
Chapter 9	119
Light detectors	
9.1 Photomultiplier tubes	
Experiment 9.1	
Experiment 9.2	
9.2 Silicon photodiodes	
Experiment 9.3	
Experiment 9.4	

Appendix	127
Optical and optomechanical components	
A.1. Optical components	
A.2 Optomechanical components	
A.3 Stock numbers and prices of optical, optomechanical, and other components	
Index.....	159

PREFACE

This book is intended for undergraduates in physics and optics. The background for the experiments in this book is based on our previous book *Introduction to Optical Components*, published by CRC Press in March 2018. There are 45 experiments in this book. Optical, optomechanical, and other components for these experiments are available from several vendors including Edmund Optics, Newport, and Thorlabs in the United States. Stock numbers for the optical, optomechanical, and other components given in this book are mostly from Edmund Optics or Thorlabs. One of each of the optical, optomechanical, and other components listed in Appendix A.3 can be purchased for a total of about \$16,000. These components will cost more than \$16,000 if more than one component is purchased. In addition, $\frac{1}{4}$ "-20 and other screws are required for mounting the optomechanical components. The experiments in this book are relatively easy to set up. However, some tinkering may be needed in mounting the optical and optomechanical components to the breadboard. Measurement and analysis of the experiments is also relatively easy.

ACKNOWLEDGMENTS

We thank Dr. William Herzog and Dr. Mordechai Rothschild for discussions regarding this work. We thank Dr. Antonio Sanchez and Lewis Farrar for their review of this book. We also thank Tara Alavi for preparing the schematics of the experiments in this book.

CHAPTER 1

LENSES

1.1 Focal length of a lens

The effective focal length of a lens is given by

$$\frac{1}{f_{\lambda}} = (n_{\lambda} - 1) \left[\frac{1}{R_1} - \frac{1}{R_2} + \frac{(n_{\lambda}-1)t_C}{n_{\lambda}R_1R_2} \right] \quad (1.1)$$

where n_{λ} is the refractive index of lens material at wavelength λ , R_1 and R_2 are radii of curvature of the left-hand side and right-hand side lens surfaces, respectively, and t_C is the center thickness of the lens. The sign convention for the radius of curvature is that it is positive if the center of curvature is to the right-hand side of the surface and negative if the center of curvature is to the left-hand side of the surface. The back focal length of the lens is given by

$$f_{\lambda B} = f_{\lambda} + \delta_2 \quad (1.2)$$

where

$$\delta_2 = -f_{\lambda} t_C \left(\frac{n_{\lambda}-1}{n_{\lambda}R_1} \right) \quad (1.3)$$

Combining Equations (1.2) and (1.3), we obtain

$$f_{\lambda B} = f_{\lambda} \left[1 - t_C \left(\frac{n_{\lambda}-1}{n_{\lambda}R_1} \right) \right] \quad (1.4)$$

Experiment 1.1: Measure the back focal length $f_{\lambda B}$ of a N-BK7 25.0-mm diameter 35-mm effective focal length plano-convex lens using a 532-nm laser. Determine the effective focal length of the lens using a value of 1.517 for n_{λ} for $\lambda = 532$ nm.

The optical components for this experiment are the following:

1. 0.9-mW 532-nm laser (Thorlabs stock no. CPS532-C2 for \$162.18 in 2018).
2. 25.0-mm diameter, 35.0-mm effective focal length, MgF₂-coated N-BK7 plano-convex lens (Edmund Optics stock no. 45-146 for \$32.50 in 2018).
3. 10- μ m ceramic aperture (Edmund Optics stock no. 84-910 for \$107.00 in 2018).
4. UV-NIR silicon power photodetector (Edmund Optics stock no. 89-310 for \$795.00 in 2018).

The optomechanical and other components for this experiment are the following:

1. 5VDC regulated power supply (Thorlabs stock no. LDS5 for \$86.96 in 2018), 11-mm diameter kinematic mount (Thorlabs stock no. MK11F for \$90.00 in 2018), 3" stainless-steel post (Edmund Optics stock no. 59-754 for \$10.25 in 2018), 3" post holder (Edmund Optics stock no. 58-979 for \$13.25 in 2018), 1/2" translation stage (Thorlabs stock no. MT1 for \$297.94 in 2018), and a base plate for the 1/2" translation stage (Thorlabs stock no. MT401 for \$23.66 in 2018) for the 0.9-mW 532-nm laser.
2. 25/25.4-mm kinematic mount (Edmund Optics stock no. 58-854 for \$109.00 in 2018), 3" stainless-steel post (Edmund Optics stock no. 59-754 for \$10.25 in 2018), 3" post holder (Edmund Optics stock no. 58-979 for \$13.25 in 2018), and a 2"x3" slotted base plate (Edmund Optics stock no. 03-655 for \$15.00 in 2018) for the 35.0-mm effective focal length lens.
3. Mount for 10-mm optics (Thorlabs stock no. LMR10 for \$20.81 in 2018), 3" stainless-steel post (Edmund Optics stock no. 59-754 for \$10.25 in 2018), 3" post holder (Edmund Optics stock no. 58-979 for \$13.25 in 2018), 1/2" translation stage (Thorlabs stock no. MT1 for \$297.94 in 2018), and a base plate for the 1/2" translation stage (Thorlabs stock no. MT401 for \$23.66 in 2018) for the 10- μ m ceramic aperture.

4. Power meter (Edmund Optics stock no. 89-305 for \$850.00 in 2018), adjustable-height V-clamp (Thorlabs stock no. VG100 for \$87.98 in 2018), 3" stainless-steel post (Edmund Optics stock no. 59-754 for \$10.25 in 2018), 3" post holder (Edmund Optics stock no. 58-979 for \$13.25 in 2018), and a 2"x3" slotted base plate (Edmund Optics stock no. 03-655 for \$15.00 in 2018) for the UV-NIR photodetector.
5. 3" spring-type caliper and divider (Starrett stock no. 274-3 for \$68.00 in 2018).

Figure 1.1 shows a schematic of experiment 1.1.

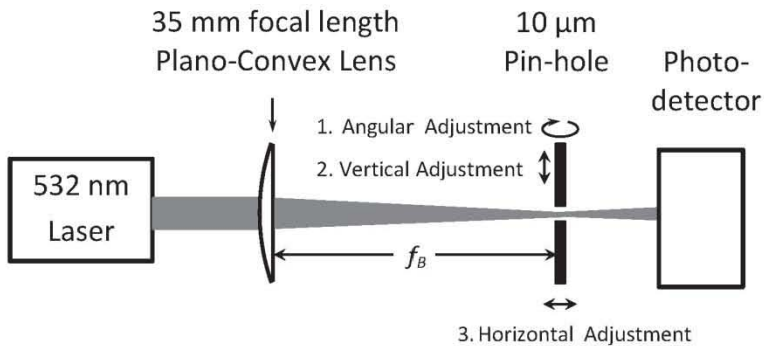


Figure 1.1 Schematic of experiment 1.1.

The schematic of experiment 1.1 is achieved through the following procedure:

1. The 0.9-mW 532-nm laser is mounted on the breadboard using the 11-mm diameter kinematic mount, 3" stainless-steel post, 3" post holder, 1/2" travel translation stage, and the base plate for the 1/2" travel translation stage.
2. The 0.9-mW 532-nm laser is aligned so that the 3.5-mm diameter collimated laser beam propagates parallel to the long edge of the breadboard at a fixed height of 6.5" above the breadboard.
3. The 35-mm effective focal length lens is attached to the breadboard using the 25/25.4-mm diameter kinematic mount, 3" stainless-steel post, 3" post holder, and 2"x3" slotted base plate.

4. The UV-NIR silicon power photodetector is attached to the breadboard using the adjustable-height V-clamp, 3" stainless-steel post, 3" post holder, and 2"x3" slotted base plate.
5. The position of the 25.0-mm diameter, 35-mm effective focal length lens is adjusted so that the 3.5-mm diameter 532-nm laser beam is incident upon the center of the lens and is perpendicular to the plane of the lens. This can be achieved by covering the back side of the lens with a washer-shaped piece of thick paper with an outer diameter of 25 mm and a central hole of 3 mm diameter, and then maximizing the output signal of the UV-NIR silicon power photodetector by adjusting the position and angle of the lens. Also, when the lens is centered and its plane surface is perpendicular to the laser beam, the back reflection from the planar face of the lens will be collinear with the incoming laser beam.
6. The 10- μ m ceramic aperture is attached to the breadboard using the adaptor for 10-mm diameter optics, mount for 18-mm optics, 3" stainless-steel post, 3" post holder, $\frac{1}{2}$ " translation stage, and base plate for the $\frac{1}{2}$ " translation stage. The center of the stage is positioned 30 mm behind the back surface of the lens.
7. The 10- μ m ceramic aperture is positioned 30 mm behind the 35-mm effective focal length lens (with the lens positioned between the laser and the 10- μ m ceramic aperture). At this distance the laser beam spot on the ceramic should be larger than the area of the opening of the 10- μ m ceramic aperture. Make vertical adjustment of the aperture until the laser spot is centered on the aperture opening (visual verification is sufficient at this time).
8. Angular adjustment of the 10- μ m ceramic aperture: the amount of laser light going through the aperture is very sensitive to the angle of the plane of the 10- μ m ceramic aperture with respect to the direction of the laser beam. Therefore angular adjustments must be made to ensure that maximum laser beam throughput is achieved. Angular optimization can be achieved by maximizing the output signal of the UV-NIR silicon power photodetector through trial and error as the angle of the plane of the aperture is adjusted.
9. Centering the 10- μ m ceramic aperture: the plane of the 10- μ m ceramic aperture is translated in a horizontal direction,

perpendicular to the laser beam, until maximal laser beam is achieved by adjusting the angle of the 3" stainless-steel post so as to maximize the output signal of the UV-NIR silicon power photodetector.

10. The 10- μm ceramic aperture is moved along the long edge of the breadboard using the $\frac{1}{2}$ " translation stage away from the lens so as to maximize the signal output of the UV-NIR silicon power photodetector.
11. As the 10- μm ceramic aperture is moved away from the lens horizontally, the UV-NIR silicon power photodetector signal will increase at first, then it may reach a plateau, and finally it decreases again. Suppose the plateau occurs over the horizontal position range D to $D+\Delta$. Move the aperture back to the middle of this range, i.e. horizontal position $D+\Delta/2$.
12. Fine tuning of the vertical position of the 10- μm ceramic aperture: the vertical position of the 10- μm ceramic aperture is optimized by adjusting the height of the 3" stainless-steel post so as to maximize the output signal of the UV-NIR silicon power photodetector. Refer to procedures in step 11 if you see a plateau in the output signal of the UV-NIR silicon power photodetector.
13. Fine tuning the position of the 10- μm ceramic aperture: the position of the 10- μm ceramic aperture is adjusted until the optimum distance from the lens is achieved (using the same procedure as described in step 12).
14. The horizontal distance between the 10- μm ceramic aperture at the above position and the back of the 35-mm effective focal length lens represents the back focal length of the lens, which may be measured using a Starrett 274-3 spring-type caliper and divider.

1.2 Focal length of a combination of two lenses

The focal length F of a combination of two lenses is given by

$$\frac{1}{F} = \frac{1}{f_1} + \frac{1}{f_2} - \frac{d}{f_1 f_2} \quad (1.5)$$

where f_1 and f_2 are the focal lengths of the two lenses and d is the distance between the centers of the two lenses. Equation (1.5) may be written as

$$F = \frac{f_1 f_2}{(f_1 + f_2) - d} \quad (1.6)$$

Equation (1.6) shows that F is negative if $d > (f_1 + f_2)$. In this case, the collimated beam of light incident upon the combination of the two lenses will focus on the right-hand side of the second lens of focal length f_2 . F is determined from a measurement of the back focal point of the second lens using the following equation

$$F = \frac{f_{B2}}{\left(1 - \frac{d}{f_1}\right)} \quad (1.7)$$

where f_{B2} is the distance between the second lens and its back focal point.

Experiment 1.2: Measure the focal length of a combination of two double-convex lenses with focal lengths $f_1 = 25.0$ mm and $f_2 = 50.0$ mm using a value of 100 mm for d and a 0.9-mW 532-nm laser.

The optical components for this experiment are the following:

1. 0.9-mW 532-nm laser (Thorlabs stock no. CPS532-C2 for \$162.18 in 2018).
2. 25.0-mm diameter, 25.0-mm effective focal length MgF₂-coated N-SF5 double-convex lens (Edmund Optics stock no. 32-490 for \$31.50 in 2018).
3. 25.0-mm diameter, 50.0-mm effective focal length MgF₂-coated N-BK7 double-convex lens (Edmund Optics stock no. 32-625 for \$31.50 in 2018).
4. 10-μm ceramic aperture (Edmund Optics stock no. 84-910 for \$107.00 in 2018).
5. UV-NIR silicon power photodetector (Edmund Optics stock no. 89-310 for \$795.00 in 2018).

The optomechanical and other components for this experiment are the following:

1. 5 VDC regulated power supply (Thorlabs stock no. LDS5 for \$86.95 in 2018), 11-mm diameter kinematic mount (Thorlabs stock no. MK11F for \$90.00 in 2018), 3" stainless-steel post, 3" post holder, 1/2" translation stage (Thorlabs stock no. MT1 for \$297.84 in 2018), and a base plate for the 1/2" translation stage (Thorlabs stock no. MT401 for \$23.66 in 2018) for the 0.9-mW 532-nm laser.
2. 25/25.4-mm kinematic mount (Edmund Optics stock no. 58-854 for \$109.00 in 2018), 3" stainless-steel post (Edmund Optics stock no. 59-754 for \$10.25 in 2018), 3" post holder (Edmund Optics stock no. 58-979 for \$13.25 in 2018), and a 2"x3" slotted base plate (Edmund Optics stock no. 03-655 for \$15.00 in 2018) for the 25.0-mm effective focal length lens.
3. 25/25.4-mm kinematic mount (Edmund Optics stock no. 58-854 for \$109.00 in 2018), 3" stainless-steel post (Edmund Optics stock no. 59-754 for \$10.25 in 2018), 3" post holder (Edmund Optics stock no. 58-979 for \$13.25 in 2018), and a 2"x3" slotted base plate (Edmund Optics stock no. 03-655 for \$15.00 in 2018) for the 50.0-mm effective focal length lens.
4. Mount for the 10-mm optics (Thorlabs stock no. LMR10 for \$20.81 in 2018), 3" stainless-steel post (Edmund Optics stock no. 59-754 for \$10.25 in 2018), 3" post holder (Edmund Optics stock no. 58-979 for \$13.25 in 2018), 1/2" translation stage (Thorlabs stock no. MT1 for \$297.94 in 2018), and a base plate for the 1/2" translation stage (Thorlabs stock no. MT401 for \$23.66 in 2018) for the 10- μ m ceramic aperture.
5. Power meter (Edmund Optics stock no. 89-305 for \$850.00 in 2018), adjustable-height V-clamp (Thorlabs stock no. VG100 for \$87.98 in 2018), 3" stainless-steel post (Edmund Optics stock no. 59-754 for \$10.25 in 2018), 3" post holder (Edmund Optics stock no. 58-979 for \$13.25 in 2018), and a 2"x3" slotted base plate (Edmund Optics stock no. 03-655 for \$15.00 in 2018) for the UV-NIR silicon power photodetector.

Figure 1.2 shows a schematic of experiment 1.2.

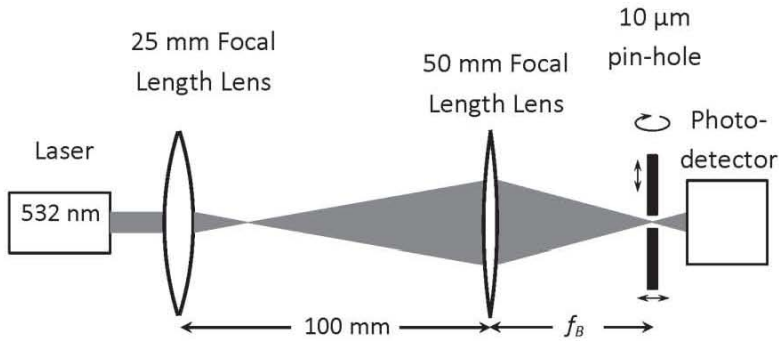


Figure 1.2 Schematic of experiment 1.2.

The schematic of experiment 1.2 is achieved through the following procedure:

1. The 0.9-mW, 532-nm laser is attached to the 36"x12" breadboard using the 11-mm diameter kinematic mount, 3" stainless-steel post, 3" post holder, 1/2" translation stage, and the base plate for the 1/2" translation stage.
2. The 0.9-mW 532-nm laser is aligned so that the 3.5-mm diameter collimated laser beam propagates parallel to the long edge of the 36"x12" breadboard at a fixed height of 6.5" above the breadboard.
3. The 25.0-mm effective focal length lens is attached to the 36"x12" breadboard using the 25/25.4-mm kinematic mount, 3" stainless-steel post, 3" post holder, and 2"x3" slotted base plate.
4. The 25.0-mm effective focal length lens is adjusted so that the 3.5-mm diameter laser beam is incident upon the center of the 25.0-mm effective focal length lens.
5. The 50.0-mm effective focal length lens is attached to the 36"x12" breadboard at a distance of 100 mm from the 25.0-mm effective focal length lens using the 25/25.4-mm kinematic mount, 3" stainless-steel post, 3" post holder, and 2"x3" slotted base plate.

6. The 25.0-mm effective focal length lens focuses the 3.5-mm diameter, 532.0-nm laser beam at a distance of 25 mm on the right-hand side of this lens.
7. The focused beam expands to a diameter of 10.5 mm when it is incident upon the center of the 50.0-mm effective focal length lens.
8. Adjust the 50.0-mm effective focal length lens so that the 532.0-nm laser beam is incident upon the center of the 50.0-mm effective focal length lens.
9. The 50.0-mm effective focal length lens focuses the 532.0-nm laser beam at a distance of 150 mm on the right-hand side of this lens.
10. The 10- μ m ceramic aperture is attached to the 36"x12" breadboard using the mount for the 10-mm diameter optics, 3" stainless-steel post, 3" post holder, $\frac{1}{2}$ " translation stage, and base plate for the $\frac{1}{2}$ " translation stage.
11. The UV-NIR silicon power photodetector is attached to the 36"x12" breadboard using the adjustable-height V-clamp, 3" stainless-steel post, 3" post holder, and 2"x3" slotted base plate.
12. The 10- μ m ceramic aperture is positioned so that the laser beam focused by the 50.0-mm effective focal length lens is centered upon the 10- μ m ceramic aperture using the stainless-steel post for the vertical motion and the base plate for the $\frac{1}{2}$ " translation stage for the horizontal motion. To achieve this optimal position, the signal from the UV-NIR silicon power photodetector is to be maximized by vertical adjustment, rotational adjustment and horizontal adjustment (perpendicular to the laser beam).
13. The 10- μ m ceramic aperture is moved along the long edge of the breadboard using the $\frac{1}{2}$ " translation stage so as to maximize the signal output of the UV-NIR silicon power photodetector.
14. As the 10- μ m ceramic aperture is moved away from or towards the 50.0-mm effective focal length lens horizontally, the UV-NIR silicon power photodetector signal may show a plateau over horizontal position range D to $D+\Delta$. Move the aperture back to the middle of this range, i.e. horizontal position $D+\Delta/2$.

15. Fine tuning of the vertical position of the 10- μm ceramic aperture: the vertical position of the 10- μm ceramic aperture is optimized by adjusting the height of the 3" stainless-steel post so as to maximize the output signal of the UV-NIR silicon power photodetector. Refer to procedures in step 12 if you see a plateau in the output signal of the UV-NIR silicon power photodetector.
16. Fine tuning the horizontal position of the 10- μm ceramic aperture: the position of the 10- μm ceramic aperture is adjusted until the optimum distance from the lens is achieved (using the same procedure as described in step 14).
15. The distance between the position of the 10- μm ceramic aperture corresponding to the middle of the maximum signal and the back center of the 50.0-mm effective focal length lens represents the back focal length f_{B2} of the 50.0-mm effective focal length lens, which may be measured using a Starrett 274-3 spring-type caliper and divider.

1.3 Spherical aberration of a lens

The longitudinal spherical aberration (LSA) for a collimated ray incident at the height h from the optical axis of a lens of focal length f is given by

$$LSA = \frac{h^2}{8fn(n-1)} \times \left[\frac{n+2}{n-1} q^2 - 4(n+1)q + (3n+2)(n-1) + \frac{n^3}{n-1} \right] \quad (1.8)$$

where n is the refractive of the lens and q is the shape factor of the lens given by

$$q = \frac{R_2 + R_1}{R_2 - R_1} \quad (1.9)$$

where R_1 and R_2 are the left-hand side and right-hand side radii of curvature of the lens, respectively. For a double-convex lens with $R_2 = -R_1$, $q = 0$ and Equation (1.8) becomes

$$LSA = \frac{h^2}{8fn(n-1)} \left[(3n+2)(n-1) + \frac{n^3}{n-1} \right] \quad (1.10)$$

Experiment 1.3: Measure the spherical aberration of a double-convex lens with n equal to 1.5, effective focal length f equal to 25.0 mm, diameter d equal to 25.0 mm, and $h = 10$ mm using a 632.8-nm He-Ne laser.

The optical components for this experiment consist of the following:

1. 0.8-mW 632.8-nm He-Ne laser (Thorlabs stock no. HNLS008L for \$889.44 in 2018).
2. 25.0-mm diameter, 25.0-mm effective focal length MgF₂-coated N-SF5 double-convex lens (Edmund Optics stock no. 32-490 for \$31.50 in 2018).
3. 10- μ m ceramic aperture (Edmund Optics stock no. 84-910 for \$107.00 in 2018).
4. UV-NIR silicon power photodetector (Edmund Optics stock no. 89-310 for \$795.00 in 2018).

The optomechanical components for this experiment consist of the following:

1. 25/25.4-mm kinematic mount (Edmund Optics stock no. 58-854 for \$109.00 in 2018), 3" stainless-steel post (Edmund Optics stock no. 59-754 for \$10.25 in 2018), 3" post holder (Edmund Optics stock no. 58-979 for \$13.25 in 2018), and a 2"x3" slotted base plate (Edmund Optics stock no. 03-655 for \$15.00 in 2018) for the 25.0-mm effective focal length lens.
2. Mount for the 10-mm optics (Thorlabs stock no. LMR10 for \$20.81 in 2018), 3" stainless-steel post (Edmund Optics stock no. 59-754 for \$10.25 in 2018), 3" post holder (Edmund Optics stock no. 58-979 for \$13.25 in 2018), 1/2" translation stage (Thorlabs stock no. MT1 for \$297.94 in 2018), and a base plate for the 1/2" translation stage (Thorlabs stock no. MT401 for \$23.66 in 2018) for the 10- μ m ceramic aperture.
3. Power meter (Edmund Optics stock no. 89-305 for \$850.00 in 2018), adjustable-height V-clamp (Thorlabs stock no. VG100 for \$87.98 in 2018), 3" stainless-steel post (Edmund Optics stock no. 59-754 for \$10.25 in 2018), 3" post holder (Edmund Optics stock no. 58-979 for \$13.25 in 2018), and 2"x3" slotted base plate (Edmund Optics stock no. 03-655 for \$15.00 in 2018) for the UV-NIR silicon power photodetector.

Figure 1.3 shows a schematic of experiment 1.3.

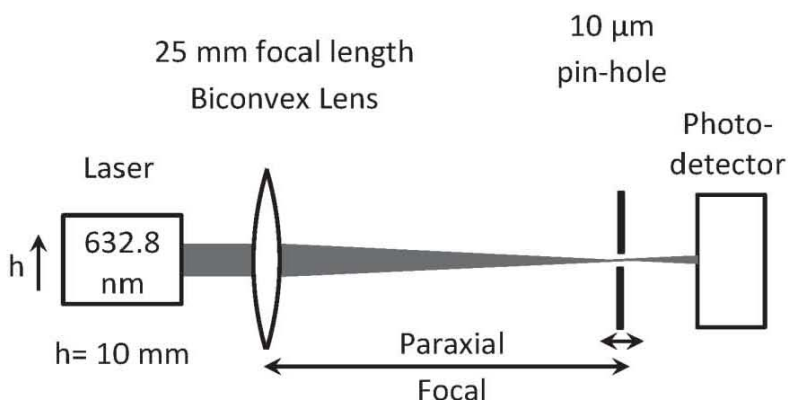


Figure 1.3 Schematic of experiment 1.3.

The schematic of experiment 1.3 is achieved through the following procedure:

1. The 0.8-mW 632.8-nm He-Ne laser is mounted on the 36"x12" breadboard using the 3" stainless-steel post, 3" post holder, ½" translation stage, and the base plate for the ½" translation stage.
2. The 632.8-nm He-Ne laser is aligned so that the 0.48-mm diameter collimated laser beam propagates parallel to the long edge of the 36"x12" breadboard at a fixed height of 6.5" above the breadboard.
3. The 25.0-mm effective focal length lens is attached to the 36"x12" breadboard using the 25/25.4-mm kinematic mount, 3" stainless-steel post, 3" post holder, and 2"x3" slotted base plate.
4. The 25.4-mm effective focal length lens is adjusted so that the 0.48-mm diameter He-Ne laser beam is incident upon the center of the 25.4-mm effective focal length lens.
5. The 10-μm ceramic aperture is attached to the 36"x12" breadboard using the mount for 10-mm diameter optics, 3" stainless-steel post, 3" post holder, ½" travel translation stage, and base plate for the ½" translation stage.

6. The 10- μm ceramic aperture is positioned so that the laser beam focused by the 25.0-mm effective focal length lens is centered upon the 10- μm ceramic aperture.
7. The 10- μm ceramic aperture is moved along the long edge of the 36"x12" breadboard using the translation stage so as to maximize the signal output of the UV-NIR silicon power photodetector.
8. The maximum detector signal will be obtained not for a unique horizontal position of the aperture, but over the range D and $D+\Delta$. Move the aperture to the middle of this range, i.e. $D+\Delta/2$.
9. The location of the 10- μm ceramic aperture in the middle of the maximum signal determines the position of the paraxial focal point of the lens.
10. The 632.8-nm He-Ne laser is then translated through a distance of 10 mm and the new position of the focal point for $h = 10$ mm is determined by translating the 10-mm ceramic aperture so that the 632.8-nm laser beam passes through the pinhole.
11. The displacement of the 10-mm ceramic aperture from the paraxial focal point to the focal point for $h = 10$ mm is a measure of the spherical aberration of the 25-mm effective focal length biconvex lens.

1.4 Chromatic aberration of a lens

The chromatic aberration CA of a lens is due the variation of the refractive index n with the wavelength of light. The focal length of a thin lens is given by

$$\frac{1}{f} = (n - 1) \left[\frac{1}{R_1} - \frac{1}{R_2} \right] \quad (1.11)$$

The fractional CA is then given by

$$\frac{CA}{f} = \frac{n_2 - n_1}{n_m - 1} \quad (1.12)$$

where n_1 and n_2 are the refractive indices at wavelengths λ_1 and λ_2 , respectively, and n_m is the refractive index at the mean wavelength $\lambda = (\lambda_1 + \lambda_2)/2$.

Experiment 1.4: Measure the chromatic aberration CA of a BK7 plano-convex lens of 100-mm focal length using 532-nm and 632-nm lasers. Using the measured value of CA , determine the value of the difference in the refractive index of the lens for the 532-nm and 632-nm wavelengths.

The optical components for this experiment consist of the following:

1. 0.9-mW 532-nm laser (Thorlabs stock no. CPS532-C2 for \$162.18 in 2018).
2. 0.8-mW 632.8-nm He-Ne laser (Thorlabs stock no. HNLS008L for \$889.44 in 2018).
3. 25.0-mm diameter, 100.0-mm effective focal length MgF_2 -coated N-BK7 plano-convex lens (Edmund Optics stock no. 32-482 for \$31.50 in 2018).
4. 10- μm diameter ceramic aperture (Edmund Optics stock no. 84-910 for \$107.00 in 2018).
5. UV-NIR silicon power photodetector (Edmund Optics stock no. 89-310 for \$795.00 in 2018).

The optomechanical components for this experiment consist of the following:

1. 5VDC regulated power supply (Thorlabs stock no. LDS5 for \$86.96 in 2018), 11-mm diameter kinematic mount (Thorlabs stock no. MK11F for \$90.00 in 2018), 3" stainless-steel post (Edmund Optics stock no. 59-754 for \$10.25 in 2018), 3" post holder (Edmund Optics stock no. 58-979 for \$13.25 in 2018), 1/2" translation stage (Thorlabs stock no. MT1 for \$297.94 in 2018), and a base plate for the 1/2" translation stage (Thorlabs stock no. MT401 for \$23.66 in 2018) for the 0.9-mW 532-nm laser.
2. 3" stainless-steel post (Edmund Optics stock no. 59-754 for \$10.25 in 2018), 3" post holder (Edmund Optics stock no. 58-979 for \$13.25 in 2018), 1/2" translation stage (Thorlabs stock no. MT1 for \$297.84 in 2018), and a base plate for the 1/2" translation

stage (Thorlabs stock no. MT401 for \$23.66 in 2018) for the 0.8-mW 632.8-nm He-Ne laser.

3. 25/25.4-mm kinematic mount (Edmund Optics stock no. 58-854 for \$109.00 in 2018), 3" stainless-steel post (Edmund Optics stock no. 59-754 for \$10.25 in 2018), 3" post holder (Edmund Optics stock no. 58-979 for \$13.25 in 2018), and a 2"x3" slotted base plate (Edmund Optics stock no. 03-655 for \$15.00 in 2018) for the 100.0-mm effective focal length lens.
4. Mount for the 10-mm optics (Thorlabs stock no. LMR10 for \$20.81 in 2018), 3" stainless-steel post (Edmund Optics stock no. 59-754 for \$10.25 in 2018), 3" post holder (Edmund Optics stock no. 58-979 for \$13.25 in 2018), $\frac{1}{2}$ " translation stage (Thorlabs stock no. MT1 for \$297.94 in 2018), and a base plate for the $\frac{1}{2}$ " translation stage (Thorlabs stock no. MT401 for \$23.66 in 2018) for the 10- μ m ceramic aperture.
5. Power meter (Edmund Optics stock no. 89-305 for \$850.00 in 2018), adjustable-height V-clamp (Thorlabs stock no. VG100 for \$87.98 in 2018), 3" stainless-steel post (Edmund Optics stock no. 59-754 for \$10.25 in 2018), 3" post holder (Edmund Optics stock no. 58-979 for \$13.25 in 2018), and a 2"x3" slotted base plate (Edmund Optics stock no. 03-655 for \$15.00 in 2018) for the UV-NIR silicon power photodetector.

Figure 1.4 shows a schematic of experiment 1.4.

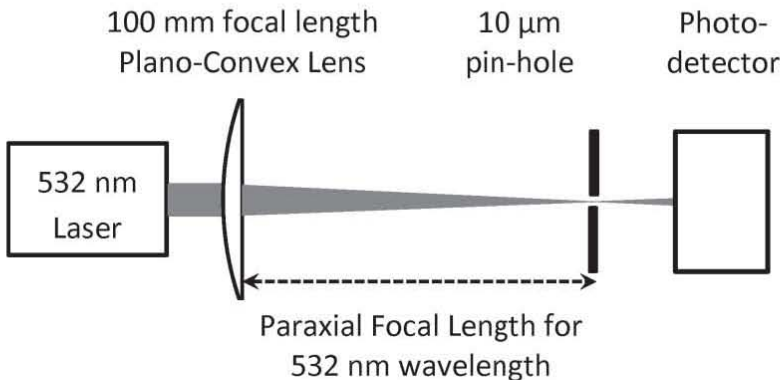


Figure 1.4 Schematic of experiment 1.4.

The schematic of experiment 1.4 is achieved through the following procedure:

1. The 0.9-mW 532-nm laser is mounted on the 36"x12" breadboard using the 11-mm kinematic mount, 3" stainless-steel post, 3" post holder, 1/2" translation stage, and the base plate for the 1/2" translation stage.
2. The 0.9-mW 532-nm laser is aligned so that the 3.5-mm diameter collimated laser beam propagates parallel to the long edge of the 36"x12" breadboard at a fixed height of 6.5" above the 36"x12" breadboard.
3. The 100.0-mm effective focal length lens is attached to the 36"x12" breadboard using the 25/25.4-mm kinematic mount, 3" stainless-steel post, 3" post holder, and 2"x3" slotted base plate.
4. The 100.0-mm effective focal length is adjusted so that the 3.5-mm diameter laser beam is incident upon the center of the 100.0-mm effective focal length lens.
5. The 10- μ m ceramic aperture is attached to the 36"x12" breadboard using the mount for the 10-mm optics, 3" stainless-steel post, 3" post holder, 1/2" translation stage, and the base plate for the 1/2" translation stage.
6. The 10- μ m ceramic aperture is positioned so that the laser beam focused by the 100.0-mm effective focal length lens is centered upon the 10- μ m ceramic aperture.
7. The UV-NIR silicon power photodetector is attached to the 36"x12" breadboard using the adjustable-height V-clamp, 3" stainless-steel post, 3" post holder, and 2"x3" slotted base plate.
8. The 10- μ m ceramic aperture is moved along the long edge of the 36"x12" breadboard using the 1/2" translation stage so as to maximize the signal output of the UV-NIR silicon power photodetector.
9. The maximum signal should be observed over some distance.
10. The position of the 10- μ m ceramic aperture corresponding to the middle of the maximum signal represents the paraxial focal spot of the 100.0-mm effective focal length lens for the 532-nm laser.

11. This process is repeated for the 632.8-nm laser without disturbing the lens, the 10- μm ceramic aperture, and the UV-NIR silicon power photodetector to determine the paraxial focal point for the 632.8-nm wavelength.
12. The distance between the two positions of the 10- μm ceramic aperture is a measure of the chromatic aberration of the lens for the 532-nm and 632.8-nm wavelengths.

1.5 Laser beam expander

A laser beam expander is used to expand the diameter of a laser beam using two lenses with focal lengths f_1 and f_2 with $f_2 > f_1$. The magnification of the laser beam diameter is given by

$$M = \frac{f_2}{f_1} \quad (1.13)$$

Experiment 1.5: Measure the expansion of the laser beam diameter using two plano-convex lenses with effective focal lengths $f_1 = 25$ mm and $f_2 = 125$ mm using a 632.8-nm He-Ne laser.

The optical components for this experiment consist of the following:

1. 0.8-mW 632.8-nm He-Ne laser (Thorlabs stock no. HNLS008L for \$889.44 in 2018).
2. 25.0-mm diameter, 25.0-mm effective focal length MgF_2 -coated N-SF5 plano-convex lens (Edmund Optics stock no. 45-098 for \$32.50 in 2018).
3. 25.0-mm diameter, 125.0-mm effective focal length MgF_2 -coated N-BK7 plano-convex lens (Edmund Optics stock no. 32-862 for \$31.50 in 2018).

The optomechanical components for this experiment consist of the following:

1. 3" stainless-steel post (Edmund Optics stock no. 59-754 for \$10.25 in 2018), 3" post holder (Edmund Optics stock no. 58-979 for \$13.25 in 2018), $\frac{1}{2}$ " translation stage (Thorlabs stock no. MT1 for \$297.84 in 2018), and a base plate for the $\frac{1}{2}$ " translation

stage (Thorlabs stock no. MT401 for \$23.66 in 2018) for the 0.8-mW 632.8-nm He-Ne laser.

2. 25/25.4-mm kinematic mount (Edmund Optics stock no. 58-854 for \$109.00 in 2018), 3" stainless-steel post (Edmund Optics stock no. 59-754 for \$10.25 in 2018), 3" post holder (Edmund Optics stock no. 58-979 for \$13.25 in 2018), and a 2"x3" slotted base plate (Edmund Optics stock no. 03-655 for \$15.00 in 2018) for the 25.0-mm diameter, 25.0-mm effective focal length lens.
3. 25/25.4-mm kinematic mount (Edmund Optics stock no. 58-854 for \$109.00 in 2018), 3" stainless-steel post (Edmund Optics stock no. 59-754 for \$10.25 in 2018), 3" post holder (Edmund Optics stock no. 58-979 for \$13.25 in 2018), and a 2"x3" slotted base plate (Edmund Optics stock no. 03-655 for \$15.00 in 2018) for the 25.0-mm diameter, 125.0-mm effective focal length lens.

Figure 1.5 shows a schematic of experiment 1.5.

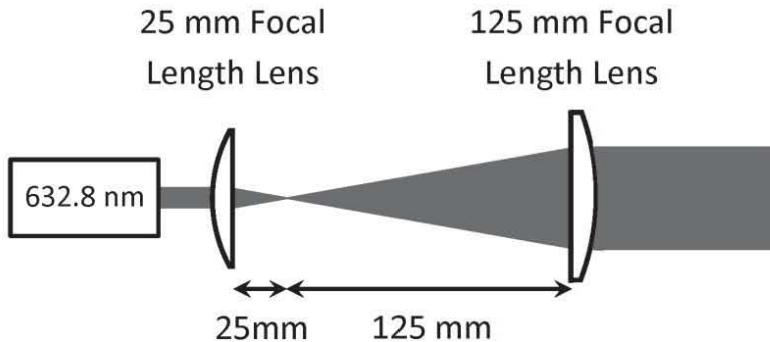


Figure 1.5 Schematic of experiment 1.5.

The schematic of experiment 1.5 is achieved through the following procedure:

1. The 632.8-nm He-Ne laser is mounted on the 36"x12" breadboard using the 3" stainless-steel post, 3" post holder, 1/2" translation stage, and the base plate for the 1/2" translation stage.
2. The 632.8-nm He-Ne laser is aligned so that the 0.48-mm diameter collimated laser beam propagates parallel to the long

edge of the 36"x12" breadboard at a fixed height of 6.5" above the 36"x12" breadboard.

3. The 25.0-mm effective focal length lens is attached to the 36"x12" breadboard using the 25/25.4-mm kinematic mount, 3" stainless-steel post, 3" post holder, and 2"x3" slotted base plate.
4. The 25.0-mm effective focal length lens is adjusted so that the 0.48-mm diameter He-Ne laser beam is incident upon the center of the 25.0-mm effective focal length lens.
5. The 125.0-mm effective focal length lens is attached to the 36"x12" breadboard using the 25/25.4-mm kinematic mount, 3" stainless-steel post, 3" post holder, and 2"x3" slotted base plate at a distance of 150 mm from the 25.0-mm effective focal length lens.
6. The 0.48-mm diameter 632.8-nm He-Ne laser beam expands to a 2.4-mm diameter beam when it is incident upon the 125.0-mm effective focal length lens.
7. The 125.0-mm effective focal length lens is adjusted so that the 2.4-mm diameter He-Ne laser beam is incident upon the center of this lens and the output beam is collimated.
8. The diameter of the laser beam transmitted by the 125.0-mm effective focal length lens determines the expansion of the laser beam diameter incident upon the 25.0-mm effective focal length lens.

1.6 Field of view of a camera

The horizontal field of view FOV of a camera with a 35-mm format is given by

$$FOV(^{\circ}) = \tan^{-1} \left(\frac{35}{f} \right) \quad (1.14)$$

where f is the focal length of the camera lens in units of mm.

Experiment 1.6: Measure the field of view of a camera with a 50-mm effective focal length lens using a 632.8-nm He-Ne laser.

The optical components for this experiment consist of the following:

1. 0.8-mW 632.8-nm He-Ne laser (Thorlabs stock no. HNLS008L for \$889.44 in 2018).
2. 25.0-mm diameter 50.0-mm effective focal length MgF₂-coated N-BK7 plano-convex lens (Edmund Optics stock no. 32-478 for \$31.50 in 2018).

The optomechanical components for this experiment consist of the following:

1. 3" stainless-steel post (Edmund Optics stock no. 59-754 for \$10.25 in 2018), 3" post holder (Edmund Optics stock no. 58-979 for \$13.25 in 2018), ½" translation stage (Thorlabs stock no. MT1 for \$297.84 in 2018), and a base plate for the ½" translation stage (Thorlabs stock no. MT401 for \$23.66 in 2018) for the 0.8-mW 632.8-nm He-Ne laser.
2. 25/25.4-mm kinematic mount (Edmund Optics stock no. 58-854 for \$109.00 in 2018), 3" stainless-steel post (Edmund Optics stock no. 59-754 for \$10.25 in 2018), 3" post holder (Edmund Optics stock no. 58-979 for \$13.25 in 2018), and a 2"x3" slotted base plate (Edmund Optics stock no. 03-655 for \$15.00 in 2018).
3. 37-mm maximum aperture mounted iris diaphragm (Edmund Optics stock no. 53-916 for \$99.00 in 2018).

Figure 1.6 shows a schematic of experiment 1.6.

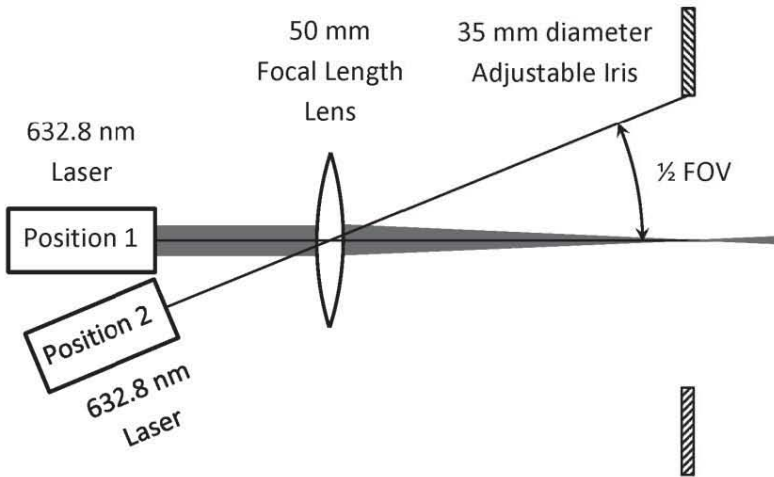


Figure 1.6 Schematic of experiment 1.6.

The schematic of experiment 1.6 is achieved through the following procedure:

1. The 0.8-mW 632.8-nm He-Ne laser is mounted on the 36"x12" breadboard using the 3" stainless-steel post, 3" post holder, $\frac{1}{2}$ " translation stage, and the base plate for the $\frac{1}{2}$ " translation stage.
2. The 0.8-mW 632.8-nm He-Ne laser is aligned so that the 0.48-mm diameter collimated laser beam propagates parallel to the long edge of the 36"x12" breadboard at a fixed height of 6.5" above the 36"x12" breadboard.
3. The 50.0-mm effective focal length lens is attached to the 36"x12" breadboard using the 25/25.4-mm kinematic mount, 3" stainless-steel post, 3" post holder, and 2"x3" slotted base plate.
4. The 50.0-mm effective focal length lens is adjusted so that the 0.48-mm diameter He-Ne laser beam is incident upon the center of this lens.
5. The 50-mm effective focal length focuses the incident laser beam at a distance of 50 mm on its right-hand side.
6. An iris with a 35-mm diameter hole is mounted on the breadboard in the focal plane of the 50.0-mm effective focal

length lens using the 3" stainless-steel post, 3" post holder, and 2"x3" slotted base plate.

7. Adjust the iris so that the focal spot of the 632.8-nm He-Ne laser due to the 50.0-mm effective focal length lens is centered upon the 35-mm hole in the iris.
8. Reposition the 632.8-nm He-Ne laser so that it passes through the center of the 50.0-mm effective focal length lens and is incident upon the edge of the 35-mm hole in the iris.
9. The angle between the two positions of the laser beam is the equal to one-half of the horizontal field of view.

1.7 Magnification of a microscope objective

The magnification of a microscope objective is given by

$$M = \frac{s_i}{s_o} \quad (1.15)$$

where s_o and s_i are the object and image distances from the objective. The value of s_o is given by

$$s_o = \left(1 + \frac{1}{M}\right)f \quad (1.16)$$

where f is the focal length of the microscope objective.

Experiment 1.7: Measure the magnification of an 18-mm focal length Olympus 10X microscope objective using a 632.8-nm He-Ne laser. Determine the value of s_o using the measured value of M and the known value of f .

The optical components for this experiment consist of the following:

1. 0.8-mW 632.8-nm He-Ne laser (Thorlabs stock no. HNLS008L for \$889.44 in 2018).
2. 19-mm diameter, 1-mm scale/100Div eyepiece reticle (Edmund Optics stock no. 54-422 for \$150.00 in 2018).

3. 24-mm diameter, 18-mm focal length Olympus PLN 10X microscope objective (Edmund Optics stock no. 86-813 for \$315.00 in 2018).
4. Mount for the 19-mm optics (Thorlabs stock no. SM1AD19 for \$22.66 in 2018), 3" stainless-steel post (Edmund Optics stock no. 59-754 for \$10.25 in 2018), 3" post holder (Edmund Optics stock no. 58-979 for \$13.25 in 2018), and a 2"x3" slotted base plate (Edmund Optics stock no. 03-655 for \$15.00 in 2018) for the 10-mm eyepiece reticle.

Figure 1.7 shows a schematic of the microscope.

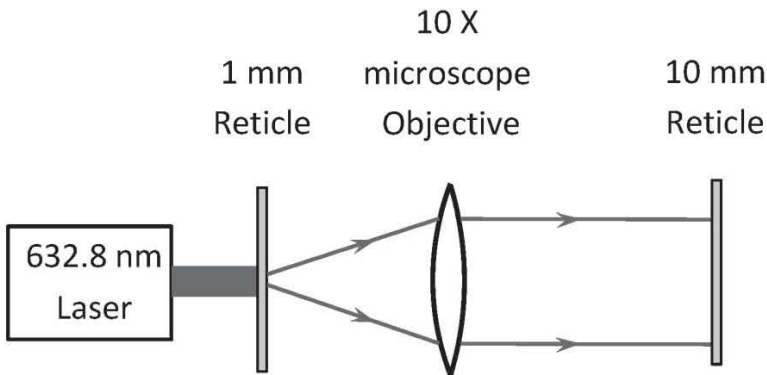


Figure 1.7 Schematic of the microscope objective.

The schematic of experiment 1.7 is achieved through the following procedure:

1. The 632.8-nm He-Ne laser is mounted on the 36"x12" breadboard using the 3" stainless-steel post, 3" post holder, $\frac{1}{2}$ " translation stage, and the base plate for the $\frac{1}{2}$ " translation stage.
2. The 632.8-nm He-Ne laser is aligned so that the 0.48-mm diameter collimated laser beam propagates parallel to the long edge of the 36"x12" breadboard at a fixed height of 6.5" above the 36"x12" breadboard.
3. The 1-mm/100Div scale eyepiece reticle is mounted on the 36"x12" breadboard using the mount for the 19-mm optics, 3" stainless-steel post, 3" post holder, and 2"x3" slotted base plate.

4. The 1-mm/100Div eyepiece reticle is rotated to be in the horizontal position.
5. The 18-mm focal length Olympus 10X microscope objective is attached to the 36"x12" breadboard at a distance of ~18 mm from the 1-mm/100Div eyepiece reticle using the adjustable ring mount for the microscope objective, 3" stainless-steel post, 3" post holder, and 2"x3" slotted base plate.
6. The 10-mm/100Div eyepiece reticle is mounted in the horizontal position on the breadboard at a distance of 200 mm using the mount for the 19-mm optics adaptor, 3" stainless-steel post, 3" post holder, and 2"x3" slotted base plate.
7. The 1-mm/100Div eyepiece reticle is translated along the long edge of the 36"x12" breadboard using the 2"x3" slotted base plate so that its image overlaps the 10-mm/100Div eyepiece reticle.
8. The magnification of the microscope objective is determined by comparing the size of the image of the 1-mm scale/100Div eyepiece reticle formed by the 10x microscope objective with the 10-mm scale/100Div eyepiece reticle.

CHAPTER 2

MIRRORS

2.1 Angle of Reflection

According to the law of reflection, the angle of reflection θ_r is given by

$$\theta_r = \theta_i \quad (2.1)$$

Experiment 2.1: Measure the angle of reflection θ_r for angle of incidence θ_i equal to 30° using a 632-nm He-Ne laser.

The optical components for this experiment are the following:

1. 0.8-mW 632.8-nm He-Ne laser (Thorlabs stock no. HNLS008L for \$889.44 in 2018).
2. 25.0-mm diameter first-surface plane mirror (Edmund Optics stock no. 87-371 for \$80.00 in 2018).

The optomechanical components for this experiment are the following:

1. 3" stainless-steel post (Edmund Optics stock no. 59-754 for \$10.25 in 2018), 3" post holder (Edmund Optics stock no. 58-979 for \$13.25 in 2018), $\frac{1}{2}$ " translation stage (Thorlabs stock no. MT1 for \$297.84 in 2018), and the base plate for the $\frac{1}{2}$ " translation stage (Thorlabs stock no. MT401 for \$23.66 in 2018) for the 0.8-mW 632.8-nm He-Ne laser.
2. Kinematic circular optical mount (Edmund Optics stock no. 58-854 for \$109.00 in 2018), 3" stainless-steel post (Edmund Optics stock no. 59-754 for \$10.25 in 2018), 3" post holder (Edmund Optics stock no. 58-979 for \$13.25 in 2018), 360° high-precision rotation mount (Thorlabs stock no. PR01 for \$331.50 in 2018), and the solid adaptor plate (Thorlabs stock no. PR01A for \$29.33 in 2018) for the 25.0-mm diameter first-surface plane mirror.

Figure 2.1 shows a schematic of experiment 2.1.

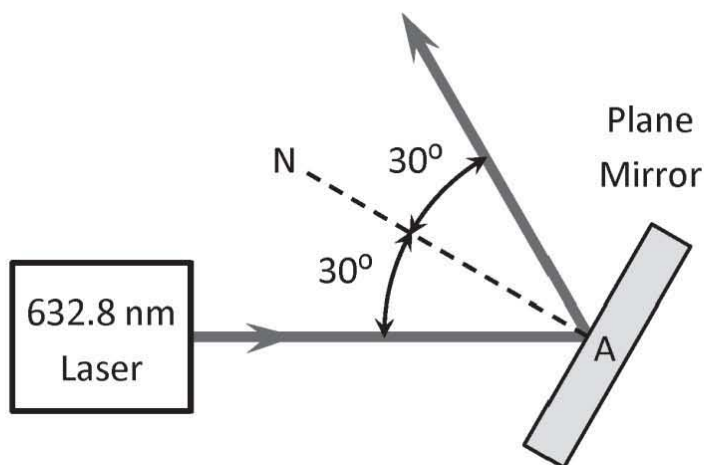


Figure 2.1 Schematic of experiment 2.1.

The schematic of experiment 2.1 is achieved through the following procedure:

1. The 0.8-mW 632.8-nm He-Ne laser is attached to the 36"x12" breadboard using the 3" stainless-steel post, 3" post holder, ½" travel translation stage, and the base plate for the ½" translation stage.
2. The 0.8-mW 632.8-nm He-Ne laser is adjusted so that the 0.48-mm diameter laser beam propagates parallel to the long edge of the 36"x12" breadboard at a fixed height of 6.5" above the breadboard.
3. The 25.0-mm diameter plane mirror is inserted into the kinematic circular optical mount using the 3" stainless-steel post, 3" post holder, 360° high-precision rotation mount, and the solid adaptor plate.
4. The plane mirror is adjusted so as to retro-reflect the 632.8-nm He-Ne laser beam.
5. The plane mirror is then rotated through an angle of 30°.

6. The 0.8-mW 632.8-nm He-Ne laser beam would be reflected from the plane mirror at an angle of 60° with respect to the incident laser beam. This implies that the angle of reflection is equal to $1/2 \times 60^\circ = 30^\circ$, which is equal to the angle of incidence.

2.2 Rotation of a mirror

If a mirror is rotated through an angle θ , the reflected ray rotates through an angle 2θ .

Experiment 2.2: Measure the angle of rotation of the reflected ray when the mirror is rotated through an angle of 20° using a 632-nm He-Ne laser. The initial angle of incidence θ_i for the incident ray is 0° .

The optical components for this experiment are the following:

1. 0.8-mW 632.8-nm He-Ne laser (Thorlabs stock no. HNLS008L for \$889.44 in 2018).
2. 25-mm diameter first-surface plane mirror (Edmund Optics stock no. 87-371 for \$80.00 in 2018).

The optomechanical components for this experiment are the following:

1. 3" stainless-steel post (Edmund Optics stock no. 59-754 for \$10.25 in 2018), 3" post holder (Edmund Optics stock no. 58-979 for \$13.25 in 2018), $\frac{1}{2}$ " translation stage (Thorlabs stock no. MT1 for \$297.84 in 2018), and the base plate for the $\frac{1}{2}$ " translation stage (Thorlabs stock no. MT401 for \$23.66 in 2018) for the 0.8-mW 632.8-nm He-Ne laser.
2. Kinematic circular optical mount (Edmund Optics stock no. 58-854 for \$109.00 in 2018), 3" stainless-steel post (Edmund Optics stock no. 59-754 for \$10.25 in 2018), 3" post holder (Edmund Optics stock no. 58-979 for \$13.25 in 2018), 360° high-precision rotation mount (Thorlabs stock no. PR01 for \$331.50 in 2018), and solid adaptor plate (Thorlabs stock no. PR01A for \$29.33 in 2018) for the 25.0-mm diameter first-surface plane mirror.

Figure 2.2 shows a schematic of experiment 2.2.

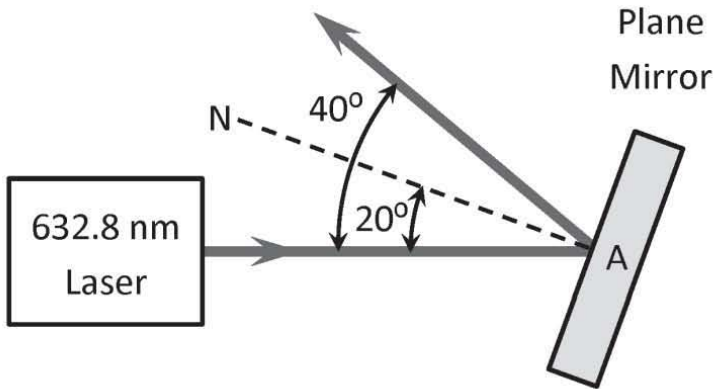


Figure 2.2 Schematic of experiment 2.2.

The schematic of experiment 2.2 is achieved through the following procedure:

1. The 0.8-mW 632.8-nm He-Ne laser is attached to the 36"x12" breadboard using the 3" stainless-steel post, 3" post holder, $\frac{1}{2}$ " translation stage, and the base plate for the $\frac{1}{2}$ " translation stage.
2. The 0.8-mW 632.8-nm He-Ne laser is adjusted so that the 0.48-mm diameter laser beam propagates parallel to the long edge of the 36"x12" breadboard at a fixed height of 6.5" above the breadboard.
3. The 25.0-mm diameter plane mirror is attached to the 36"x12" breadboard using the 25.0/25.4-mm kinematic circular optical mount, 3" stainless-steel post, 3" post holder, 360° high-precision rotation mount, and the solid adaptor plate for the 360° high-precision rotation mount.
4. The plane mirror is adjusted so as to retro-reflect the 0.8-mW 632.8-nm He-Ne laser beam.
5. The plane mirror is then rotated through an angle of 20° using the 360° high-precision rotation mount.
6. The 0.8-mW 632.8-nm He-Ne laser beam would be reflected from the plane mirror at an angle of 40° with respect to the

incident laser beam, which is twice the 20° angle of rotation of the plane mirror.

2.3 Longitudinal spherical aberration of a spherical mirror

A mirror shows spherical aberration like that of a lens. The focal point F for the paraxial rays lies at a distance from the vertex V of the spherical mirror, which is given by

$$FV = \frac{1}{2}CV \quad (2.2)$$

where C is the center of curvature of the mirror. Rays incident at the height h above the axis of the mirror come to focus F' , which is closer to the vertex V , that is

$$F'V < FV \quad (2.3)$$

The longitudinal spherical aberration is then given by

$$LSA = FV - F'V \quad (2.4)$$

Experiment 2.3: Measure the longitudinal spherical aberration of a 25.4-mm diameter, 25.4-mm focal length spherical mirror for a ray incident at a height $h = 10$ mm above the axis of the mirror using a 0.8-mW 632.8-nm He-Ne laser.

The optical components for this experiment are the following:

1. 0.8-mW 632.8-nm He-Ne laser (Thorlabs stock no. HNLS008L for \$889.44 in 2018).
2. 25.4-mm diameter, 25.4-mm focal length enhanced-aluminum spherical mirror (Edmund Optics stock no. 43-536 for \$105.00 in 2018).

The optomechanical components for this experiment are the following:

1. 3" stainless-steel post (Edmund Optics stock no. 59-754 for \$10.25 in 2018), 3" post holder (Edmund Optics stock no. 58-979 for \$13.25 in 2018), $\frac{1}{2}$ " translation stage (Thorlabs stock no.

MT1 for \$297.84 in 2018), and the base plate for the $\frac{1}{2}$ " translation stage (Thorlabs stock no. MT401 for \$23.66 in 2018) for the 0.8-mW 632.8-nm He-Ne laser.

2. 12-mm mounted iris diaphragm (Edmund Optics stock no. 53-914 for \$62.50 in 2018).
3. 3" stainless-steel post (Edmund Optics stock no. 59-754 for \$10.25 in 2018), 3" post holder (Edmund Optics stock no. 58-979 for \$13.25 in 2018), $\frac{1}{2}$ " travel translation stage (Thorlabs stock no. MT1 for \$297.94 in 2018), and base plate for the $\frac{1}{2}$ " translation stage (Thorlabs stock no. MT401 for \$23.66 in 2018) for the 12-mm mounted iris diaphragm.
4. 25.0/25.4-mm kinematic circular optical mount (Edmund Optics stock no. 58-854 for \$109.00 in 2018), 3" stainless-steel post (Edmund Optics stock no. 59-754 for \$10.25 in 2018), 3" post holder (Edmund Optics stock no. 58-979 for \$13.25 in 2018), and a 2"x3" slotted base plate (Edmund Optics stock no. 03-655 for \$15.00 in 2018) for the 2.54-mm focal length enhanced-aluminum spherical mirror.

Figure 2.3 shows a schematic of experiment 2.3.

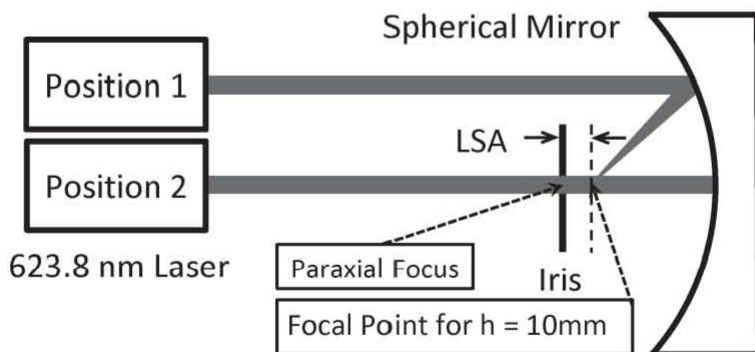


Figure 2.3 Schematic of experiment 2.3.

The schematic of experiment 2.3 is achieved through the following procedure:

1. The 0.8-mW 632.8-nm He-Ne laser is attached to the 36"x12" breadboard using the 3" stainless-steel post, 3" post holder, 1/2" translation stage, and the base plate for the 1/2" translation stage.
2. The 0.8-mW 632.8-nm He-Ne laser is adjusted so that the 0.48-mm diameter laser beam propagates parallel to the long edge of the 36"x12" breadboard at a fixed height of 6.5" above the breadboard.
3. The 12-mm mounted iris diaphragm is attached to the 36"x12" breadboard using the 3" stainless-steel post, 3" post holder, 1/2" translation stage, and the base plate for the 1/2" translation stage.
4. The 2.54-mm focal length enhanced-aluminum spherical mirror is attached to the 36"x12" breadboard using the 25.0/25.4-mm kinematic circular optical mount, 3" stainless-steel post, 3" post holder, and 2"x3" slotted base plate.
5. The spherical mirror is adjusted so as to retro-reflect the 0.8-mW 632.8-nm He-Ne laser beam.
6. The 12-mm mounted iris diaphragm is translated so as to center the paraxial focal spot of the spherical mirror on the 12-mm iris diaphragm.
7. The 0.8-mW 632.8-nm He-Ne laser is translated through a distance of 10 mm.
8. The 12-mm iris diaphragm is translated until the focal spot of the 632.8-nm laser beam for $h = 10$ mm is centered upon the 12-mm iris diaphragm.
9. The translation of the 12-mm mounted iris diaphragm from the paraxial focus to the focus for the $h = 10$ mm rays is a measure of the spherical aberration of the spherical mirror.

2.4 Off-axis concave parabolic mirror

A plane parallel beam of light incident upon an off-axis concave parabolic mirror comes to a common focal point, which is located away from the axis of the mirror.

Experiment 2.4: Determine the effective focal length of a 25.4-mm diameter, 50.8-mm focal length, 30° off-axis parabolic mirror using a 0.9-mW 532-nm laser.

The optical components for this experiment are the following:

1. 0.9-mW 532-nm laser (Thorlabs stock no. CPS532-C2 for \$162.18 in 2018).
2. 25.4-mm diameter, 50.8-mm focal length, 30° off-axis parabolic mirror (Edmund Optics stock no. 35-490 for \$205.00 in 2018).
3. 10- μ m ceramic aperture (Edmund Optics stock no. 84-910 for \$107.00 in 2018).
4. UV-NIR silicon power photodetector (Edmund Optics stock no. 89-310 for \$795.00 in 2018).

The optomechanical components for this experiment are the following:

1. 5VDC regulated power supply (Thorlabs stock no. LDS5 for \$86.96 in 2018), 11-mm kinematic mount (Thorlabs stock no. MK11F for \$90.00 in 2018), 3" stainless-steel post (Edmund Optics stock no. 59-754 for \$10.25 in 2018), 3" post holder (Edmund Optics stock no. 58-979 for \$13.25 in 2018), 1/2" translation stage (Thorlabs stock no. MT1 for \$297.94 in 2018), and the base plate for the travel translation stage (Thorlabs stock no. MT401 for \$23.66 in 2018) for the 0.9-mW 532-nm laser.
2. Mounting plate (Edmund Optics stock no. 47-111 for \$95.00 in 2018), 3" stainless-steel post (Edmund Optics stock no. 59-754 for \$10.25 in 2018), 3" post holder (Edmund Optics stock no. 58-979 for \$13.25 in 2018), and a 2"x3" slotted base plate (Edmund Optics stock no. 03-655 for \$15.00 in 2018) for the 30° off-axis parabolic mirror.
3. Lens mount for the 10-mm optics (Thorlabs stock no. LMR10 for \$20.81 in 2018), 3" stainless-steel post (Edmund Optics stock no. 59-754 for \$10.25 in 2018), 3" post holder (Edmund Optics stock no. 58-979 for \$13.25 in 2018), 1/2" translation stage (Thorlabs stock no. MT1 for \$297.94 in 2018), and a base plate for the 1/2" translation stage (Thorlabs stock no. MT401 for \$23.66 in 2018) for the 10- μ m ceramic aperture.

4. Power meter (Edmund Optics stock no. 89-305 for \$850.00 in 2018), adjustable-height V-clamp (Thorlabs stock no. VG100 for \$87.98 in 2018), 3" stainless-steel post (Edmund Optics stock no. 59-754 for \$10.25 in 2018), 3" post holder (Edmund Optics stock no. 58-979 for \$13.25 in 2018), and a 2"x3" slotted base plate (Edmund Optics stock no. 03-655 for \$15.00 in 2018) for the UV-NIR silicon power photodetector.

Figure 2.4 shows a schematic of experiment 2.4.

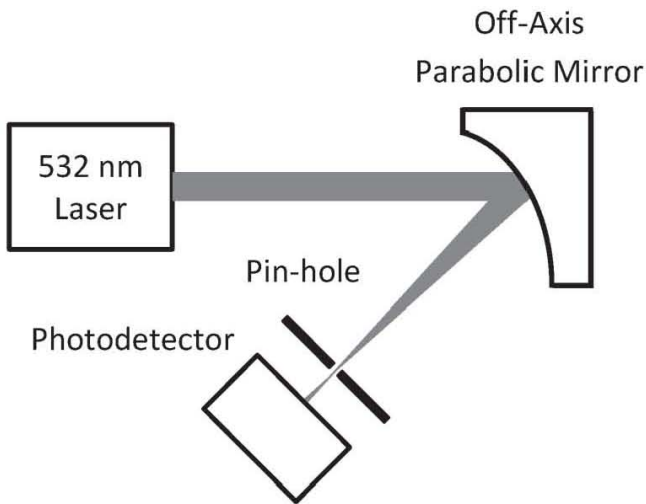


Figure 2.4 Schematic of experiment 2.4.

The schematic of experiment 2.4 is achieved through the following procedure:

1. The 0.9-mW 532.0-nm laser is attached to the 36"x12" breadboard using the 11-mm kinematic mount, 3" stainless-steel post, 3" post holder, 1/2" translation stage, and the base plate for the 1/2" translation stage.
2. The 0.9-mW 532.0-nm laser is adjusted so that the 3.5-mm diameter 0.9-mW 532-nm laser beam propagates parallel to the long edge of the breadboard at a fixed height of 6.5" above the breadboard.

3. The 30° off-axis parabolic mirror is attached to the 36"x12" breadboard using the mounting plate, 3" stainless-steel post, 3" post holder, and 2"x3" slotted base plate.
4. The 30° off-axis parabolic mirror is adjusted so that the 3.5-mm diameter 0.9-mW 532.0-nm laser beam is incident upon the center of the 30° off-axis parabolic mirror, which focuses the 0.9-mW 532.0-nm laser beam on the axis of the parabola.
5. The 10-μm ceramic aperture is attached to the 36"x12" breadboard using the lens mount for the 10-mm optics, 3" stainless-steel post, 3" post holder (Edmund Optics stock no. 58-979 for \$13.25 in 2018), 1/2" translation stage, and the base plate for the 1/2" translation stage.
6. The 10-μm ceramic aperture is adjusted so that the focal spot of the 30° off-axis parabolic mirror is centered upon the 10-μm ceramic aperture.
7. The UV-NIR silicon power photodetector is attached to the 36"x12" breadboard using the adjustable-height V-clamp, 3" stainless-steel post, 3" post holder, and 2"x3" slotted base plate.
8. The 10-μm ceramic aperture is translated to maximize the UV-NIR silicon power photodetector signal.
9. The maximum photodetector signal should be observed over some distance of the translation of the 10-μm ceramic aperture.
10. The middle of the maximum photodetector signal represents the focal point of the 30° off-axis parabolic mirror.
11. The effective focal length is the distance of the 10-μm ceramic aperture from the center of the 30° off-axis parabolic mirror.

2.5 Ellipsoidal mirror

An ellipsoidal mirror has two focal lengths, which are given by

$$f_1 = a - \sqrt{a^2 - b^2} \quad (2.6)$$

and

$$f_2 = a + \sqrt{a^2 - b^2} \quad (2.7)$$

where a and b are the semi-major and semi-minor axes of the ellipse, respectively. The first focal point is closer to the mirror than the second.

Experiment 2.5: Determine the first focal point of a 64-mm diameter ellipsoidal mirror with focal lengths $f_1 = 11$ mm and $f_2 = 78$ mm using a 0.9-mW 532-nm laser focused at the second focal point.

The optical components for this experiment consist of the following:

1. 0.9-mW 532-nm laser (Thorlabs stock no. CPS532-C2 for \$162.18 in 2018).
2. 12.7-mm diameter 12.7-mm effective focal length MgF₂-coated plano-convex lens (Edmund Optics stock no. 49-854 for \$30.50 in 2018).
3. 64-mm diameter ellipsoidal mirror with 11-mm and 78-mm focal lengths (Edmund Optics stock no. 90-968 for \$195.00 in 2018).

The optomechanical components for this experiment consist of the following:

1. 5VDC regulated power supply (Thorlabs stock no. LDS5 for \$86.96 in 2018), 11-mm kinematic mount (Thorlabs stock no. MK11F for \$90.00 in 2018), 3" stainless-steel post (Edmund Optics stock no. 59-754 for \$10.25 in 2018), 3" post holder (Edmund Optics stock no. 58-979 for \$13.25 in 2018), 1/2" translation stage (Thorlabs stock no. MT1 for \$297.94 in 2018), and a base plate for the 1/2" translation stage (Thorlabs stock no. MT401 for \$23.66 in 2018) for the 0.9-mW 532-nm laser.
2. 12.7-mm optic component mount (Edmund Optics stock no. 64-556 for \$39.00 in 2018), 3" stainless-steel post (Edmund Optics stock no. 59-754 for \$10.25 in 2018), 3" post holder (Edmund Optics stock no. 58-979 for \$13.25 in 2018), and a 2"x3" slotted base plate (Edmund Optics stock no. 03-655 for \$15.00 in 2018) for the 12.7-mm diameter plano-convex lens.

- Adjustable ring mount (Edmund Optics stock no. 36-605 for \$55.00 in 2018), 3" stainless-steel post (Edmund Optics stock no. 59-754 for \$10.25 in 2018), 3" post holder (Edmund Optics stock no. 58-979 for \$13.25 in 2018), and a 2"x3" slotted base plate (Edmund Optics stock no. 03-655 for \$15.00 in 2018) for the ellipsoidal mirror.

Figure 2.5 shows a schematic of experiment 2.5.

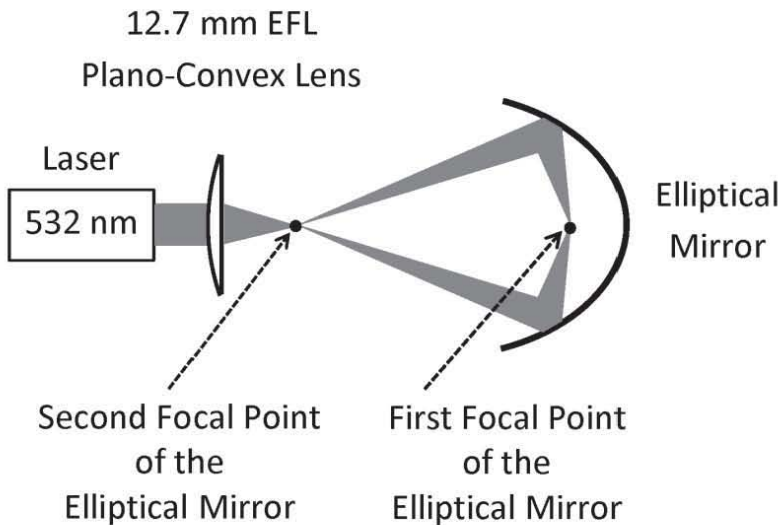


Figure 2.5 Schematic of experiment 2.5.

The schematic of experiment 2.5 is achieved through the following procedure:

- The 0.9-mW 532.0-nm laser is mounted on the 36"x12" breadboard using the 11-mm kinematic mount, 3" stainless-steel post, 3" post holder, $\frac{1}{2}$ " translation stage, and the base plate for the $\frac{1}{2}$ " translation stage.
- The 0.9-mW 532-nm laser is aligned so that the 3.5-mm diameter laser beam propagates parallel to the long edge of the 36"x12" breadboard at a fixed height of 6.5" above the 36"x12" breadboard.

3. The 12.7-mm effective focal length lens is attached to the 36"x12" breadboard using the 12.7-mm optic component mount, 3" stainless-steel post, 3" post holder, and 2"x3" slotted base plate.
4. The 12.7-mm effective focal length lens is adjusted so that the 3.5-mm diameter 532.0-nm laser beam is incident upon the center of this lens.
5. The 12.7-mm effective focal lens focuses the incident laser beam and expands it to an approximately 20-mm diameter beam.
6. The 64-mm ellipsoidal mirror is attached to the 36"x12" breadboard using the adjustable ring mount, 3" stainless-steel post, 3" post holder, and 2"x3" slotted base plate.
7. The 64-mm ellipsoidal mirror is adjusted so that the focal point of the 12.7-mm effective focal length lens is located at the second focal point of the ellipsoidal mirror.
8. An image of the focal spot of the 12.7-mm focal length lens will be produced by the 64-mm ellipsoidal mirror at its first focal point.

CHAPTER 3

GRATINGS

3.1 Grating Equation

Light incident upon a grating is diffracted according to the grating equation

$$d(\sin\theta_m - \sin\theta_i) = m\lambda \quad (3.1)$$

where d is the grating groove spacing, λ is the wavelength of light, θ_i is the angle of incidence, and θ_m is the angle of diffraction for order m that is equal to 0, ± 1 , ± 2 , and so on.

Experiment 3.1: A 632.8-nm He-Ne laser light is incident at a zero-degree angle of incidence θ_i upon a transmission grating with 1200 grooves/mm. Determine the angle of diffraction θ_m for all possible orders m .

The optical components for this experiment are the following:

1. 0.8-mW 632.8-nm He-Ne laser (Thorlabs stock no. HNLS008L for \$889.44 in 2018).
2. 1200 grooves/mm, 25-mm square transmission diffraction grating (Edmund Optics stock no. 49-582 for \$105.00 in 2018).

The optomechanical components for this experiment are the following:

1. 3" stainless-steel post (Edmund Optics stock no. 59-754 for \$10.25 in 2018), 3" post holder (Edmund Optics stock no. 58-979 for \$13.25 in 2018), $\frac{1}{2}$ " translation stage (Thorlabs stock no. MT1 for \$297.84 in 2018), and the base plate for the $\frac{1}{2}$ " translation stage (Thorlabs stock no. MT401 for \$23.66 in 2018) for the 0.8-mW 632.8-nm He-Ne laser.
2. 25.0/25.4-mm square kinematic mount (Edmund Optics stock no. 58-857 for \$105.00 in 2018), 3" stainless-steel post (Edmund

Optics stock no. 59-754 for \$10.25), 3" post holder (Edmund Optics stock no. 58-979 for \$13.25 in 2018), and a 2"x3" slotted base plate (Edmund Optics stock no. 03-655 for \$15.00 in 2018) for the 25-mm square transmission grating.

Figure 3.1 shows a schematic of experiment 3.1.

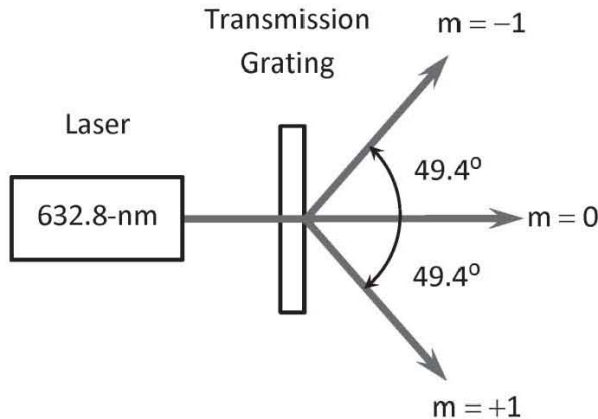


Figure 3.1 Schematic of experiment 3.1.

The schematic of experiment 3.1 is achieved through the following procedure:

1. The 0.8-mW 632.8-nm He-Ne laser is attached to the 36"x12" breadboard using the 3" stainless-steel post, 3" post holder, $\frac{1}{2}$ " translation stage, and the base plate for the $\frac{1}{2}$ " translation stage.
2. The 0.8-mW 632.8-nm He-Ne laser is adjusted so that the 0.48-mm diameter laser beam propagates parallel to the long edge of the 36"x12" breadboard at a fixed height of 6.5" above the 36"x12" breadboard.
3. The transmission grating is attached to the 36"x12" breadboard using the 25.0/25.4-mm square kinematic mount, 3" stainless-steel post, 3" post holder, and 2"x3" slotted base plate.
4. The transmission grating is aligned so that the 0.8-mW 632.8-nm He-Ne laser beam is incident upon the transmission grating at a zero angle of incidence by overlapping the zero-order ($m = 0$)

diffracted beam with the transmitted 0.632.8-nm He-Ne laser beam.

5. The $m = \pm 1$ order diffraction will occur at an angle of 49.4° on either side of the zero-order diffraction.

Experiment 3.2: A 532-nm laser light is incident at a zero-degree angle of incidence θ_i upon a transmission diffraction grating with 1200 grooves/mm. Determine the angle of diffraction θ_m for all possible orders m .

The optical components for this experiment are the following:

1. 0.9-mW 532-nm laser (Thorlabs stock no. CPS532-C2 for \$162.18 in 2018).
2. 1200 grooves/mm, 25-mm square transmission diffraction grating (Edmund Optics stock no. 49-582 for \$105.00 in 2018).

The optomechanical and other components for this experiment are the following:

1. 5VDC regulated power supply (Thorlabs stock no. LDS5 for \$86.96 in 2018), 11-mm kinematic mount (Thorlabs stock no. MK11F for \$90.00 in 2018), 3" stainless-steel post (Edmund Optics stock no. 59-754 for \$10.25 in 2018), 3" post holder (Edmund Optics stock no. 58-979 for \$13.25 in 2018), 1/2" translation stage (Thorlabs stock no. MT1 for \$297.94 in 2018), and the base plate for the 1/2" translation stage (Thorlabs stock no. MT401 for \$23.66 in 2018) for the 0.9-mW 532-nm laser.
2. 25/25.4-mm square kinematic mount (Edmund Optics stock no. 58-857 for \$105.00 in 2018), 3" stainless-steel post (Edmund Optics stock no. 59-754 for \$10.25 in 2018), 3" post holder (Edmund Optics stock no. 58-979 for \$13.25 in 2018), and a 2"x3" slotted base plate (Edmund Optics stock no. 03-655 for \$15.00 in 2018) for the 25-mm square transmission grating.

Figure 3.2 shows a schematic of experiment 3.2.

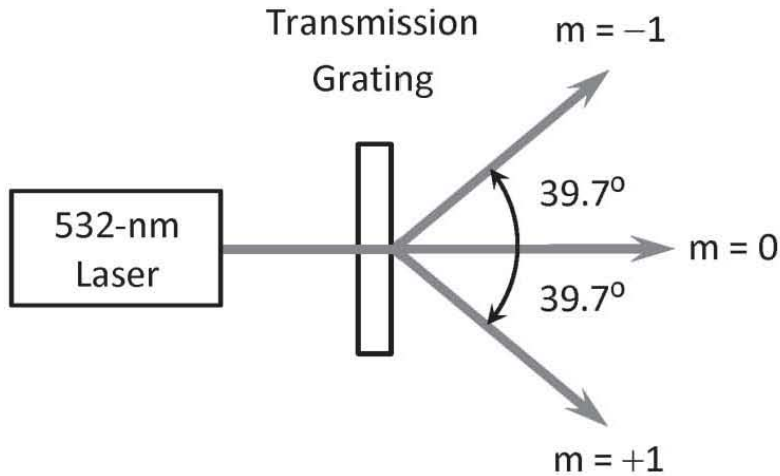


Figure 3.2 Schematic of experiment 3.2.

The schematic of experiment 3.2 is achieved through the following procedure:

1. The 0.9-mW 532-nm laser is attached to the 36"x12" breadboard using the 11-mm kinematic mount, 3" stainless-steel post, 3" post holder, ½" translation stage, and the base plate for the ½" translation stage.
2. The 0.9-mW 532-nm laser is adjusted so that the 3.5-mm diameter 532-nm laser beam propagates parallel to the long edge of the 36"x12" breadboard at a fixed height of 6.5" above the 36"x12" breadboard.
3. The transmission grating is attached to the 36"x12" breadboard using the 25.0/25.4-mm square kinematic mount, 3" stainless-steel post, 3" post holder, and 2"x3" slotted base plate.
4. The transmission grating is aligned so that the 0.9-mW 532-nm laser beam is incident upon the transmission grating at a zero angle of incidence by overlapping the zero-order ($m = 0$) diffracted beam with the transmitted 0.9-mW 532-nm laser beam.
5. The $m = \pm 1$ order diffraction will occur at an angle of 39.7° on either side of the zero-order diffraction.

3.2 Diffraction efficiency

The diffraction efficiency θ of a grating depends upon the wavelength of light and its polarization relative to the grooves of the grating.

Experiment 3.3: A 532-nm laser light is incident at an angle of incidence θ_i equal to 19° upon a 1200 grooves/mm, 25-mm square ruled diffraction grating with a blaze angle θ of $17^\circ 27'$. Determine the grating efficiency θ for the light diffracted in the $m = -1$ order for incident light polarization parallel and perpendicular to the grooves of the grating.

The optical components for this experiment are the following:

1. 0.9-mW 532-nm laser (Thorlabs stock no. CPS532-C2 for \$162.18 in 2018).
2. 25.4-mm diameter half-wave plate (Edmund Optics stock no. 43-697 for \$430.00 in 2018) for setting the polarization of the 0.9-mW 532-nm laser parallel and perpendicular to the grooves of the grating.
3. 1200 grooves/mm, 25-mm square ruled diffraction grating with blaze angle θ of $17^\circ 27'$ (Edmund Optics stock no. 43-005 for \$107.50 in 2018).
4. 25.0-mm diameter front-surface mirror (Edmund Optics stock no. 87-371 for \$80.00 in 2018).
5. UV-NIR silicon power photodetector (Edmund Optics stock no. 89-310 for \$795.00 in 2018).

The optomechanical components for this experiment are the following:

1. 5VDC regulated power supply (Thorlabs stock no. LDS5 for \$86.96 in 2018), 11-mm kinematic mount (Thorlabs stock no. MK11F for \$90.00 in 2018), 3" stainless-steel post (Edmund Optics stock no. 59-754 for \$10.25 in 2018), 3" post holder (Edmund Optics stock no. 58-979 for \$13.25 in 2018), 1/2" translation stage (Thorlabs stock no. MT1 for \$297.94 in 2018), and the base plate for the 1/2" translation stage (Thorlabs stock no. MT401 for \$23.66 in 2018) for the 0.9-mW 532-nm laser.
2. 25.0/25.4-mm kinematic circular optical mount (Edmund Optics stock no. 58-851 for \$99.00 in 2018), 3" stainless-steel post

(Edmund Optics stock no. 59-754 for \$10.25 in 2018), 3" post holder (Edmund Optics stock no. 58-979 for \$13.25 in 2018), and a 2"x3" slotted base plate (Edmund Optics stock no. 03-655 for \$15.00 in 2018) for the half-wave plate.

3. 25.0/25.4-mm square kinematic mount (Edmund Optics stock no. 58-857 for \$105.00 in 2018), 3" stainless-steel post (Edmund Optics stock no. 59-754 for \$10.25 in 2018), 3" post holder (Edmund Optics stock no. 58-979 for \$13.25 in 2018), 360° high-precision rotation mount (Thorlabs stock no. PR01 for \$331.50 in 2018), and a solid adaptor plate (Thorlabs stock no. PR01A for \$29.33 in 2018) for the 25-mm square ruled diffraction grating.
4. 25.0/25.4-mm kinematic circular optical mount (Edmund Optics stock no. 58-851 for \$99.00 in 2018), 3" stainless-steel post (Edmund Optics stock no. 59-754 for \$10.25 in 2018), 3" post holder (Edmund Optics stock no. 58-979 for \$13.25 in 2018), and a 2"x3" slotted base plate (Edmund Optics stock no. 03-655 for \$15.00 in 2018) for the 25.0-mm diameter plane mirror.
5. Power meter (Edmund Optics stock no. 89-305 for \$850.00 in 2018), adjustable-height V-clamp (Thorlabs stock no. VG100 for \$87.98 in 2018), 3" stainless-steel post (Edmund Optics stock no. 59-754 for \$10.25 in 2018), 3" post holder (Edmund Optics stock no. 58-979 for \$13.25 in 2018), and a 2"x3" slotted base plate (Edmund Optics stock no. 03-655 for \$15.00 in 2018) for the UV-NIR silicon power photodetector.

Figure 3.3 shows a schematic of experiment 3.3.

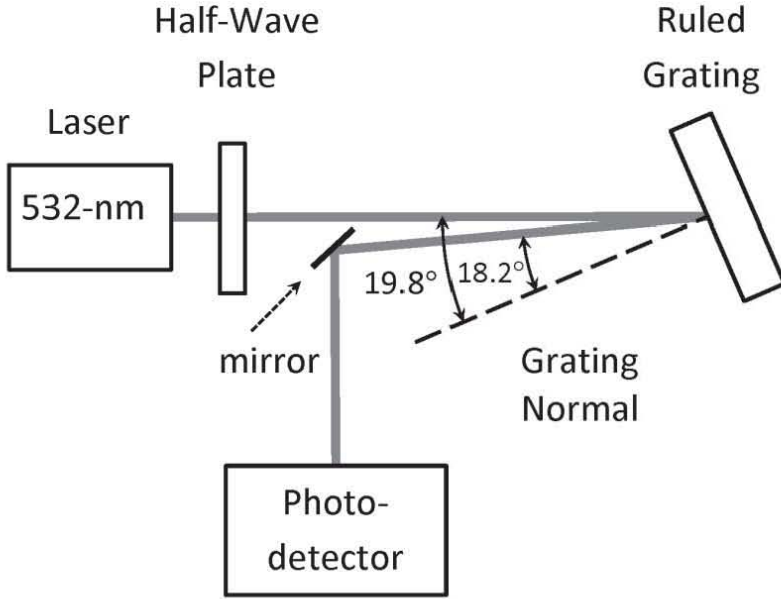


Figure 3.3 Schematic of experiment 3.3.

The schematic of experiment 3.3 is achieved through the following procedure:

1. The 0.9-mW 532-nm laser is attached to the 36"x12" breadboard using the 11-mm kinematic mount, 3" stainless-steel post, 3" post holder, $\frac{1}{2}$ " translation stage, and the base plate for the $\frac{1}{2}$ " translation stage.
2. The 0.9-mW 532-nm laser is adjusted so that the 3.5-mm diameter laser beam propagates parallel to the long edge of the breadboard at a fixed height of 6.5" above the 36"x12" breadboard.
3. The power of the 0.9-mW 532-nm laser is measured using the UV-NIR silicon power photodetector.
4. The half-wave plate is attached to the 36"x12" breadboard using the 25.0/25.4-mm kinematic circular optical mount, 3" stainless-steel post, 3" post holder, and 2"x3" slotted base plate.

5. The half-wave plate is adjusted so that the 3.5-mm diameter 532-nm laser beam is incident normally upon the center of the half-wave plate.
6. The half-wave plate is used to set the 532-nm laser polarization parallel or perpendicular to the grooves of the grating.
7. The ruled diffraction grating is attached to the 36"x12" breadboard using the 25.0/25.4-mm square kinematic mount, 3" stainless-steel post, 3" post holder, 360° high-precision rotation mount (Thorlabs stock no. PR01 for \$331.50 in 2018), and the solid adaptor plate (Thorlabs stock no. PR01A for \$29.33 in 2018).
8. The ruled diffraction grating is adjusted so that the zero-order ($m = 0$) diffracted beam is retro-reflected from the ruled grating.
9. The ruled diffraction grating is then rotated through an angle of 19° so that the 0.9-mW 532-nm laser beam is incident upon the grating at a 19° angle of incidence.
10. The plane mirror is attached to the 36"x12" breadboard using the 25/25.4-mm kinematic circular optical mount, 3" stainless-steel post, 3" post holder, and 2"x3" slotted base plate.
11. The plane mirror is adjusted to reflect the $m = -1$ diffracted order along the short edge of the 36"x12" breadboard.
12. The UV-NIR silicon power photodetector is attached to the 36"x12" breadboard using the adjustable-height V-clamp, 3" stainless-steel post, 3" post holder, and 2"x3" slotted base plate.
13. The UV-NIR silicon power photodetector is used to measure the power of the $m = -1$ diffracted order for laser polarization parallel and perpendicular to the grating grooves.

Experiment 3.4: A 632.8-nm He-Ne laser light is incident at an angle of incidence θ_i equal to 22° upon a 1200 grooves/mm, 25-mm square ruled diffraction grating with a blaze angle θ of $17^\circ 27'$. Determine the grating efficiency η for the light diffracted in the $m = -1$ order for incident laser light polarization parallel and perpendicular to the grating grooves.

The optical components for this experiment are the following:

1. 0.8-mW 632.8-nm He-Ne laser (Thorlabs stock no. HNLS008L for \$889.44 in 2018).
2. 25.4-mm diameter 632.8-nm half-wave plate (Edmund Optics stock no. 43-701 for \$430.00 in 2018) for setting the polarization of the 0.8-mW He-Ne laser parallel and perpendicular to the grooves of the grating.
3. 1200 grooves/mm, 25-mm square ruled diffraction grating with blaze angle θ of $17^\circ 27'$ (Edmund Optics stock no. 43-005 for \$107.50 in 2018).
4. 25.0-mm diameter front-surface mirror (Edmund Optics stock no. 87-371 for \$80.00 in 2018).
5. UV-NIR silicon power photodetector (Edmund Optics stock no. 89-310 for \$795.00 in 2018).

The optomechanical components for this experiment consist of the following:

1. 3" stainless-steel post (Edmund Optics stock no. 59-754 for \$10.25 in 2018), 3" post holder (Edmund Optics stock no. 58-979 for \$13.25 in 2018), $\frac{1}{2}$ " translation stage (Thorlabs stock no. MT1 for \$297.84 in 2018), and the base plate for the $\frac{1}{2}$ " translation stage (Thorlabs stock no. MT401 for \$23.66 in 2018) for the 0.8-mW 632.8-nm He-Ne laser.
2. 25/25.4-mm kinematic circular optical mount (Edmund Optics stock no. 58-851 for \$99.00 in 2018), 3" stainless-steel post (Edmund Optics stock no. 59-754 for \$10.25 in 2018), 3" post holder (Edmund Optics stock no. 58-979 for \$13.25 in 2018), and a 2"x3" slotted base plate (Edmund Optics stock no. 03-655 for \$15.00 in 2018) for the half-wave plate.
3. 25/25.4-mm square kinematic mount (Edmund Optics stock no. 58-857 for \$105.00 in 2018), 3" stainless-steel post (Edmund Optics stock no. 59-754 for \$10.25 in 2018), 3" post holder (Edmund Optics stock no. 58-979 for \$13.25 in 2018), 360° high-precision rotation mount (Thorlabs stock no. PR01 for \$301.50 in

- 2018), and a solid adaptor plate (Thorlabs stock no. PR01A for \$29.33 in 2018) for the 25-mm square ruled diffraction grating.
4. 25/25.4-mm kinematic circular optical mount (Edmund Optics stock no. 58-851 for \$99.00 in 2018), 3" stainless-steel post (Edmund Optics stock no. 59-754 for \$10.25 in 2018), 3" post holder (Edmund Optics stock no. 58-979 for \$13.25 in 2018), and a 2"x3" slotted base plate (Edmund Optics stock no. 03-655 for \$15.00 in 2018) for the 25.0-mm diameter plane mirror.
 5. Power meter (Edmund Optics stock no. 89-305 for \$850.00 in 2018), adjustable-height V-clamp (Thorlabs stock no. VG100 for \$87.98 in 2018), 3" stainless-steel post (Edmund Optics stock no. 59-754 for \$10.25 in 2018), 3" post holder (Edmund Optics stock no. 58-979 for \$13.25 in 2018), and a 2"x3" slotted base plate (Edmund Optics stock no. 03-655 for \$15.00 in 2018) for the UV-NIR silicon power photodetector.

Figure 3.4 shows a schematic of experiment 3.4.

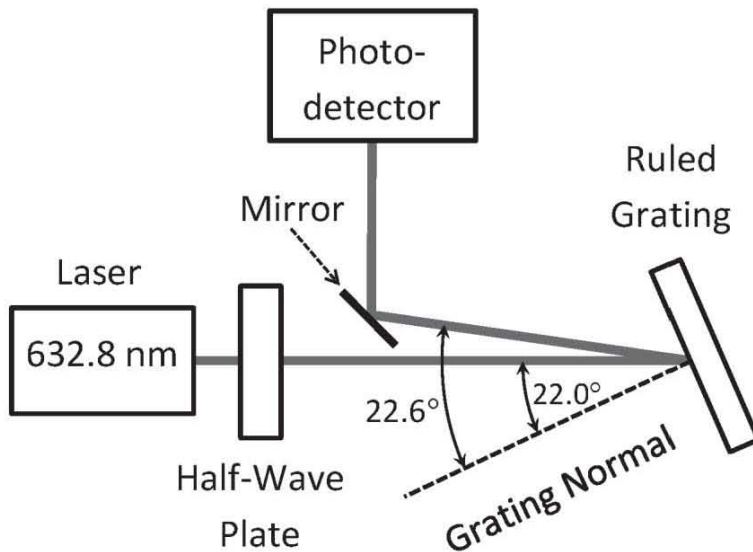


Figure 3.4 Schematic of experiment 3.4.

The schematic of experiment 3.4 is achieved through the following procedure:

1. The 0.8-mW 632.8-nm He-Ne laser is attached to the 36"x12" breadboard using the 3" stainless-steel post, 3" post holder, 1/2" translation stage, and the base plate for the 1/2" translation stage.
2. The 0.8-mW 632.8-nm He-Ne laser is adjusted so that the 0.48-mm diameter laser beam propagates parallel to the long edge of the 36"x12" breadboard at a fixed height of 6.5" above the 36"x12" breadboard.
3. The power of the 0.8-mW 632.8-nm He-Ne laser is measured using the UV-NIR silicon power photodetector.
4. The half-wave plate is attached to the 36"x12" breadboard using the 25/25.4-mm kinematic circular optical mount, 3" stainless-steel post, 3" post holder, and 2"x3" slotted base plate.
5. The half-wave plate is adjusted so that the 0.48-mm diameter 632.8-nm He-Ne laser beam is incident normally upon the center of the half-wave plate.
6. The half-wave plate is used to set the laser polarization parallel or perpendicular to the grooves of the grating.
7. The ruled diffraction grating is attached to the 36"x12" breadboard using the 25-mm square kinematic mount, 3" stainless-steel post, 3" post holder, 360° high-precision rotation mount, and the solid adaptor plate for the rotation mount.
8. The ruled diffraction grating is adjusted so that the zero-order ($m = 0$) diffracted beam is retro-reflected from the ruled grating.
9. The ruled grating is then rotated through an angle of 22° so that the laser beam is incident upon the grating at a 22° angle of incidence.
10. The plane mirror is attached to the 36"x12" breadboard using the 25/25.4-mm kinematic circular optical mount, 3" stainless-steel post, 3" post holder, and 2"x3" slotted base plate.
11. The plane mirror is adjusted to reflect the $m = -1$ diffracted order along the short edge of the 36"x12" breadboard.

12. The UV-NIR silicon power photodetector is attached to the 36"x12" breadboard using the adjustable-height V-clamp, 3" stainless-steel post, 3" post holder, and 2"x3" slotted base plate.
13. The UV-NIR silicon power photodetector is used to measure the power of the $m = -1$ diffracted order for laser polarization parallel and perpendicular to the grooves of the grating.

Experiment 3.5: A 532-nm laser light incident at an angle of incidence θ_i equal to 19° upon a 1200 grooves/mm, 25-mm square holographic grating. Determine the grating efficiency η for the light diffracted in the $m = -1$ order for incident light polarization parallel and perpendicular to the grooves of the grating.

The optical components for this experiment are the following:

1. 0.9-mW 532-nm laser (Thorlabs stock no. CPS532-C2 for \$162.18 in 2018).
2. 25.4-mm diameter, 532-nm quartz zero-order half-wave plate (Edmund Optics stock no. 43-697 for \$430.00 in 2018).
3. 1200-grooves/mm, 25-mm square holographic diffraction grating (Edmund Optics stock no. 43-216 for \$140.00 in 2018).
4. 25.0-mm diameter front-surface mirror (Edmund Optics stock no. 87-371 for \$80.00 in 2018).
5. UV-NIR silicon power photodetector (Edmund Optics stock no. 89-310 for \$795.00 in 2018).

The optomechanical components for this experiment consist of the following:

1. 5VDC regulated power supply (Thorlabs stock no. LDS5 for \$86.96 in 2018), 11-mm kinematic mount (Thorlabs stock no. MK11F for \$90.00 in 2018), 3" stainless-steel post (Edmund Optics stock no. 59-754 for \$10.25 in 2018), 3" post holder (Edmund Optics stock no. 58-979 for \$13.25 in 2018), 1/2" translation stage (Thorlabs stock no. MT1 for \$297.94 in 2018), and the base plate for the 1/2" translation stage (Thorlabs stock no. MT401 for \$23.66 in 2018) for the 0.9-mW 532-nm laser.

2. 25/25.4-mm kinematic circular optical mount (Edmund Optics stock no. 58-851 for \$99.00 in 2018), 3" stainless-steel post (Edmund Optics stock no. 59-754 for \$10.25 in 2018), 3" post holder (Edmund Optics stock no. 58-979 for \$13.25 in 2018), and a 2"x3" slotted base plate (Edmund Optics stock no. 03-655 for \$15.00 in 2018) for the half-wave plate.
3. 25-mm square kinematic mount (Edmund Optics stock no. 58-857 for \$105.00 in 2018), 3" stainless-steel post (Edmund Optics stock no. 59-754 for \$10.25 in 2018), 3" post holder (Edmund Optics stock no. 58-979 for \$13.25 in 2018), 360° high-precision rotation mount (Thorlabs stock no. PR01 for \$331.50 in 2018), and a solid adaptor plate (Thorlabs stock no. PR01A for \$29.33 in 2018) for the 25-mm square holographic grating.
4. 25/25.4-mm kinematic circular optical mount (Edmund Optics stock no. 58-851 for \$99.00 in 2018), 3" stainless-steel post (Edmund Optics stock no. 59-754 for \$10.25 in 2018), 3" post holder (Edmund Optics stock no. 58-979 for \$13.25 in 2018), and a 2"x3" slotted base plate (Edmund Optics stock no. 03-655 for \$15.00 in 2018) for the 25.0-mm diameter plane mirror.
5. Power meter (Edmund Optics stock no. 89-305 for \$850.00 in 2018), adjustable-height V-clamp (Thorlabs stock no. VG100 for \$87.98 in 2018), 3" stainless-steel post (Edmund Optics stock no. 59-754 for \$10.25 in 2018), 3" post holder (Edmund Optics stock no. 58-979 for \$13.25 in 2018), and a 2"x3" slotted base plate (Edmund Optics stock no. 03-655 for \$15.00 in 2018) for the UV-NIR silicon power photodetector.

Figure 3.5 shows a schematic of experiment 3.5.

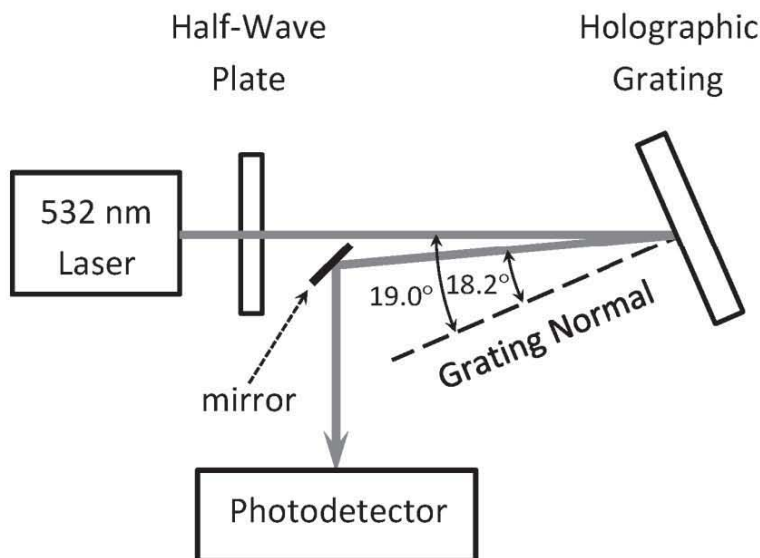


Figure 3.5 Schematic of experiment 3.5.

The schematic of experiment 3.5 is achieved through the following procedure:

1. The 0.9-mW 532-nm laser is attached to the 36"x12" breadboard using the 11-mm kinematic mount, 3" stainless-steel post, 3" post holder, ½" translation stage, and the base plate for the ½" translation stage.
2. The 0.9-mW 532-nm laser is adjusted so that the 3.5-mm diameter laser beam propagates parallel to the long edge of the breadboard at a fixed height of 6.5" above the breadboard.
3. The power of the 0.9-mW 532-nm laser is measured using the UV-NIR silicon power photodetector.
4. The half-wave plate is attached to the 36"x12" breadboard using the 25/25.4-mm kinematic circular optical mount, 3" stainless-steel post, 3" post holder, and 2"x3" slotted base plate.

5. The half-wave plate is adjusted so that the 3.5-mm diameter 532-nm laser beam is incident normally upon the center of the half-wave plate.
6. The half-wave plate is used to set the polarization of the 0.9-mW 532-nm laser parallel or perpendicular to the grooves of the grating.
7. The holographic grating is attached to the 36"x12" breadboard using the 25-mm square kinematic mount, 3" stainless-steel post, 3" post holder, 360° high-precision rotation mount, and the solid adaptor plate for the rotation mount.
8. The holographic grating is adjusted so that the zero-order ($m = 0$) diffracted beam is retro-reflected from the holographic grating.
9. The holographic grating is then rotated through an angle of 19° so that the laser beam is incident upon the grating at a 19° angle of incidence.
10. The plane mirror is attached to the 36"x12" breadboard using the 25/25.4-mm kinematic circular optical mount, 3" stainless-steel post, 3" post holder, and 2"x3" slotted base plate.
11. The plane mirror is adjusted to reflect the $m = -1$ diffracted order along the short edge of the 36"x12" breadboard.
12. The UV-NIR silicon power photodetector is attached to the 36"x12" bread board using the adjustable-height V-clamp, 3" stainless-steel post, 3" post holder, and 2"x3" slotted base plate.
13. The UV-NIR silicon power photodetector is used to measure the power of the $m = -1$ diffracted order for laser polarization parallel and perpendicular to the grooves of the grating.

Experiment 3.6: A 632.8-nm He-Ne laser light incident at an angle of incidence θ_i equal to 22° upon a 1200 grooves/mm, 25-mm square holographic grating. Determine the grating efficiency η for the laser light diffracted in the $m = -1$ order for incident light polarization parallel and perpendicular to the grooves of the grating.

The optical components for this experiment are the following:

1. 0.8-mW 632.8-nm He-Ne laser (Thorlabs stock no. HNLS008L for \$889.44 in 2018).
2. 25.4-mm diameter 632.8-nm zero-order half-wave plate (Edmund Optics stock no. 43-701 for \$430.00 in 2018).
3. 1200 grooves/mm, 25-mm square holographic diffraction grating (Edmund Optics stock no. 43-216 for \$140.00 in 2018).
4. 25.0-mm diameter front-surface mirror (Edmund Optics stock no. 87-371 for \$80.00 in 2018).
5. UV-NIR silicon power photodetector (Edmund Optics stock no. 89-310 for \$795.00 in 2018).

The optomechanical and other components for this experiment are the following:

1. 3" stainless-steel post (Edmund Optics stock no. 59-754 for \$10.25 in 2018), 3" post holder (Edmund Optics stock no. 58-979 for \$13.25 in 2018), $\frac{1}{2}$ " translation stage (Thorlabs stock no. MT1 for \$297.84 in 2018), and the base plate for the $\frac{1}{2}$ " translation stage (Thorlabs stock no. MT401 for \$23.66 in 2018) for the 0.8-mW 632.8-nm He-Ne laser.
2. 25/25.4-mm kinematic circular optical mount (Edmund Optics stock no. 58-851 for \$99.00 in 2018), 3" stainless-steel post (Edmund Optics stock no. 59-754 for \$10.25 in 2018), 3" post holder (Edmund Optics stock no. 58-979 for \$13.25 in 2018), and a 2"x3" slotted base plate (Edmund Optics stock no. 03-655 for \$15.00 in 2018) for the half-wave plate.
3. 25-mm square kinematic mount (Edmund Optics stock no. 58-857 for \$105.00 in 2018), 3" stainless-steel post (Edmund Optics stock no. 59-754 for \$10.25 in 2018), 3" post holder (Edmund Optics stock no. 58-979 for \$13.25 in 2018), 360° high-precision rotation mount (Thorlabs stock no. PR01 for \$331.50 in 2018), and a solid adaptor plate (Thorlabs stock no. PR01A for \$29.33 in 2018) for the 25-mm square holographic diffraction grating.

4. 25/25.4-mm kinematic circular optical mount (Edmund Optics stock no. 58-851 for \$99.00 in 2018), 3" stainless-steel post (Edmund Optics stock no. 59-754 for \$10.25 in 2018), 3" post holder (Edmund Optics stock no. 58-979 for \$13.25 in 2018), and a 2"x3" slotted base plate (Edmund Optics stock no. 03-655 for \$15.00 in 2018) for the 25.0-mm diameter plane mirror.
5. Power meter (Edmund Optics stock no. 89-305 for \$850.00 in 2018), adjustable-height V-clamp (Thorlabs stock no. VG100 for \$87.98 in 2018), 3" stainless-steel post (Edmund Optics stock no. 59-754 for \$10.25 in 2018), 3" post holder (Edmund Optics stock no. 58-979 for \$13.25 in 2018), and a 2"x3" slotted base plate (Edmund Optics stock no. 03-655 for \$15.00 in 2018) for the UV-NIR silicon power photodetector.

Figure 3.6 shows a schematic of experiment 3.6.

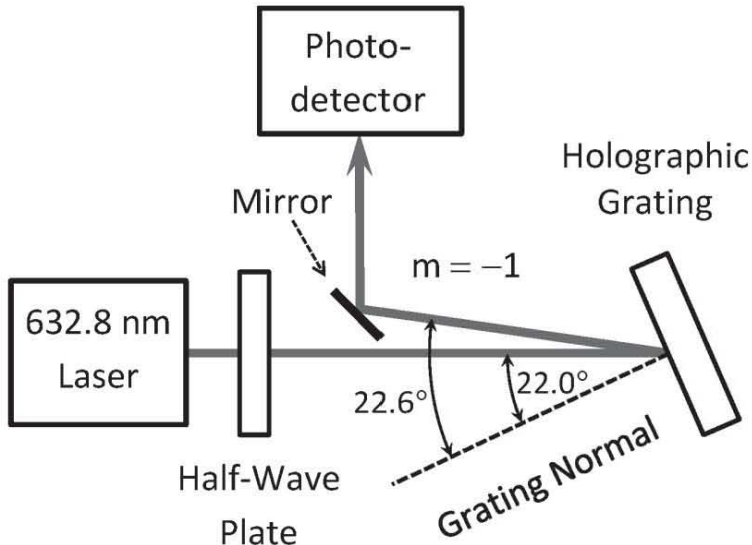


Figure 3.6 Schematic of experiment 3.6.

The schematic of experiment 3.6 is achieved through the following procedure:

1. The 0.8-mW 632.8-nm He-Ne laser is attached to the 36"x12" breadboard using the 3" stainless-steel post, 3" post holder, 1/2" translation stage, and the base plate for the 1/2" translation stage.
2. The 0.8-mW 632.8-nm He-Ne laser is adjusted so that the 0.48-mm diameter laser beam propagates parallel to the long edge of the 36"x12" breadboard at a fixed height of 6.5" above the breadboard.
3. The half-wave plate is attached to the 36"x12" breadboard using the 25/25.4-mm kinematic circular optical mount, 3" stainless-steel post, 3" post holder, and 2"x3" slotted base plate.
4. The half-wave plate is adjusted so that the 0.48-mm diameter 632.8-nm He-Ne laser beam is incident normally upon the center of the half-wave plate.
5. The half-wave plate is used to set the laser polarization parallel or perpendicular to the grooves of the grating.
6. The holographic grating is attached to the 36"x12" breadboard using the 25-mm square kinematic mount, 3" stainless-steel post, 3" post holder, 360° high-precision rotation mount, and the solid adaptor plate for the rotation mount.
7. The holographic grating is adjusted so that the zero-order ($m = 0$) diffracted beam is retro-reflected from the holographic grating.
8. The holographic grating is then rotated through an angle of 22° so that the 632.8-nm He-Ne laser beam is incident upon the grating at a 22° angle of incidence.
9. The plane mirror is attached to the 36"x12" breadboard using the 25/25.4-mm kinematic circular optical mount, 3" stainless-steel post, 3" post holder, and 2"x3" slotted base plate.
10. The plane mirror is adjusted to reflect the $m = -1$ diffracted order along the short edge of the 36"x12" breadboard.
11. The UV-NIR silicon power photodetector is attached to the 36"x12" breadboard using the adjustable-height V-clamp, 3" stainless-steel post, 3" post holder, and 2"x3" slotted base plate.

12. The UV-NIR silicon power photodetector is used to measure the power of the $m = -1$ diffracted order for the 632.8-nm He-Ne laser beam polarization parallel and perpendicular to the grooves of the grating.

CHAPTER 4

POLARIZERS

4.1 Malus' law

Malus' law gives the transmittance of an ideal polarizer for linearly polarized light as

$$T = (\cos\theta)^2 \quad (4.1)$$

where θ is the angle of the linear polarizer with that of the linear polarization of light.

Experiment 4.1: A 632.8-nm, linearly-polarized He-Ne laser light is incident upon a linear polarizer with a transmittance of 84% for linearly polarized light. Determine the transmittance of the linear polarizer for θ equal to 45° .

The optical components for this experiment are the following:

1. 0.8-mW 632.8-nm He-Ne laser (Thorlabs stock no. HNLS008L for \$889.44 in 2018).
2. 25.0-mm diameter high-contrast glass linear polarizer (Edmund Optics stock no. 47-216 for \$160.00 each in 2018).
3. UV-NIR silicon power photodetector (Edmund Optics stock no. 89-310 for \$795.00 in 2018).

The optomechanical and other components for this experiment are the following:

1. 3" stainless-steel post (Edmund Optics stock no. 59-754 for \$10.25 in 2018), 3" post holder (Edmund Optics stock no. 58-979 for \$13.25 in 2018), $\frac{1}{2}$ " translation stage (Thorlabs stock no. MT1 for \$297.84 in 2018), and the base plate for the $\frac{1}{2}$ " translation stage (Thorlabs stock no. MT401 for \$23.66 in 2018) for the 0.8-mW 632.8-nm He-Ne laser.

2. 25/25.4-mm diameter kinematic circular optical mount (Edmund Optics stock no. 58-851 for \$99.00 in 2018), 3" stainless-steel post (Edmund Optics stock no. 59-754 for \$10.25 in 2018), 3" post holder (Edmund Optics stock no. 58-979 for \$13.25 in 2018), and a 2"x3" slotted base plate (Edmund Optics stock no. 03-655 for \$15.00 in 2018) for the glass linear polarizer.
3. Power meter (Edmund Optics stock no. 89-305 for \$850.00 in 2018), adjustable-height V-clamp (Thorlabs stock no. VG100 for \$87.98 in 2018), 3" stainless-steel post (Edmund Optics stock no. 59-754 for \$10.25 in 2018), 3" post holder (Edmund Optics stock no. 58-979 for \$13.25 in 2018), and a 2"x3" slotted base plate (Edmund Optics stock no. 03-655 for \$15.00 in 2018) for the UV-NIR silicon power photodetector.

Figure 4.1 shows a schematic of experiment 4.1.

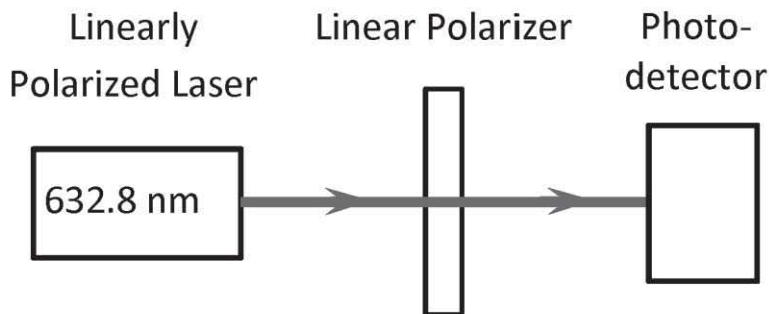


Figure 4.1 Schematic of experiment 4.1.

The schematic of experiment 4.1 is achieved through the following procedure:

1. The 0.8-mW 632.8-nm He-Ne laser is attached to the 36"x12" breadboard using the 3" stainless-steel post, 3" post holder, and $\frac{1}{2}$ " translation stage, and the base plate for the $\frac{1}{2}$ " translation stage.
2. The 0.8-mW 632.8-nm He-Ne laser is adjusted so that the 0.48-mm diameter laser beam propagates parallel to the long edge of the 36"x12" breadboard at a fixed height of 6.5" above the breadboard.

3. The linear polarizer is attached to the 36"x12" breadboard using the 25/25.4-mm kinematic circular optical mount, 3" stainless-steel post, 3" post holder, and 2"x3" slotted base plate.
4. The linear polarizer is adjusted so that the 0.48-mm diameter 632.8-nm He-Ne laser beam is incident normally upon the center of the linear polarizer.
5. The UV-NIR silicon power photodetector is attached to the 36"x12" breadboard using the adjustable-height V-clamp, 3" stainless-steel post, 3" post holder, and 2"x3" slotted base plate.
6. The power of the 632.8-nm He-Ne laser beam is measured using the UV-NIR silicon power photodetector.
7. The transmission axis of the linear polarizer is set at 45° with respect to the polarization of the 0.8-mW 632.8-nm He-Ne laser beam.
8. The power of the 0.8-mW 632.8-nm He-Ne laser beam transmitted through the linear polarizer is measured with the UV-NIR silicon power photodetector to determine the transmittance of the linear polarizer at 45°.

4.2 Wollaston polarizer

Wollaston polarizers separate an unpolarized light beam into two orthogonal, linearly polarized light beams that leave the polarizer through the exit port with a divergence angle of δ . A Wollaston calcite prism linear polarizer consists of two right-angled calcite prisms, which are cemented together. The optic axes of the two prisms are orthogonal to each other.

Experiment 4.2: A 632.8-nm He-Ne polarized laser beam is incident upon a calcite Wollaston linear polarizer. Determine the divergence angle δ between the two orthogonal linearly polarized O- and E-beams.

The optical components for this experiment are the following:

1. 0.8-mW 632.8-nm He-Ne laser (Thorlabs stock no. HNLS008L for \$889.44 in 2018).
2. 632.8-nm 25-mm diameter half-wave plate (Edmund Optics stock no. 43-701 for \$430.00 in 2018).

3. Calcite Wollaston polarizer (Edmund Optics stock no. 68-821 for \$570.00 in 2018).

The optomechanical components for this experiment are the following:

1. 3" stainless-steel post (Edmund Optics stock no. 59-754 for \$10.25 in 2018), 3" post holder (Edmund Optics stock no. 58-979 for \$13.25 in 2018), $\frac{1}{2}$ " translation stage (Thorlabs stock no. MT1 for \$297.84 in 2018), and the base plate for the $\frac{1}{2}$ " translation stage (Thorlabs stock no. MT401 for \$23.66 in 2018) for the 0.8-mW 632.8-nm He-Ne laser.
2. 25/25.4-mm kinematic circular optical mount (Edmund Optics stock no. 58-851 for \$99.00 in 2018), 3" stainless-steel post (Edmund Optics stock no. 59-754 for \$10.25 in 2018), 3" post holder (Edmund Optics stock no. 58-979 for \$13.25 in 2018), and a 2"x3" slotted base plate (Edmund Optics stock no. 03-655 for \$15.00 in 2018) for the 632.8-nm half-wave plate.
3. 25.4-mm diameter polarizer mount (Edmund Optics stock no. 55-010 for \$165.00 in 2018), 3" stainless-steel post (Edmund Optics stock no. 59-754 for \$10.25 in 2018), 3" post holder (Edmund Optics stock no. 58-979 for \$13.25 in 2018), and a 2"x3" slotted base plate (Edmund Optics stock no. 03-655 for \$15.00 in 2018) for the calcite Wollaston polarizer.

Figure 4.2 shows a schematic of experiment 4.2.

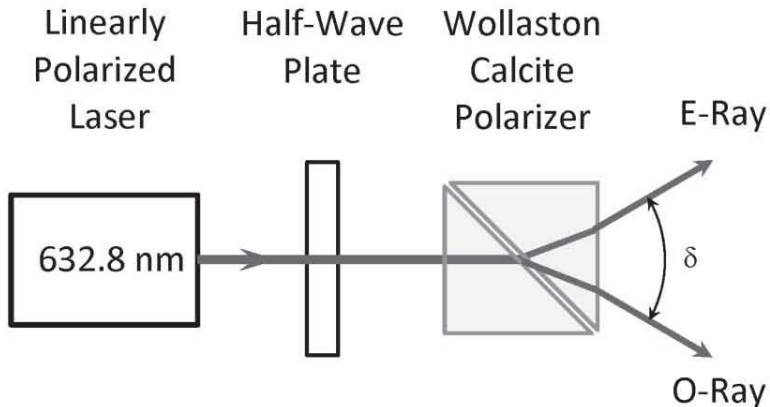


Figure 4.2 Schematic of experiment 4.2.

The schematic of experiment 4.2 is achieved through the following procedure:

1. The 0.8-mW 632.8-nm He-Ne laser is attached to the 36"x12" breadboard using the 3" stainless-steel post, 3" post holder, and $\frac{1}{2}$ " translation stage, and the base plate for the $\frac{1}{2}$ " translation stage.
2. The 0.8-mW 632.8-nm He-Ne laser is adjusted so that the 0.48-mm diameter 632.8-nm He-Ne laser beam propagates parallel to the long edge of the 36"x12" breadboard at a fixed height of 6.5" above the breadboard.
3. The 632.8-nm half-wave plate is attached to the 36"x12" breadboard using the 25/25.4-mm kinematic circular optical mount, 3" stainless-steel post, 3" post holder, and 2"x3" slotted base plate.
4. The 632.8-nm half-wave plate is adjusted so that the 0.8-mW 632.8-nm He-Ne laser beam is incident at a zero angle of incidence upon the half-wave plate.
5. The 632.8-nm half-wave is set to rotate the polarization of the 0.8-mW 632.8-nm He-Ne laser beam through an angle of 45° .
6. The calcite Wollaston polarizer is attached to the 36"x12" breadboard using the 25.4-mm diameter polarizer mount, 3" stainless-steel post, 3" post holder, and 2"x3" slotted base plate.
7. The calcite Wollaston polarizer is adjusted so that the 0.8-mW 632.8-nm He-Ne laser beam transmitted through the half-wave plate is incident at a zero angle of incidence upon the calcite Wollaston polarizer.
8. The calcite Wollaston polarizer produces two orthogonally polarized O- and E-beams with a divergence angle δ , which is measured.

4.3 Rochon polarizer

Rochon polarizer is similar to the Wollaston polarizer except that the optic axis in the first prism is parallel to the length of the polarizer. Therefore, the O-beam propagates through the Rochon polarizer without any

deviation. However, the E-beam suffers the same deviation as in the Wollaston polarizer.

Experiment 4.3: A 632.8-nm He-Ne polarized laser beam is incident upon a quartz Rochon polarizer. Determine the divergence angle δ between the orthogonal linearly polarized O- and E-beams.

The optical components for this experiment are the following:

1. 0.8-mW 632.8-nm He-Ne laser (Thorlabs stock no. HNLS008L for \$889.44 in 2018).
2. 632.8-nm 25-mm diameter half-wave plate (Edmund Optics stock no. 43-701 for \$430.00 in 2018).
3. Quartz Rochon polarizer (Edmund Optics stock no. 68-824 for \$685.00 in 2018).

The optomechanical components for this experiment are the following:

1. 3" stainless-steel post (Edmund Optics stock no. 59-754 for \$10.25 in 2018), 3" post holder (Edmund Optics stock no. 58-979 for \$13.25 in 2018), $\frac{1}{2}$ " translation stage (Thorlabs stock no. MT1 for \$297.84 in 2018), and the base plate for the $\frac{1}{2}$ " translation stage (Thorlabs stock no. MT401 for \$23.66 in 2018) for the 0.8-mW 632.8-nm He-Ne laser.
2. 25/25.4-mm kinematic circular optical mount (Edmund Optics stock no. 58-851 for \$99.00 in 2018), 3" stainless-steel post (Edmund Optics stock no. 59-754 for \$10.25 in 2018), 3" post holder (Edmund Optics stock no. 58-979 for \$13.25 in 2018), and a 2"x3" slotted base plate (Edmund Optics stock no. 03-655 for \$15.00 in 2018) for the 632.8-nm half-wave plate.
3. 25.4-mm diameter polarizer mount (Edmund Optics stock no. 55-010 for \$165.00 in 2018), 3" stainless-steel post (Edmund Optics stock no. 59-754 for \$10.25 in 2018), 3" post holder (Edmund Optics stock no. 58-979 for \$13.25 in 2018), and a 2"x3" slotted base plate (Edmund Optics stock no. 03-655 for \$15.00 in 2018) for the quartz Rochon polarizer.

Figure 4.3 shows a schematic of experiment 4.3.

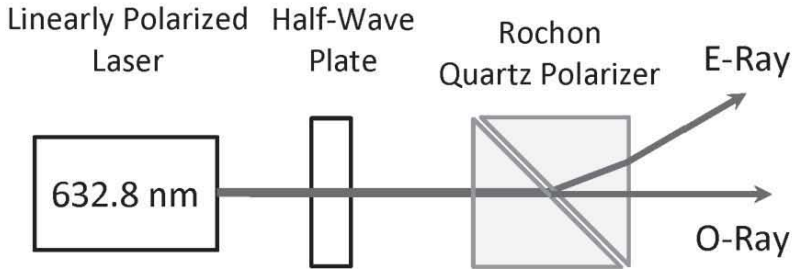


Figure 4.3 Schematic of experiment 4.3.

The schematic of experiment 4.3 is achieved through the following procedure:

1. The 0.8-mW 632.8-nm He-Ne laser is attached to the 36"x12" breadboard using the 3" stainless-steel post, 3" post holder, $\frac{1}{2}$ " translation stage, and the base plate for the $\frac{1}{2}$ " translation stage.
2. The 0.8-mW 632.8-nm He-Ne laser is adjusted so that the 0.48-mm diameter 632.8-nm He-Ne laser beam propagates parallel to the long edge of the 36"x12" breadboard at a fixed height of 6.5" above the 36"x12" breadboard.
3. The 632.8-nm half-wave plate is attached to the 36"x12" breadboard using the 25/25.4-mm kinematic circular optical mount, 3" stainless-steel post, 3" post holder, and 2"x3" slotted base plate.
4. The 632.8-nm half-wave plate is adjusted so that the 632.8-nm laser beam is incident at a zero angle of incidence upon the 632.8-nm half-wave plate.
5. The 632.8-nm half-wave is set to rotate the polarization of the 0.8-mW 632.8-nm He-Ne laser beam through an angle of 45° .
6. The quartz Rochon polarizer is attached to the 36"x12" breadboard using the 25.4-mm diameter polarizer mount, 3" stainless-steel post, 3" post holder, and 2"x3" slotted base plate.
7. The quartz Rochon polarizer is adjusted so that the 0.8-mW 632.8-nm He-Ne laser beam transmitted through the half-wave plate is incident at a zero angle of incidence upon the quartz Rochon polarizer.

8. The quartz Rochon polarizer produces two orthogonally polarized O- and E-beams with a divergence angle δ , which is measured.

4.4 Brewster window polarizer

When unpolarized light is incident upon an uncoated surface of a dielectric window at the Brewster angle, the reflectance for light with an **E**-field in the plane of incidence (TM polarization) is zero and the reflectance for light with an **E**-field perpendicular to the plane of incidence (TE polarization) is finite.

Experiment 4.4: A 632.8-nm He-Ne laser beam is incident upon a fused silica Brewster window. The He-Ne laser beam is polarized at 45° to the plane of incidence. Determine the reflectance R of the TE-polarized beam and the transmittance T of the partially polarized beam.

The optical components for this experiment are the following:

1. 0.8-mW 632.8-nm He-Ne laser (Thorlabs stock no. HNLS008L for \$889.44 in 2018).
2. 6328-nm, 25-mm diameter half-wave plate (Edmund Optics stock no. 43-701 for \$430.00 in 2018).
3. 25-mm diameter, 2.0-mm thick fused silica Brewster window (Edmund Optics stock no. 65-825 for \$120.00 in 2018).
4. UV-NIR silicon power photodetector (Edmund Optics stock no. 89-310 for \$795.00 in 2018).

The optomechanical and other components for this experiment are the following:

1. 3" stainless-steel post (Edmund Optics stock no. 59-754 for \$10.25 in 2018), 3" post holder (Edmund Optics stock no. 58-979 for \$13.25 in 2018), $\frac{1}{2}$ " translation stage (Thorlabs stock no. MT1 for \$297.84 in 2018), and the base plate for the $\frac{1}{2}$ " translation stage (Thorlabs stock no. MT401 for \$23.66 in 2018) for the 0.8-mW 632.8-nm He-Ne laser.
2. 25/25.4-mm kinematic circular optical mount (Edmund Optics stock no. 58-851 for \$99.00 in 2018), 3" stainless-steel post (Edmund Optics stock no. 59-754 for \$10.25 in 2018), 3" post holder (Edmund Optics stock no. 58-979 for \$13.25 in 2018), and

- a 2"x3" slotted base plate (Edmund Optics stock no. 03-655 for \$15.00 in 2018) for the half-wave plate.
3. 25/25.4-mm kinematic circular optical mount (Edmund Optics stock no. 58-851 for \$99.00 in 2018), 3" stainless-steel post (Edmund Optics stock no. 59-754 for \$10.25 in 2018), 3" post holder (Edmund Optics stock no. 58-979 for \$13.25 in 2018), and a 2"x3" slotted base plate (Edmund Optics stock no. 03-655 for \$15.00 in 2018) for the fused silica Brewster window.
 4. Power meter (Edmund Optics stock no. 89-305 for \$850.00 in 2018), adjustable-height V-clamp (Thorlabs stock no. VG100 for \$87.98 in 2018), 3" stainless-steel post (Edmund Optics stock no. 59-754 for \$10.25 in 2018), 3" post holder (Edmund Optics stock no. 58-979 for \$13.25 in 2018), and a 2"x3" slotted base plate (Edmund Optics stock no. 03-655 for \$15.00 in 2018) for the UV-NIR photodetector.

Figure 4.4 shows a schematic of experiment 4.4.

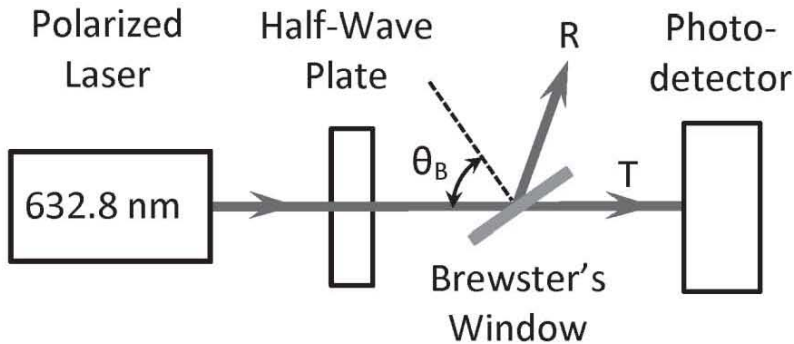


Figure 4.4 Schematic of experiment 4.4.

The schematic of experiment 4.4 is achieved through the following procedure:

1. The 0.8-mW 632.8-nm He-Ne laser is attached to the 36"x12" breadboard using the 3" stainless-steel post, 3" post holder, $\frac{1}{2}$ " translation stage, and the base plate for the $\frac{1}{2}$ " translation stage.
2. The 0.8mW 632.8-nm He-Ne laser is adjusted so that the 0.48-mm diameter 632.8-nm laser beam propagates parallel to the long

edge of the 36"x12" breadboard at a fixed height of 6.5" above the breadboard.

3. The power of the 0.8-mW 632.8-nm He-Ne laser beam is measured using the UV-NIR silicon power photodetector.
4. The 632.8-nm half-wave plate is attached to the 36"x12" breadboard using the 25/25.4-mm kinematic circular optical mount, 3" stainless-steel post, 3" post holder, and 2"x3" slotted base plate.
5. The 632.8-nm half-wave plate is adjusted so that the 0.8-mW 632.8-nm He-Ne laser beam is incident at a zero angle of incidence upon the half-wave plate.
6. The 632.8-nm half-wave plate is set to rotate the polarization of the 0.8-mW 632.8-nm He-Ne laser beam through an angle of 45°.
7. The fused silica Brewster window is attached to the 36"x12" breadboard using the 25/25.4-mm kinematic circular optical mount, 3" stainless-steel post, 3" post holder, and 2"x3" slotted base plate.
8. The fused silica Brewster window is adjusted so that the 632.8-nm laser beam transmitted through the 632.8-nm half-wave plate is incident at the Brewster angle of ~56° upon the fused silica Brewster window.
9. The UV-NIR silicon power photodetector is attached to the 36"x12" breadboard using the adjustable-height V-clamp, 3" stainless-steel post, 3" post holder, and 2"x3" slotted base plate.
10. The power of the partially-polarized transmitted beam is measured to determine the value of T for the fused silica Brewster window using the UV-NIR silicon power photodetector.
11. The UV-NIR silicon power photodetector is relocated to measure the power of the TE-polarized reflected beam to determine the value of R for the fused silica Brewster window.

4.5 Wire-grid polarizer

A wire-grid polarizer consists of many thin metal wires on a substrate. Light polarized along the direction of these wires (TE polarization) is reflected while light polarized perpendicular to these wires (TM polarization) is transmitted.

Experiment 4.5: A 632.8-nm, linearly-polarized He-Ne laser beam is incident upon a wire-grid polarizer for the 420-700-nm wavelength range. Determine the maximum transmittance of the wire-grid polarizer.

The optical components for this experiment are the following:

1. 0.8-mW 632.8-nm He-Ne laser (Thorlabs stock no. HNLS008L for \$889.44 in 2018).
2. 25-mm diameter wire-grid polarizer (Edmund Optics stock no. 34-318 for \$499.00 in 2018).
3. UV-NIR silicon power photodetector (Edmund Optics stock no. 89-310 for \$795.00 in 2018).

The optomechanical and other components for this experiment are the following:

1. 3" stainless-steel post (Edmund Optics stock no. 59-754 for \$10.25 in 2018), 3" post holder (Edmund Optics stock no. 58-979 for \$13.25 in 2018), $\frac{1}{2}$ " translation stage (Thorlabs stock no. MT1 for \$297.84 in 2018), and the base plate for the $\frac{1}{2}$ " translation stage (Thorlabs stock no. MT401 for \$23.66 in 2018) for the 0.8-mW 632.8-nm He-Ne laser.
2. 25/25.4-mm kinematic circular optical mount (Edmund Optics stock no. 58-851 for \$99.00 in 2018), 3" stainless-steel post (Edmund Optics stock no. 59-754 for \$10.25 in 2018), 3" post holder (Edmund Optics stock no. 58-979 for \$13.25 in 2018), and a 2"x3" slotted base plate (Edmund Optics stock no. 03-655 for \$15.00 in 2018) for the wire-grid polarizer.
3. Power meter (Edmund Optics stock no. 89-305 for \$850.00 in 2018), adjustable-height V-clamp (Thorlabs stock no. VG100 for \$87.98 in 2018), 3" stainless-steel post (Edmund Optics stock no. 59-754 for \$10.25 in 2018), 3" post holder (Edmund Optics stock no. 58-979 for \$13.25 in 2018), and a 2"x3" slotted base plate

(Edmund Optics stock no. 03-655 for \$15.00 in 2018) for the UV-NIR silicon power photodetector.

Figure 4.5 shows a schematic of experiment 4.5.

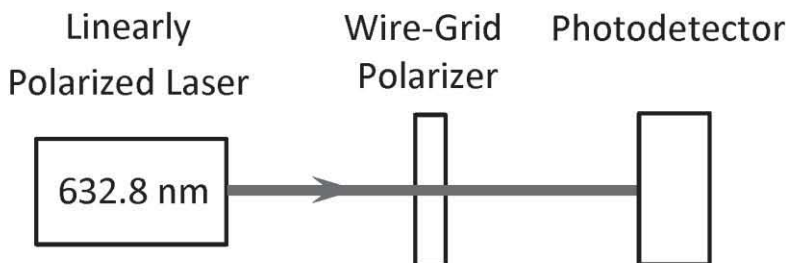


Figure 4.5 Schematic of experiment 4.5.

The schematic of experiment 4.5 is achieved through the following procedure:

1. The 0.8-mW 632.8-nm He-Ne laser is attached to the 36"x12" breadboard using the 3" stainless-steel post, 3" post holder, ½" translation stage, and the base plate for the ½" translation stage.
2. The 0.8-mW 632.8-nm He-Ne laser is adjusted so that the 0.48-mm diameter 632.8-nm laser beam propagates parallel to the long edge of the breadboard at a fixed height of 6.5" above the breadboard.
3. The power of the 0.8-mW 632.8-nm laser beam is measured using the UV-NIR silicon power photodetector.
4. The wire-grid polarizer is attached to the 36"x12" breadboard using the 25/25.4-mm kinematic circular optical mount, 3" stainless-steel post, 3" post holder, and 2"x3" slotted base plate.
5. The wire-grid polarizer is adjusted so that the 0.8-mW 632.8-nm He-Ne laser beam is incident at a zero angle of incidence upon the wire-grid polarizer.
6. The UV-NIR silicon power photodetector is attached to the 36"x12" breadboard using the adjustable-height V-clamp, 3" stainless-steel post, 3" post holder, and 2"x3" slotted base plate.

7. The 0.8-mW 632.8-nm He-Ne laser beam transmitted by the wire-grid polarizer is incident upon the UV-NIR silicon power photodetector.
8. The UV-NIR silicon power photodetector is adjusted so that the 0.8-mW 632.8-nm He-Ne laser beam transmitted by the wire-grid polarizer is centered upon the UV-NIR silicon power photodetector.
9. The wire-grid polarizer is rotated to maximize the signal of the UV-NIR silicon power photodetector.
10. The ratio of the maximum power of the 0.8-mW 632.8-nm He-Ne laser beam transmitted by the wire-grid polarizer and the power of the 0.8-mW 632.8-nm He-Ne laser beam is a measure of the maximum transmittance of the wire-grid polarizer at 632.8 nm.

CHAPTER 5

OPTICAL WINDOWS

5.1 External Transmittance

The external transmittance T_E of a plane parallel window with a negligible absorption coefficient α for a normal incidence of light is given by

$$T_E = \frac{1-R}{1+R} \quad (5.1)$$

where R is the single-surface reflectance.

Experiment 5.1: Measure the external transmittance T_E of an uncoated UV grade fused silica window using a 632.8-nm He-Ne laser. Determine the value of the single-surface reflectance R using the measured value of T_E .

The optical components for this experiment are the following:

1. 0.8-mW 632.8-nm He-Ne laser (Thorlabs stock no. HNLS008L for \$889.44 in 2018).
2. 25.0-mm diameter, 3.0-mm thick uncoated UV grade fused silica window (Edmund Optics stock no.47-195 for \$105.00 in 2018).
3. UV-NIR silicon power photodetector (Edmund Optics stock no. 89-310 for \$795.00 in 2018).

The optomechanical and other components for this experiment are the following:

1. 3" stainless-steel post (Edmund Optics stock no. 59-754 for \$10.25 in 2018), 3" post holder (Edmund Optics stock no. 58-979 for \$13.25 in 2018), $\frac{1}{2}$ " translation stage (Thorlabs stock no. MT1 for \$297.84 in 2018), and a base plate for the $\frac{1}{2}$ " translation stage (Thorlabs stock no. MT401 for \$23.66 in 2018) for the 0.8-mW 632.8-nm He-Ne laser.

2. 25/25.4-mm kinematic circular optical mount (Edmund Optics stock no. 58-851 for \$99.00 in 2018), 3" stainless-steel post (Edmund Optics stock no. 59-754 for \$10.25 in 2018), 3" post holder (Edmund Optics stock no. 58-979 for \$13.25 in 2018), and a 2"x3" slotted base plate (Edmund Optics stock no. 03-655 for \$15.00 in 2018) for the fused silica window.
3. Power meter (Edmund Optics stock no. 89-305 for \$850.00 in 2018), adjustable-height V-clamp (Thorlabs stock no. VG100 for \$87.98 in 2018), 3" stainless-steel post (Edmund Optics stock no. 59-754 for \$10.25 in 2018), 3" post holder (Edmund Optics stock no. 58-979 for \$13.25 in 2018), and a 2"x3" slotted base plate (Edmund Optics stock no. 03-655 for \$15.00 in 2018) for the UV-NIR silicon power photodetector.

Figure 5.1 shows a schematic of experiment 5.1.

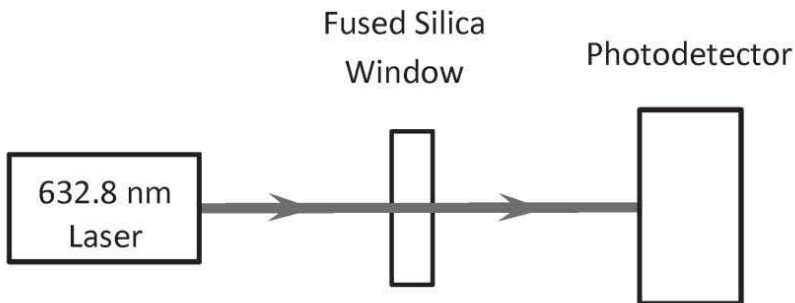


Figure 5.1 Schematic of experiment 5.1.

The schematic of experiment 5.1 is achieved through the following procedure:

1. The 0.8-mW 632.8-nm He-Ne laser is attached to the 36"x12" breadboard using the 3" stainless-steel post, 3" post holder, and 1/2" translation stage, and the base plate for the 1/2" translation stage.
2. The 0.8-mW 632.8-nm He-Ne laser is adjusted so that the 0.48-mm diameter 632.8-nm He-Ne laser beam propagates parallel to the long edge of the 36"x12" breadboard at a fixed height of 6.5" above the 36"x12" breadboard.

3. The power of the 0.8-mW 632.8-nm He-Ne laser beam is measured using the UV-NIR silicon power photodetector.
4. The fused silica window is attached to the 36"x12" breadboard using the 25/25.4-mm kinematic circular optical mount, 3" stainless-steel post, 3" post holder, and 2"x3" slotted base plate.
5. The fused silica window is adjusted so that the 0.8-mW 632.8-nm laser beam is incident upon the center of the fused silica window at a zero angle of incidence.
6. The UV-NIR silicon power photodetector is attached to the 36"x12" breadboard using the adjustable-height V-clamp, 3" stainless-steel post, 3" post holder, and 2"x3" slotted base plate.
7. The power of the 0.8-mW 632.8-nm He-Ne laser beam transmitted by the fused silica window is measured using the UV-NIR silicon power photodetector.
8. The ratio of the power of the 0.8-mW 632.8-nm He-Ne laser beam transmitted by the fused silica window and the power of the 0.8-mW 632.8-nm He-Ne laser beam is a measure of the external transmittance T_E of the fused silica window.

5.2 Single-surface reflectance

The single-surface reflectance R of a window for a near-normal incidence of light is given by

$$R \approx \frac{(n-1)^2 + \kappa^2}{(n+1)^2 + \kappa^2} \quad (5.2)$$

where n and k are the optical constants of the window material.

Experiment 5.2: Measure the single-surface reflectance R of a germanium window for a 5° angle of incidence at 632.8 nm. Determine the value of the refractive index n of germanium using the measured value of R .

The optical components for this experiment are the following:

1. 0.8-mW 632.8-nm He-Ne laser (Thorlabs stock no. HNLS008L for \$889.44 in 2018).

2. 25.0-mm diameter, 3.0-mm thick uncoated germanium window (Edmund Optics stock no. 68-737 for \$175.00 in 2018).
3. UV-NIR silicon power photodetector (Edmund Optics stock no. 89-310 for \$795.00 in 2018).

The optomechanical and other components for this experiment are the following:

1. 3" stainless-steel post (Edmund Optics stock no. 59-754 for \$10.25 in 2018), 3" post holder (Edmund Optics stock no. 58-979 for \$13.25 in 2018), $\frac{1}{2}$ " translation stage (Thorlabs stock no. MT1 for \$297.84 in 2018), and a base plate for the $\frac{1}{2}$ " translation stage (Thorlabs stock no. MT401 for \$23.66 in 2018) for the 0.8-mW 632.8-nm He-Ne laser.
2. 25/25.4-mm kinematic circular optical mount (Edmund Optics stock no. 58-851 for \$99.00 in 2018), 3" stainless-steel post (Edmund Optics stock no. 59-754 for \$10.25 in 2018), 3" post holder (Edmund Optics stock no. 58-979 for \$13.25 in 2018), and a 2"x3" slotted base plate (Edmund Optics stock no. 03-655 for \$15.00 in 2018) for the germanium window.
3. Power meter (Edmund Optics stock no. 89-305 for \$850.00 in 2018), adjustable-height V-clamp (Thorlabs stock no. VG100 for \$87.98 in 2018), 3" stainless-steel post (Edmund Optics stock no. 59-754 for \$10.25 in 2018), 3" post holder (Edmund Optics stock no. 58-979 for \$13.25 in 2018), and a 2"x3" slotted base plate (Edmund Optics stock no. 03-655 for \$15.00 in 2018) for the UV-NIR silicon power photodetector.

Figure 5.2 shows a schematic of experiment 5.2.

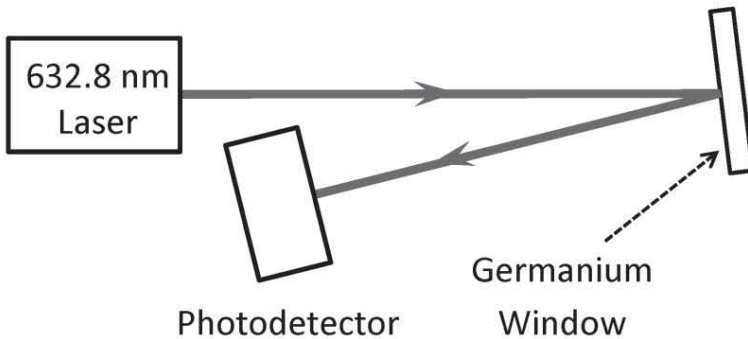


Figure 5.2 Schematic of experiment 5.2.

The schematic of experiment 5.2 is achieved through the following procedure:

1. The 0.8-mW 632.8-nm He-Ne laser is attached to the 36"x12" breadboard using the 3" stainless-steel post, 3" post holder, ½" translation stage, and the base plate for the ½" translation stage.
2. The 0.8-mW 632.8-nm He-Ne laser is adjusted so that the 0.48-mm diameter 632.8-nm He-Ne laser beam propagates parallel to the long edge of the 36"x12" breadboard at a fixed height of 6.5" above the 36"x12" breadboard.
3. The power of the 0.8-mW 632.8-nm He-Ne laser beam is measured using the UV-NIR silicon power photodetector.
4. The germanium window is attached to the 36"x12" breadboard using the 25/25.4-mm kinematic circular optical mount, 3" stainless-steel post, 3" post holder, and 2"x3" slotted base plate.
5. The germanium window is adjusted so that the 0.8-mW 632.8-nm He-Ne laser beam is incident upon the center of the fused silica window at a 5° angle of incidence.
6. The UV-NIR silicon power photodetector is attached to the 36"x12" breadboard using the adjustable-height V-clamp, 3" stainless-steel post, 3" long post holder, and 2"x3" slotted base plate.

7. The power of the 0.8-mW 632.8-nm He-Ne laser beam reflected by the germanium window is measured using the UV-NIR silicon power photodetector.
8. The ratio of the power of the 0.8-mW 632.8-nm He-Ne laser beam reflected by the germanium window and the power of the 0.8-mW 632.8-nm He-Ne laser is a measure of the reflectance R of the germanium window at near-normal incidence.

5.3 Reflection loss

The reflection loss R_L for a plane parallel window with a negligible absorption coefficient α for a near-normal incidence of light is given by

$$R_L \approx \frac{2R}{1+R} \quad (5.3)$$

where R is the single-surface reflectance for near-normal incidence.

Experiment 5.3: Measure the single-surface reflectance R of a silicon window for a 5° angle of incidence at 632.8 nm. Determine the reflection loss R_L using the measured value of R .

The optical components for this experiment are the following:

1. 0.8-mW 632.8-nm He-Ne laser (Thorlabs stock no. HNLS008L for \$889.44 in 2018).
2. 25.0-mm diameter, 3.0-mm thick uncoated silicon window (Edmund Optics stock no.68-527 for \$125.00 in 2018).
3. UV-NIR silicon power photodetector (Edmund Optics stock no. 89-310 for \$795.00 in 2018).

The optomechanical and other components for this experiment are the following:

1. 3" stainless-steel post (Edmund Optics stock no. 59-754 for \$10.25 in 2018), 3" post holder (Edmund Optics stock no. 58-979 for \$13.25 in 2018), $\frac{1}{2}$ " translation stage (Thorlabs stock no. MT1 for \$297.84 in 2018), and a base plate for the $\frac{1}{2}$ " translation stage (Thorlabs stock no. MT401 for \$23.66 in 2018) for the 0.8-mW 632.8-nm He-Ne laser.

2. 25/25.4-mm kinematic circular optical mount (Edmund Optics stock no. 58-851 for \$99.00 in 2018), 3" stainless-steel post (Edmund Optics stock no. 59-754 for \$10.25 in 2018), 3" post holder (Edmund Optics stock no. 58-979 for \$13.25 in 2018), and a 2"x3" slotted base plate (Edmund Optics stock no. 03-655 for \$15.00 in 2018) for the silicon window.
3. Power meter (Edmund Optics stock no. 89-305 for \$850.00 in 2018), adjustable-height V-clamp (Thorlabs stock no. VG100 for \$87.98 in 2018), 3" stainless-steel post (Edmund Optics stock no. 59-754 for \$10.25 in 2018), 3" post holder (Edmund Optics stock no. 58-979 for \$13.25 in 2018), and a 2"x3" slotted base plate (Edmund Optics stock no. 03-655 for \$15.00 in 2018) for the UV-NIR silicon power photodetector.

Figure 5.3 shows a schematic of experiment 5.3.

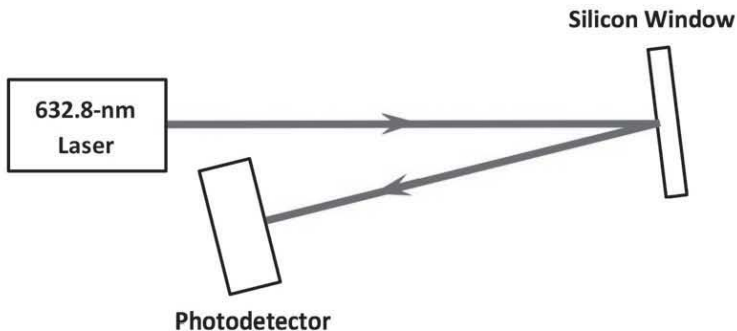


Figure 5.3 Schematic of experiment 5.3.

The schematic of experiment 5.3 is achieved through the following procedure:

1. The 0.8-mW 632.8-nm He-Ne laser is attached to the 36"x12" breadboard using the 3" stainless-steel post, 3" post holder, ½" translation stage, and the base plate for the ½" translation stage.
2. The 0.8-mW 632.8-nm He-Ne laser is adjusted so that the 0.48-mm diameter 632.8-nm He-Ne laser beam propagates parallel to the long edge of the 36"x12" breadboard at a fixed height of 6.5" above the breadboard.

3. The power of the 0.8-mW 632.8-nm He-Ne laser beam is measured using the UV-NIR silicon power photodetector.
4. The silicon window is attached to the 36"x12" breadboard using the 25/25.4-mm kinematic circular optical mount, 3" stainless-steel post, 3" post holder, and 2"x3" slotted base plate.
5. The silicon window is adjusted so that the 0.8-mW 632.8-nm He-Ne laser beam is incident upon the center of the silicon window at a 5° angle of incidence.
6. The UV-NIR silicon power photodetector is attached to the 36"x12" breadboard using the adjustable-height V-clamp, 3" stainless-steel post, 3" post holder, and 2"x3" slotted base plate.
7. The power of the 0.8-mW 632.8-nm He-Ne laser beam reflected by the silicon window is measured using the UV-NIR silicon power photodetector.
8. The ratio of the power of the 0.8-mW 632.8-nm He-Ne laser beam reflected by the silicon window and the power of the 0.8-mW 632.8-nm He-Ne laser is a measure of the reflectance R of the silicon window at near-normal incidence.

Experiment 5.4: Measure the single-surface reflectance R of a zinc selenide window for a 5° angle of incidence at 632.8 nm. Determine the reflection loss R_L using the measured value of R .

The optical components for this experiment are the following:

1. 0.8-mW 632.8-nm He-Ne laser (Thorlabs stock no. HNLS008L for \$889.44 in 2018).
2. 25.0-mm diameter, 2.0-mm thick uncoated zinc selenide window (Edmund Optics stock no.68-508 for \$249.00 in 2018).
3. UV-NIR silicon power photodetector (Edmund Optics stock no. 89-310 for \$795.00 in 2018).

The optomechanical and other components for this experiment are the following:

1. 3" stainless-steel post (Edmund Optics stock no. 59-754 for \$10.25 in 2018), 3" post holder (Edmund Optics stock no. 58-979

for \$13.25 in 2018), $\frac{1}{2}$ " translation stage (Thorlabs stock no. MT1 for \$297.84 in 2018), and a base plate for the $\frac{1}{2}$ " translation stage (Thorlabs stock no. MT401 for \$23.66 in 2018) for the 0.8-mW 632.8-nm He-Ne laser.

2. 25/25.4-mm kinematic circular optical mount (Edmund Optics stock no. 58-851 for \$99.00 in 2018), 3" stainless-steel post (Edmund Optics stock no. 59-754 for \$10.25 in 2018), 3" post holder (Edmund Optics stock no. 58-979 for \$13.25 in 2018), and a 2"x3" slotted base plate (Edmund Optics stock no. 03-655 for \$15.00 in 2018) for the zinc selenide window.
3. Power meter (Edmund Optics stock no. 89-305 for \$850.00 in 2018), adjustable-height V-clamp (Thorlabs stock no. VG100 for \$87.98 in 2018), 3" stainless-steel post (Edmund Optics stock no. 59-754 for \$10.25 in 2018), 3" post holder (Edmund Optics stock no. 58-979 for \$13.25 in 2018), and a 2"x3" slotted base plate (Edmund Optics stock no. 03-655 for \$15.00 in 2018) for the UV-NIR silicon power photodetector.

Figure 5.4 shows a schematic of experiment 5.4.

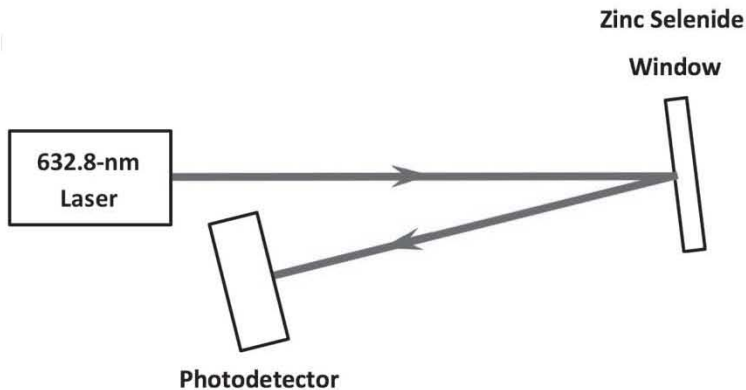


Figure 5.4 Schematic of experiment 5.4.

The schematic of experiment 5.4 is achieved through the following procedure:

1. The 0.8-mW 632.8-nm He-Ne laser is attached to the 36"x12" breadboard using the 3" stainless-steel post, 3" post holder, 1/2" translation stage, and the base plate for the 1/2" translation stage.
2. The 0.8-mW 632.8-nm He-Ne laser is adjusted so that the 0.48-mm diameter 632.8-nm He-Ne laser beam propagates parallel to the long edge of the 36"x12" breadboard at a fixed height of 6.5" above the breadboard.
3. The power of the 0.8-mW 632.8-nm He-Ne laser beam is measured using the UV-NIR silicon power photodetector.
4. The zinc selenide window is attached to the 36"x12" breadboard using the 25/25.4-mm kinematic circular optical mount, 3" stainless-steel post, 3" post holder, and 2"x3" slotted base plate.
5. The zinc selenide window is adjusted so that the 0.8-mW 632.8-nm He-Ne laser beam is incident upon the center of the zinc selenide window at a 5° angle of incidence.
6. The UV-NIR silicon power photodetector is attached to the 36"x12" breadboard using the adjustable-height V-clamp, 3" stainless-steel post, 3" long post holder, and 2"x3" slotted base plate.
7. The power of the 0.8-mW 632.8-nm He-Ne laser beam reflected by the zinc selenide window is measured using the UV-NIR silicon power photodetector.

The ratio of the power of the 0.8-mW 632.8-nm He-Ne laser beam reflected by the zinc selenide window and the power of the 0.8-mW 632.8-nm He-Ne laser is a measure of the reflectance R of the zinc selenide window at near-normal incidence.

CHAPTER 6

OPTICAL FILTERS

6.1 Bandpass filters

Bandpass filters have high transmittance in a narrow band (25-50 nm) and high absorption elsewhere.

Experiment 6.1: Determine the transmittance of a 525-nm bandpass filter at 532 nm.

The optical components for this experiment are the following:

1. 0.9-mW 532-nm laser (Thorlabs stock no. CPS532-C2 for \$162.18 in 2018).
2. 25.0-mm diameter, 525-nm bandpass filter (Edmund Optics stock no. 87-789 for \$195.00 in 2018).
3. UV-NIR silicon power photodetector (Edmund Optics stock no. 89-310 for \$795.00 in 2018).

The optomechanical and other components for this experiment are the following:

1. 5VDC regulated power supply (Thorlabs stock no. LDS5 for \$86.96 in 2018), 11-mm kinematic mount (Thorlabs stock no. MK11F for \$90.00 in 2018), 3" stainless-steel post (Edmund Optics stock no. 59-754 for \$10.25 in 2018), 3" post holder (Edmund Optics stock no. 58-979 for \$13.25 in 2018), 1/2" translation stage (Thorlabs stock no. MT1 for \$297.94 in 2018), and a base plate for the 1/2" translation stage (Thorlabs stock no. MT401 for \$23.66 in 2018) for the 0.9-mW 532-nm laser.
2. 25/25.4-mm kinematic circular optical mount (Edmund Optics stock no. 58-851 for \$99.00 in 2018), 3" stainless-steel post (Edmund Optics stock no. 59-754 for \$10.25 in 2018), 3" post

holder (Edmund Optics stock no. 58-979 for \$13.25 in 2018), and a 2"x3" slotted base plate (Edmund Optics stock no. 03-655 for \$15.00 in 2018) for the 525-nm bandpass filter.

3. Power meter (Edmund Optics stock no. 89-305 for \$850.00 in 2018), adjustable-height V-clamp (Thorlabs stock no. VG100 for \$87.98 in 2018), 3" stainless-steel post (Edmund Optics stock no. 59-754 for \$10.25 in 2018), 3" post holder (Edmund Optics stock no. 58-979 for \$13.25 in 2018), and a 2"x3" slotted base plate (Edmund Optics stock no. 03-655 for \$15.00 in 2018) for the UV-NIR silicon power photodetector.

Figure 6.1 shows a schematic of experiment 6.1.

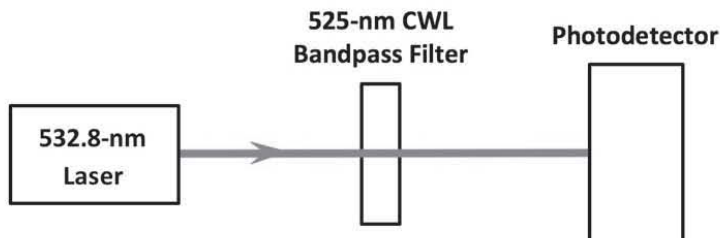


Figure 6.1 Schematic of experiment 6.1.

The schematic of experiment 6.1 is achieved through the following procedure:

1. The 0.9-mW 532-nm laser is attached to the 36"x12" breadboard using the 11-mm kinematic mount, 3" stainless-steel post, 3" post holder, 1/2" translation stage, and the base plate for the 1/2" translation stage.
2. The 0.9-mW 532-nm laser is adjusted so that the 3.5-mm diameter 0.9-mW 532-nm laser beam propagates parallel to the long edge of the 36"x12" breadboard at a fixed height of 6.5" above the breadboard.
3. The power of the 0.9-mW 532-nm laser beam is measured using the UV-NIR silicon power photodetector.
4. The 525-nm bandpass filter is attached to the 36"x12" breadboard using the 25/25.4-mm kinematic circular optical mount, 3" stainless-steel post, 3" post holder, and 2"x3" slotted base plate.

5. The 525-nm bandpass filter is adjusted so that the 0.9-mW 532-nm laser beam is incident normally upon the 525-nm bandpass filter by retro-reflection of the 0.9-mW 532-nm laser beam from the 525-nm bandpass filter.
6. The UV-NIR silicon power photodetector is attached to the 36"x12" breadboard using the adjustable-height V-clamp, 3" stainless-steel post, 3" post holder, and 2"x3" slotted base plate.
7. The UV-NIR silicon power photodetector is adjusted so that the 0.9-mW 532-nm laser beam transmitted by the 525-nm bandpass filter is centered upon the UV-NIR silicon power photodetector.
8. The power of the 0.9-mW 532-nm laser beam transmitted through the 525-nm bandpass filter is measured by the UV-NIR silicon power photodetector.
9. The ratio of the power of the 0.9-mW 532-nm laser beam transmitted through the 525-nm bandpass filter and the power of the 0.9-mW 532-nm laser beam is a measure of the transmittance of the 525-nm CWL bandpass filter at 532 nm.

Experiment 6.2: Determine the transmittance of a 625-nm bandpass filter at 632.8 nm.

The optical components for this experiment are the following:

1. 0.8-mW 632.8-nm He-Ne laser (Thorlabs stock no. HNLS008L for \$889.44 in 2018).
2. 25.0-mm diameter, 625-nm bandpass filter (Edmund Optics stock no. 87-791 for \$195.00 in 2018).
3. UV-NIR silicon power photodetector (Edmund Optics stock no. 89-310 for \$795.00 in 2018).

The optomechanical components for this experiment are the following:

1. 3" stainless-steel post (Edmund Optics stock no. 59-754 for \$10.25 in 2018), 3" post holder (Edmund Optics stock no. 58-979 for \$13.25 in 2018), $\frac{1}{2}$ " translation stage (Thorlabs stock no. MT1 for \$297.84 in 2018), and a base plate for the $\frac{1}{2}$ " translation stage (Thorlabs stock no. MT401 for \$23.66 in 2018) for the 0.8-mW 632.8-nm He-Ne laser.

2. 25/25.4-mm kinematic circular optical mount (Edmund Optics stock no. 58-851 for \$99.00 in 2018), 3" stainless-steel post (Edmund Optics stock no. 59-754 for \$10.25 in 2018), 3" post holder (Edmund Optics stock no. 58-979 for \$13.25 in 2018), and a 2"x3" slotted base plate (Edmund Optics stock no. 03-655 for \$15.00 in 2018) for the 625-nm bandpass filter.
3. Power meter (Edmund Optics stock no. 89-305 for \$850.00 in 2018), adjustable-height V-clamp (Thorlabs stock no. VG100 for \$87.98 in 2018), 3" stainless-steel post (Edmund Optics stock no. 59-754 for \$10.25 in 2018), 3" post holder (Edmund Optics stock no. 58-979 for \$13.25 in 2018), and a 2"x3" slotted base plate (Edmund Optics stock no. 03-655 for \$15.00 in 2018) for the UV-NIR photodetector.

Figure 6.2 shows a schematic of experiment 6.2.

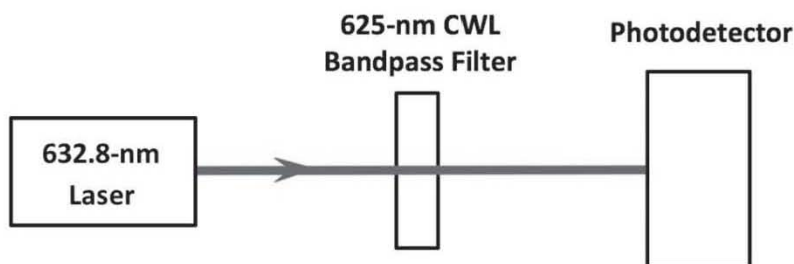


Figure 6.2 Schematic of experiment 6.2.

The schematic of experiment 6.2 is achieved through the following procedure:

1. The 0.8-mW 632.8-nm He-Ne laser is attached to the 36"x12" breadboard using the 3" stainless-steel post, 3" post holder, ½" translation stage, and the base plate for the ½" translation stage.
2. The 0.8-mW 632.8-nm He-Ne laser is adjusted so that the 0.48-mm diameter 632.8-nm He-Ne laser beam propagates parallel to the long edge of the 36"x12" breadboard at a fixed height of 6.5" above the breadboard.
3. The power of the 0.8-mW 632.8-nm He-Ne laser beam is measured using the UV-NIR silicon power photodetector.

4. The 625-nm bandpass filter is attached to the 36"x12" breadboard using the 25/25.4-mm kinematic circular optical mount, 3" stainless-steel post, 3" post holder, and 2"x3" slotted base plate.
5. The 625-nm bandpass filter is adjusted so that the 0.8-mW 632.8-nm He-Ne laser beam is incident normally upon the 625-nm bandpass filter by retro-reflection of the 0.8-mW 632.8-nm He-Ne laser beam from the 625-nm bandpass filter.
6. The UV-NIR silicon power photodetector is attached to the 36"x12" breadboard using the adjustable-height V-clamp, 3" stainless-steel post, 3" post holder, and 2"x3" slotted base plate.
7. The UV-NIR silicon power photodetector is adjusted so that the 0.8-mW 632.8-nm He-Ne laser beam transmitted by the 625-nm bandpass filter is centered upon the UV-NIR silicon power photodetector.
8. The power of the 0.8-mW 632.8-nm He-Ne laser beam transmitted through the 625-nm bandpass filter is measured by the UV-NIR silicon power photodetector.
9. The ratio of the power of the 0.8-mW 632.8-nm He-Ne laser beam transmitted through the 625-nm bandpass filter and the power of the 0.8-mW 632.8-nm He-Ne laser beam is a measure of the transmittance of the 625-nm bandpass filter at 632.8 nm.

6.2 Longpass filters

Longpass filters are available with a specified cut-on wavelength.

Experiment 6.3: Determine the transmittance of a longpass filter with a 500-nm cut-on wavelength at 632.8 nm.

The optical components for this experiment are the following:

1. 0.8-mW 632.8-nm He-Ne laser (Thorlabs stock no. HNLS008L for \$889.44 in 2018).
2. 25.0-mm diameter, 500-nm cut-on wavelength longpass filter (Edmund Optics stock no. 47-616 for \$125.00 in 2018).

3. UV-NIR silicon power photodetector (Edmund Optics stock no. 89-310 for \$795.00 in 2018).

The optomechanical and other components for this experiment are the following:

1. 3" stainless-steel post (Edmund Optics stock no. 59-754 for \$10.25 in 2018), 3" post holder (Edmund Optics stock no. 58-979 for \$13.25 in 2018), $\frac{1}{2}$ " translation stage (Thorlabs stock no. MT1 for \$297.84 in 2018), and a base plate for the $\frac{1}{2}$ " translation stage (Thorlabs stock no. MT401 for \$23.66 in 2018) for the 0.8-mW 632.8-nm He-Ne laser.
2. 25/25.4-mm kinematic circular optical mount (Edmund Optics stock no. 58-851 for \$99.00 in 2018), 3" stainless-steel post (Edmund Optics stock no. 59-754 for \$10.25 in 2018), 3" post holder (Edmund Optics stock no. 58-979 for \$13.25 in 2018), and a 2"x3" slotted base plate (Edmund Optics stock no. 03-655 for \$15.00 in 2018) for the 25.0-mm diameter, 500-nm cut-on longpass filter.
3. Power meter (Edmund Optics stock no. 89-305 for \$850.00 in 2018), adjustable-height V-clamp (Thorlabs stock no. VG100 for \$87.98 in 2018), 3" stainless-steel post (Edmund Optics stock no. 59-754 for \$10.25 in 2018), 3" post holder (Edmund Optics stock no. 58-979 for \$13.25 in 2018), and a 2"x3" slotted base plate (Edmund Optics stock no. 03-655 for \$15.00 in 2018) for the UV-NIR silicon power photodetector.

Figure 6.3 shows a schematic of experiment 6.3.

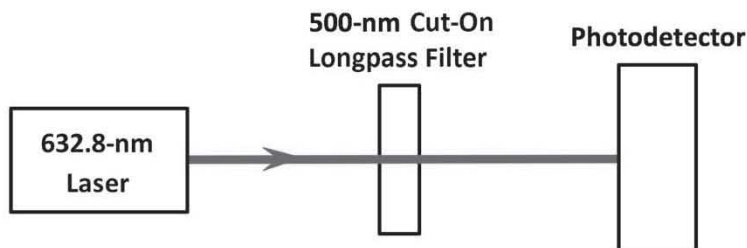


Figure 6.3 Schematic of experiment 6.3.

The schematic of experiment 6.3 is achieved through the following procedure:

1. The 0.8-mW 632.8-nm He-Ne laser is attached to the 36"x12" breadboard using the 3" stainless-steel post, 3" post holder, 1/2" translation stage, and the base plate for the 1/2" translation stage.
2. The 0.8-mW 632.8-nm He-Ne laser is adjusted so that the 0.48-mm diameter 632.8-nm laser beam propagates parallel to the long edge of the 36"x12" breadboard at a fixed height of 6.5" above the breadboard.
3. The power of the 0.8-mW 632.8-nm He-Ne laser beam is measured using the UV-NIR silicon power photodetector.
4. The 500-nm cut-on wavelength longpass filter is attached to the 36"x12" breadboard using the 25/25.4-mm kinematic circular optical mount, 3" stainless-steel post, 3" post holder, and 2"x3" slotted base plate.
5. The 500-nm cut-on wavelength longpass filter is adjusted so that the 0.8-mW 632.8-nm He-Ne laser beam is incident normally upon the 500-nm cut-on wavelength longpass filter by retro-reflection of the 0.8-mW 632.8-nm He-Ne laser beam from the 500-nm cut-on wavelength longpass filter.
6. The UV-NIR silicon power photodetector is attached to the 36"x12" breadboard using the adjustable-height V-clamp, 3" stainless-steel post, 3" post holder, and 2"x3" slotted base plate.
7. The UV-NIR silicon power photodetector is adjusted so that the 0.8-mW 632.8-nm He-Ne laser beam transmitted by the 500-nm cut-on wavelength longpass filter is centered upon the UV-NIR silicon power photodetector.
8. The power of the 0.8-mW 632.8-nm He-Ne laser beam transmitted through the 500-nm cut-on wavelength longpass filter is measured by the UV-NIR silicon power photodetector.
9. The ratio of the power of the 0.8-mW 632.8-nm He-Ne laser beam transmitted through the 500-nm cut-on wavelength longpass filter and the power of the 0.8-mW 632.8-nm He-Ne

laser beam is a measure of the transmittance of the 500-nm cut-on wavelength longpass filter at 632.8 nm.

6.3 Raman filters

Raman filters are used to block the pump laser light from entering the Raman spectrometer. Both longpass and shortpass Raman filters are available.

Experiment 6.4: Measure the transmittance of a 532-nm longpass Raman filter at 632.8 nm.

The optical components for this experiment are the following:

1. 0.8-mW 632.8-nm He-Ne laser (Thorlabs stock no. HNLS008L for \$889.44 in 2018).
2. 25-mm diameter, 532.0-nm longpass Raman filter (Semrock stock no. LP03-532RU-25 for \$695.00 in 2018).
3. UV-NIR silicon power photodetector (Edmund Optics stock no. 89-310 for \$795.00 in 2018).

The optomechanical and other components for this experiment are the following:

1. 3" stainless-steel post (Edmund Optics stock no. 59-754 for \$10.25 in 2018), 3" post holder (Edmund Optics stock no. 58-979 for \$13.25 in 2018), $\frac{1}{2}$ " translation stage (Thorlabs stock no. MT1 for \$297.84 in 2018), and a base plate for the $\frac{1}{2}$ " translation stage (Thorlabs stock no. MT401 for \$23.66 in 2018) for the 0.8-mW 632.8-nm He-Ne laser.
2. 25/25.4-mm kinematic circular optical mount (Edmund Optics stock no. 58-851 for \$99.00 in 2018), 3" stainless-steel post (Edmund Optics stock no. 59-754 for \$10.25 in 2018), 3" post holder (Edmund Optics stock no. 58-979 for \$13.25 in 2018), and a 2"x3" slotted base plate (Edmund Optics stock no. 03-655 for \$15.00 in 2018) for the 532.0-nm longpass Raman filter.
3. Power meter (Edmund Optics stock no. 89-305 for \$850.00 in 2018), adjustable-height V-clamp (Thorlabs stock no. VG100 for \$87.98 in 2018), 3" stainless-steel post (Edmund Optics stock no. 59-754 for \$10.25 in 2018), 3" post holder (Edmund Optics stock

no. 58-979 for \$13.25 in 2018), and a 2"x3" slotted base plate (Edmund Optics stock no. 03-655 for \$15.00 in 2018) for the UV-NIR silicon power photodetector.

Figure 6.4 shows a schematic of experiment 6.4.

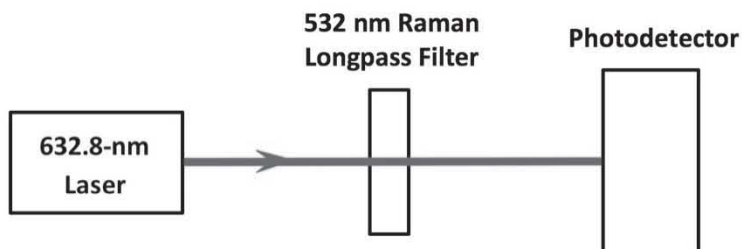


Figure 6.4 Schematic of experiment 6.4

The schematic of experiment 6.4 is achieved through the following procedure:

1. The 0.8-mW 632.8-nm He-Ne laser is attached to the 36"x12" breadboard using the 3" stainless-steel post, 3" post holder, ½" translation stage, and the base plate for the ½" translation stage.
2. The 0.8-mW 632.8-nm He-Ne laser is adjusted so that the 0.48-mm diameter 632.8-nm He-Ne laser beam propagates parallel to the long edge of the 36"x2" breadboard at a fixed height of 6.5" above the breadboard.
3. The power of the 0.8-mW 632.8-nm He-Ne laser is measured using the UV-NIR silicon power photodetector
4. The 532.0-nm longpass Raman filter is attached to the 36"x12" breadboard using the 25/25.4-mm kinematic circular optical mount, 3" stainless-steel post, 3" post holder, and 2"x3" slotted base plate.
5. The 532.0-nm longpass Raman filter is adjusted so that the 0.8-mW 632.8-nm He-Ne laser beam is incident normally upon the 532.0-nm longpass Raman filter by retro-reflection of the 0.8-mW 632.8-nm He-Ne laser beam from the 532.0-nm longpass Raman filter.

6. The UV-NIR silicon power photodetector is attached to the 36"x12" breadboard using the adjustable-height V-clamp, 3" stainless-steel post, 3" post holder, and 2"x3" slotted base plate.
7. The UV-NIR silicon power photodetector is adjusted so that the 0.8-mW 632.8-nm He-Ne laser beam transmitted by the 532.0-nm longpass Raman filter is centered upon the UV-NIR silicon power photodetector.
8. The power of the 0.8-mW 632.8-nm He-Ne laser beam transmitted through the 532.0-nm longpass Raman filter is measured by the UV-NIR silicon power photodetector.
9. The ratio of the power of the 0.8-mW 632.8-nm He-Ne laser beam transmitted through the 532.0-nm longpass Raman filter and the power of the 0.8-mW 632.8-nm He-Ne laser is a measure of the transmittance of the 532.0-nm longpass Raman filter at 632.8 nm.

Experiment 6.5: Measure the transmittance of a 532.0-nm longpass Raman filter at 532.0 nm.

The optical components for this experiment are the following:

1. 0.9-mW 532-nm laser (Thorlabs stock no. CPS532-C2 for \$162.18 in 2018).
2. 25-mm diameter, 532.0-nm longpass Raman filter (Semrock stock no. LP03-532RU-25 for \$695.00 in 2018).
3. UV-NIR silicon power photodetector (Edmund Optics stock no. 89-310 for \$795.00 in 2018).

The optomechanical and other components for this experiment are the following:

1. 5VDC regulated power supply (Thorlabs stock no. LDS5 for \$86.96 in 2018), 11-mm kinematic mount (Thorlabs stock no. MK11F for \$90.00 in 2018), 3" stainless-steel post (Edmund Optics stock no. 59-754 for \$10.25 in 2018), 3" post holder (Edmund Optics stock no. 58-979 for \$13.25 in 2018), 1/2" translation stage (Thorlabs stock no. MT1 for \$297.94 in 2018), and a base plate for the 1/2" translation stage (Thorlabs stock no. MT401 for \$23.66 in 2018) for the 0.9-mW 532-nm laser.

2. 25/25.4-mm kinematic circular optical mount (Edmund Optics stock no. 58-851 for \$99.00 in 2018), 3" stainless-steel post (Edmund Optics stock no. 59-754 for \$10.25 in 2018), 3" post holder (Edmund Optics stock no. 58-979 for \$13.25 in 2018), and a 2"x3" slotted base plate (Edmund Optics stock no. 03-655 for \$15.00 in 2018) for the 532.0-nm longpass Raman filter.
3. Power meter (Edmund Optics stock no. 89-305 for \$850.00 in 2018), adjustable-height V-clamp (Thorlabs stock no. VG100 for \$87.98 in 2018), 3" stainless-steel post (Edmund Optics stock no. 59-754 for \$10.25 in 2018), 3" post holder (Edmund Optics stock no. 58-979 for \$13.25 in 2018), and a 2"x3" slotted base plate (Edmund Optics stock no. 03-655 for \$15.00 in 2018) for the UV-NIR silicon power photodetector.

Figure 6.5 shows a schematic of experiment 6.5.

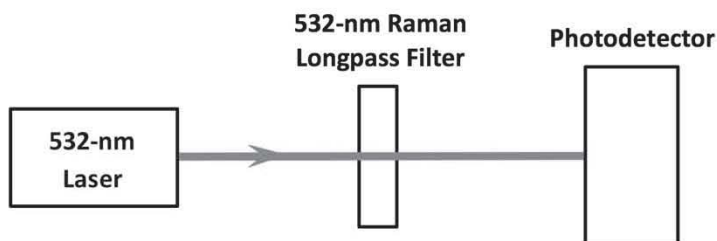


Figure 6.5 Schematic of experiment 6.5.

The schematic of experiment 6.5 is achieved through the following procedure:

1. The 0.9-mW 532-nm laser is attached to the 36"x12" breadboard using the 11-mm kinematic mount, 3" stainless-steel post, 3" post holder, 1/2" translation stage, and the base plate for the 1/2" translation stage.
2. The 0.9-mW 532-nm laser is adjusted so that the 3.5-mm diameter, 532-nm laser beam propagates parallel to the long edge of the 36"x12" breadboard at a fixed height of 6.5" above the breadboard.
3. The power of the 0.9-mW 532.0-nm laser beam is measured using the UV-NIR silicon power photodetector.

4. The 532.0-nm longpass Raman filter is attached to the 36"x12" breadboard using the 25/25.4-mm kinematic circular optical mount, 3" stainless-steel post, 3" post holder, and 2"x3" slotted base plate.
5. The 532.0-nm longpass Raman filter is adjusted so that the 0.9-mW 532.0-nm laser beam is incident normally upon the 532.0-nm longpass Raman filter by retro-reflection of the 0.9-mW 532.0-nm laser beam from the 532.0-nm longpass Raman filter.
6. The UV-NIR silicon power photodetector is attached to the 36"x12" breadboard using the adjustable-height V-clamp, 3" stainless-steel post, 3" post holder, and 2"x3" slotted base plate.
7. The UV-NIR silicon power photodetector is adjusted so that the 0.9-mW 532.0-nm laser beam transmitted by the 532.0-nm longpass Raman filter is centered upon the UV-NIR silicon power photodetector.
8. The power of the 532.0-nm laser beam transmitted through the 532.0-nm longpass Raman filter is measured by the UV-NIR silicon power photodetector.
9. The ratio of the power of the 0.9-mW 532.0-nm laser beam transmitted through the 532.0-nm longpass Raman filter and the power of the 0.9-mW 532.0-nm laser is a measure of the transmittance of the 532.0-nm longpass Raman filter at 532.0 nm.

CHAPTER 7

BEAMSPLITTERS

7.1 Plate beamsplitters

The displacement δ of the transmitted beam from the incident beam for a 45° angle of incidence is given by

$$\delta = \frac{t}{\sqrt{2}}(1 - \tan\theta_t) \quad (7.1)$$

where t is the thickness of the plate and θ_t is the angle of transmission, which is given by

$$\sin\theta_t = \frac{1}{n\sqrt{2}} \quad (7.2)$$

Experiment 7.1: Measure the displacement δ for a plate beamsplitter for a 45° angle of incidence at 632.8 nm.

The optical components for this experiment are the following:

1. 0.8-mW 632.8-nm He-Ne laser (Thorlabs stock no. HNLS008L for \$889.44 in 2018).
2. 25-mm diameter, 1.0-mm thick 50/50 glass plate beamsplitter (Edmund Optics stock no. 43-736 for \$40.00 in 2018).

The optomechanical components for this experiment consist of the following:

1. 3" stainless-steel post (Edmund Optics stock no. 59-754 for \$10.25 in 2018), 3" post holder (Edmund Optics stock no. 58-979 for \$13.25 in 2018), $\frac{1}{2}$ " translation stage (Thorlabs stock no. MT1 for \$297.84 in 2018), and a base plate for the $\frac{1}{2}$ " translation stage (Thorlabs stock no. MT401 for \$23.66 in 2018) for the 0.8-mW 632.8-nm He-Ne laser.

2. 25/25.4-mm kinematic circular optical mount (Edmund Optics stock no. 58-851 for \$99.00 in 2018), 3" stainless-steel post (Edmund Optics stock no. 59-754 for \$10.25 in 2018), 3" post holder (Edmund Optics stock no. 58-979 for \$13.25 in 2018), and a 2"x3" slotted base plate (Edmund Optics stock no. 03-655 for \$15.00 in 2018) for the 50/50 glass plate beamsplitter.

Figure 7.1 shows a schematic of experiment 7.1.

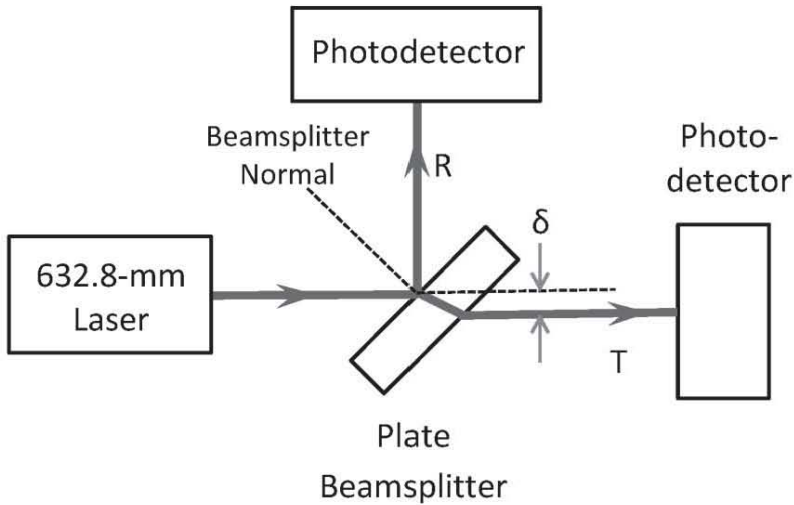


Figure 7.1 Schematic of experiment 7.1.

The schematic of experiment 7.1 is achieved through the following procedure:

1. The 0.8-mW 632.8-nm He-Ne laser is attached to the 36"x12" breadboard using the 3" stainless-steel post, 3" post holder, $\frac{1}{2}$ " translation stage, and the base plate for the $\frac{1}{2}$ " translation stage.
2. The 0.8-mW 632.8-nm He-Ne laser is adjusted so that the 0.48-mm diameter 632.8-nm He-Ne laser beam propagates parallel to the long edge of the 36"x12" breadboard at a fixed height of 6.5" above the breadboard.
3. Mark the direction of propagation of the 0.8-mW 632.8-nm He-Ne laser beam.

4. The 50/50 glass plate beamsplitter is attached to the 36"x12" breadboard using the 25/25.4-mm kinematic circular optical mount, 3" stainless-steel post, 3" post holder, and 2"x3" slotted base plate.
5. The 50/50 glass plate beamsplitter is set at a 45° angle of incidence to the 0.8-mW 632.8-nm He-Ne laser beam.
6. Determine the displacement of the 0.8-mW 632.8-nm He-Ne laser beam transmitted by the plate beamsplitter from its original direction of propagation marked in step 3.

7.2 Polka dot beamsplitters

Polka dot beamsplitters are fabricated by depositing square dots of aluminum on a substrate. These beamsplitters have a fairly constant reflectance/transmittance (R/T) ratio over a large spectral range.

Experiment 7.2: Measure the reflectance R of a 50/50 polka dot beamsplitter at 632.8 nm.

The optical components for this experiment are the following:

1. 0.8-mW 632.8-nm He-Ne laser (Thorlabs stock no. HNLS008L for \$889.44 in 2018).
2. 25.4-mm diameter 50/50 polka dot beamsplitter (Edmund Optics stock no. 46-458 for \$135.00 in 2018).
3. UV-NIR silicon power photodetector (Edmund Optics stock no. 89-310 for \$795.00 in 2018).

The optomechanical and other components for this experiment are the following:

1. 3" stainless-steel post (Edmund Optics stock no. 59-754 for \$10.25 in 2018), 3" post holder (Edmund Optics stock no. 58-979 for \$13.25 in 2018), ½" translation stage (Thorlabs stock no. MT1 for \$297.84 in 2018), and a base plate for the ½" translation stage (Thorlabs stock no. MT401 for \$23.66 in 2018) for the 0.8-mW 632.8-nm He-Ne laser.

2. 25/25.4-mm kinematic circular optical mount (Edmund Optics stock no. 58-851 for \$99.00 in 2018), 3" stainless-steel post (Edmund Optics stock no. 59-754 for \$10.25 in 2018), 3" post holder (Edmund Optics stock no. 58-979 for \$13.25 in 2018), and a 2"x3" slotted base plate (Edmund Optics stock no. 03-655 for \$15.00 in 2018) for the 50/50 polka dot beamsplitter.
3. Power meter (Edmund Optics stock no. 89-305 for \$850.00 in 2018), adjustable-height V-clamp (Thorlabs stock no. VG100 for \$87.98 in 2018), 3" stainless-steel post (Edmund Optics stock no. 59-754 for \$10.25 in 2018), 3" post holder (Edmund Optics stock no. 58-979 for \$13.25 in 2018), and a 2"x3" slotted base plate (Edmund Optics stock no. 03-655 for \$15.00 in 2018) for the UV-NIR silicon power photodetector.

Figure 7.2 shows a schematic of experiment 7.2.

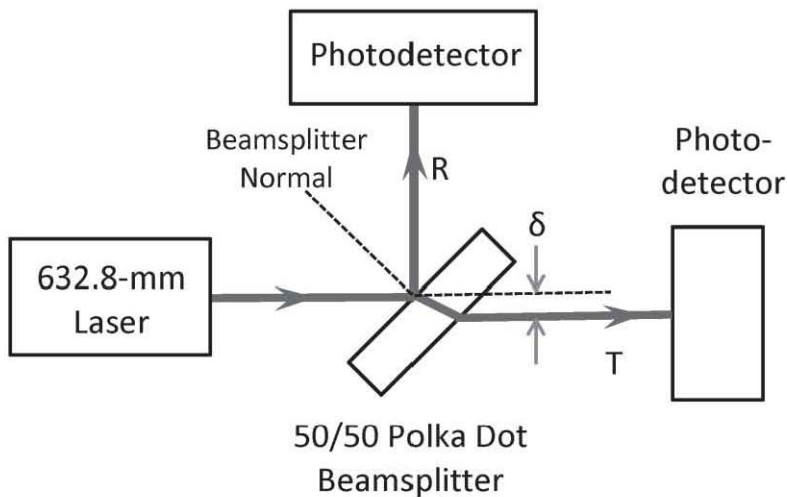


Figure 7.2 Schematic of experiment 7.2.

The schematic of experiment 7.2 is achieved through the following procedure:

1. The 0.8-mW 632.8-nm He-Ne laser is attached to the 36"x12" breadboard using the 3" stainless-steel post, 3" post holder, $\frac{1}{2}$ " translation stage, and the base plate for the $\frac{1}{2}$ " translation stage.

2. The 0.8-mW 632.8-nm He-Ne laser is adjusted so that the 0.48-mm diameter 632.8-nm He-Ne laser beam propagates parallel to the long edge of the 36"x12" breadboard at a fixed height of 6.5" above the breadboard.
3. Measure the power of the 0.8-mW 632.8-nm He-Ne laser beam using the UV-NIR silicon power photodetector.
4. The 50/50 polka dot beamsplitter is attached to the 36"x12" breadboard using the 25/25.4-mm kinematic circular optical mount, 3" stainless-steel post, 3" post holder, and 2"x3" slotted base plate.
5. The 50/50 polka dot beamsplitter is set at a 45° angle of incidence to the 0.8-mW 632.8-nm He-Ne laser beam.
6. The UV-NIR silicon power photodetector is attached to the 36"x12" breadboard using the adjustable-height V-clamp, 3" stainless-steel post, 3" post holder, and 2"x3" slotted base plate.
7. Measure the power of the 0.8-mW 632.8-nm He-Ne laser beam reflected by the polka dot beamsplitter using the UV-NIR silicon power photodetector.
8. The reflectance R of the polka dot beamsplitter is the ratio of the power of the 0.8-mW 632.8-nm He-Ne laser beam reflected by the polka dot beamsplitter (measured in step 7) and the power of the 0.8-mW 632.8-nm He-Ne laser beam (measured in step 3).

7.3 Pellicle beamsplitters

Pellicle beamsplitters are made of very thin (2 μm) nitrocellulose film bonded to lapped aluminum frames. Uncoated pellicle beamsplitters have an R/T ratio of 8/92. Dielectric-coated pellicle beamsplitters are available with R/T ratios of 33/67, 45/55, and 50/50.

Experiment 7.3: Measure the transmittance T of a 50/50 pellicle beamsplitter at 632.8 nm.

The optical components for this experiment are the following:

1. 0.8-mW 632.8-nm He-Ne laser (Thorlabs stock no. HNLS008L for \$889.44 in 2018).

2. 25.4-mm diameter 50/50 pellicle beamsplitter (Edmund Optics stock no. 39-481 for \$160.00 in 2018).
3. UV-NIR silicon power photodetector (Edmund Optics stock no. 89-310 for \$795.00 in 2018).

The optomechanical and other components for this experiment are the following:

1. 3" stainless-steel post (Edmund Optics stock no. 59-754 for \$10.25 in 2018), 3" post holder (Edmund Optics stock no. 58-979 for \$13.25 in 2018), $\frac{1}{2}$ " translation stage (Thorlabs stock no. MT1 for \$297.84 in 2018), and a base plate for the $\frac{1}{2}$ " translation stage (Thorlabs stock no. MT401 for \$23.66 in 2018) for the 0.8-mW 632.8-nm He-Ne laser.
2. 25/25.4-mm kinematic circular optical mount (Edmund Optics stock no. 58-851 for \$99.00 in 2018), 3" stainless-steel post (Edmund Optics stock no. 59-754 for \$10.25 in 2018), 3" post holder (Edmund Optics stock no. 58-979 for \$13.25 in 2018), and a 2"x3" slotted base plate (Edmund Optics stock no. 03-655 for \$15.00 in 2018) for the pellicle beamsplitter.
3. Power meter (Edmund Optics stock no. 89-305 for \$850.00 in 2018), adjustable-height V-clamp (Thorlabs stock no. VG100 for \$87.98 in 2018), 3" stainless-steel post (Edmund Optics stock no. 59-754 for \$10.25 in 2018), 3" post holder (Edmund Optics stock no. 58-979 for \$13.25 in 2018), and a 2"x3" slotted base plate (Edmund Optics stock no. 03-655 for \$15.00 in 2018) for the UV-NIR silicon power photodetector.

Figure 7.3 shows a schematic of experiment 7.3.

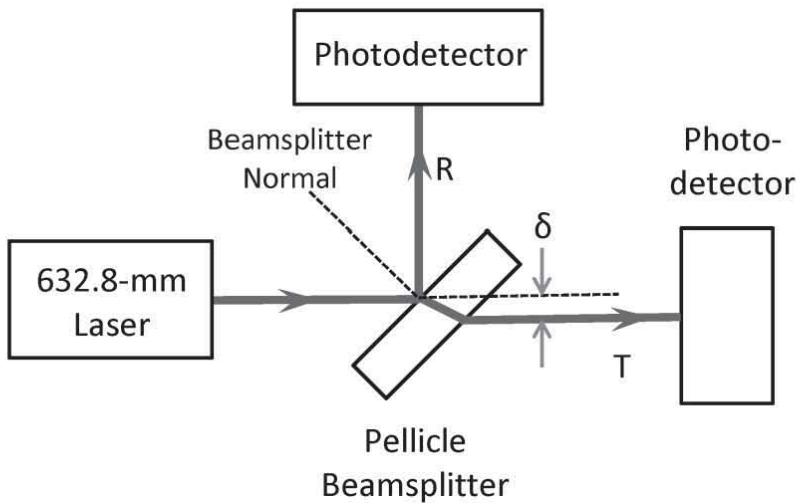


Figure 7.3 Schematic of experiment 7.3.

The schematic of experiment 7.3 is achieved through the following procedure:

1. The 0.8-mW 632.8-nm He-Ne laser is attached to the 36"x12" breadboard using the 3" stainless-steel post, 3" post holder, 1/2" translation stage, and the base plate for the 1/2" translation stage.
2. The 0.8-mW 632.8-nm He-Ne laser is adjusted so that the 0.48-mm diameter 632.8-nm laser beam propagates parallel to the long edge of the 36"x12" breadboard at a fixed height of 6.5" above the breadboard.
3. Measure the power of the 0.8-mW 632.8-nm He-Ne laser beam using the UV-NIR silicon power photodetector.
4. The 50/50 pellicle beamsplitter is attached to the 36"x12" breadboard using the 25/25.4-mm kinematic circular optical mount, 3" stainless-steel post, 3" post holder, and 2"x3" slotted base plate.
5. The 50/50 pellicle beamsplitter is set at a 45° angle of incidence to the 0.8-mW 632.8-nm He-Ne laser beam.

6. The UV-NIR silicon power photodetector is attached to the 36"x12" breadboard using the adjustable-height V-clamp, 3" stainless-steel post, 3" post holder, and 2"x3" slotted base plate.
7. Measure the power of the 0.8-mW 632.8-nm He-Ne laser beam transmitted by the pellicle beamsplitter using the UV-NIR silicon power photodetector.
8. The transmittance T of the pellicle beamsplitter is the ratio of the power of the 0.8-mW 632.8-nm He-Ne laser beam transmitted by the 50/50 pellicle beamsplitter (measured in step 7) and the power of the 0.8-mW 632.8-nm He-Ne laser beam (measured in step 3).

7.4 Cube beamsplitters

Cube beamsplitters are fabricated using two right angle prisms. The hypotenuse of one prism is coated and the two prisms are cemented together to form a cube. Standard cube beamsplitters are available with R/T ratios of 30/70, 50/50, and 70/30.

Experiment 7.4: Measure the transmittance T of a 50/50 cube beamsplitter at 632.8 nm.

The optical components for this experiment are the following:

1. 0.8-mW 632.8-nm He-Ne laser (Thorlabs stock no. HNLS008L for \$889.44 in 2018).
2. 25.0-mm diameter 50/50 cube beamsplitter (Edmund Optics stock no. 47-009 for \$220.00 in 2018).
3. UV-NIR silicon power photodetector (Edmund Optics stock no. 89-310 for \$795.00 in 2018).

The optomechanical and other components for this experiment are the following:

1. 3" stainless-steel post (Edmund Optics stock no. 59-754 for \$10.25 in 2018), 3" post holder (Edmund Optics stock no. 58-979 for \$13.25 in 2018), $\frac{1}{2}$ " translation stage (Thorlabs stock no. MT1 for \$297.84 in 2018), and a base plate for the $\frac{1}{2}$ " translation stage (Thorlabs stock no. MT401 for \$23.66 in 2018) for the 0.8-mW 632.8-nm He-Ne laser.

2. C-mount (Edmund Optics stock no. 56-263 for \$219.00 in 2018), 3" stainless-steel post (Edmund Optics stock no. 59-754 for \$10.25 in 2018), 3" post holder (Edmund Optics stock no. 58-979 for \$13.25 in 2018), and a 2"x3" slotted base plate (Edmund Optics stock no. 03-655 for \$15.00 in 2018) for the 50/50 cube beamsplitter.
3. Power meter (Edmund Optics stock no. 89-305 for \$850.00 in 2018), adjustable-height V-clamp (Thorlabs stock no. VG100 for \$87.98 in 2018), 3" stainless-steel post (Edmund Optics stock no. 59-754 for \$10.25 in 2018), 3" post holder (Edmund Optics stock no. 58-979 for \$13.25 in 2018), and a 2"x3" slotted base plate (Edmund Optics stock no. 03-655 for \$15.00 in 2018) for the UV-NIR silicon power photodetector.

Figure 7.4 shows a schematic of experiment 7.4.

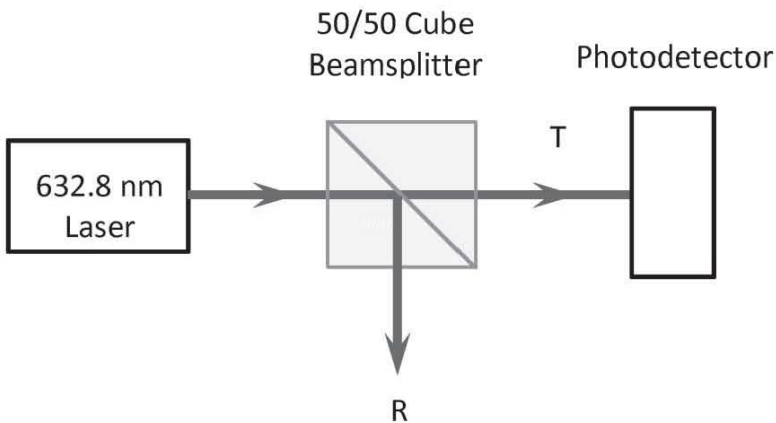


Figure 7.4 Schematic of experiment 7.4.

The schematic of experiment 7.4 is achieved through the following procedure:

1. The 0.8-mW 632.8-nm He-Ne laser is attached to the 36"x12" breadboard using the 3" stainless-steel post, 3" post holder, $\frac{1}{2}$ " translation stage, and the base plate for the $\frac{1}{2}$ " translation stage.

2. The 0.8-mW 632.8-nm He-Ne laser is adjusted so that the 0.48-mm diameter 632.8-nm He-Ne laser beam propagates parallel to the long edge of the 36"x12" breadboard at a fixed height of 6.5" above the breadboard.
3. Measure the power of the 0.8-mW 632.8-nm He-Ne laser beam using the UV-NIR silicon power photodetector.
4. The 50/50 cube beamsplitter is attached to the 36"x12" breadboard using the C-mount, 3" stainless-steel post, 3" post holder, and 2"x3" slotted base plate.
5. The 50/50 cube beamsplitter is set at a 0° angle of incidence to the 0.8-mW 632.8-nm He-Ne laser beam.
6. The UV-NIR silicon power photodetector is attached to the 36"x12" breadboard using the adjustable-height V-clamp, 3" stainless-steel post, 3" post holder, and 2"x3" slotted base plate.
7. Measure the power of the 0.8-mW 632.8-nm He-Ne laser beam transmitted by the 50/50 cube beamsplitter.
8. The transmittance T of the 50/50 cube beamsplitter is the ratio of the power of the 0.8-mW 632.8-nm He-Ne laser beam transmitted by the 50/50 cube beamsplitter (measured in step 7) and that of the 0.8-mW 632.8-nm He-Ne laser beam (measured in step 3).

7.5 Dichroic beamsplitters

Dichroic longpass and shortpass beamsplitters are designed for a 45° angle of incidence and have a cut-on wavelength. The longpass beamsplitters transmit the long wavelength band and reflect the shorter wavelength band than the cut-on wavelength. The shortpass beamsplitters transmit the short wavelength band and reflect the long wavelength band.

Experiment 7.5: Combine the 532-nm and 632.8-nm laser beams using a 45° longpass dichroic beamsplitter with a 600-nm cut-on wavelength.

The optical components for this experiment are the following:

1. 0.8-mW 632.8-nm He-Ne laser (Thorlabs stock no. HNLS008L for \$889.44 in 2018).

2. 25.0-mm diameter 45° dichroic longpass beamsplitter with a 600-nm cut-on wavelength (Edmund Optics stock no. 69-890 for \$115.00 in 2018).
3. 0.9-mW 532-nm laser (Thorlabs stock no. CPS532-C2 for \$162.18 in 2018).

The optomechanical and other components for this experiment are the following:

1. 3" stainless-steel post (Edmund Optics stock no. 59-754 for \$10.25 in 2018), 3" post holder (Edmund Optics stock no. 58-979 for \$13.25 in 2018), ½" translation stage (Thorlabs stock no. MT1 for \$297.84 in 2018), and a base plate for the ½" translation stage (Thorlabs stock no. MT401 for \$23.66 in 2018) for the 0.8-mW 632.8-nm He-Ne laser.
2. 25/25.4-mm kinematic circular optical mount (Edmund Optics stock no. 58-851 for \$99.00 in 2018), 3" stainless-steel post (Edmund Optics stock no. 59-754 for \$10.25 in 2018), 3" post holder (Edmund Optics stock no. 58-979 for \$13.25 in 2018), and a 2"x3" slotted base plate (Edmund Optics stock no. 03-655 for \$15.00 in 2018) for the 45° dichroic dielectric longpass beamsplitter.
3. 5VDC regulated power supply (Thorlabs stock no. LDS5 for \$86.96 in 2018), 11-mm kinematic mount (Thorlabs stock no. MK11F for \$90.00 in 2018), 3" stainless-steel post (Edmund Optics stock no. 59-754 for \$10.25 in 2018), 3" post holder (Edmund Optics stock no. 58-979 for \$13.25 in 2018), 1/2" translation stage (Thorlabs stock no. MT1 for \$297.94 in 2018), and a base plate for the ½" translation stage (Thorlabs stock no. MT401 for \$23.66 in 2018) for the 0.9-mW 532-nm laser.

Figure 7.5 shows a schematic of experiment 7.5.

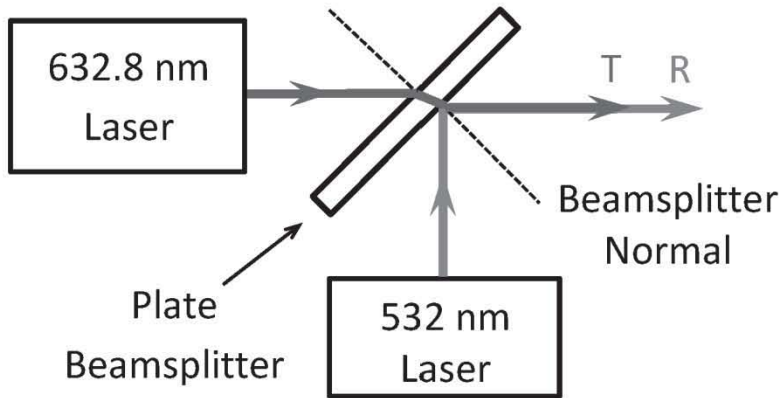


Figure 7.5 Schematic of experiment 7.5

The schematic of experiment 7.5 is achieved through the following procedure:

1. The 0.8-mW 632.8-nm He-Ne laser is attached to the 36"x12" breadboard using the 3" stainless-steel post, 3" post holder, 1/2" translation stage, and the base plate for the 1/2" translation stage.
2. The 0.8-mW 632.8-nm He-Ne laser is adjusted so that the 0.48-mm diameter 632.8-nm He-Ne laser beam propagates parallel to the long edge of the 36"x12" breadboard at a fixed height of 6.5" above the breadboard.
3. The 45° dichroic dielectric longpass beamsplitter is attached to the 36"x12" breadboard using the 25/25.4-mm kinematic circular optical mount, 3" stainless-steel post, 3" post holder, and 2"x3" slotted base plate.
4. The 45° dichroic dielectric longpass beamsplitter is set at a 45° angle of incidence to the 0.8-mW 632.8-nm He-Ne laser beam.
5. The 0.8-mW 632.8-nm He-Ne laser beam is transmitted by the dichroic dielectric longpass beamsplitter.
6. The 0.9-mW 532.0-nm laser is attached to the 36"x12" breadboard using the 11-mm kinematic mount, 3" stainless-steel post, 3" post holder, 1/2" translation stage, and the base plate for the 1/2" translation stage.

7. The 0.9-mW 532.0-nm laser is adjusted so that the 3.5-mm diameter 532-nm laser beam propagates parallel to the short edge of the 36"x12" breadboard at a fixed height of 6.5".
8. The 0.9-mW 532.0-nm laser is adjusted so that the 532-nm laser beam is incident upon the back side of the dichroic dielectric longpass beamsplitter at the same location as the transmitted 0.8-mW 632.8-nm He-Ne laser beam.
9. The 0.9-mW 532.0-nm laser beam is reflected by the 45° dichroic dielectric beamsplitter and propagates together with the transmitted 0.8-mW 632.8-nm He-Ne laser beam.

CHAPTER 8

LIGHT SOURCES

8.1 Incandescent tungsten lamps

The filament of an incandescent tungsten lamp operates at a temperature of about 3000 K. At this operating temperature, the efficiency of the incandescent tungsten lamp in the visible region is only 8%.

Experiment 8.1: Measure the UV-NIR efficiency of a 60-W incandescent tungsten lamp using a UV-NIR silicon power photodetector placed at a distance of 0.3 m from the 60-W incandescent tungsten lamp.

The optical components for this experiment are the following:

1. 60-W incandescent tungsten lamp.
2. UV-NIR silicon power photodetector (Edmund Optics stock no. 89-310 for \$795.00 in 2018).

The optomechanical and other components for this experiment are the following:

1. Power meter (Edmund Optics stock no. 89-305 for \$850.00 in 2018), adjustable-height V-clamp (Thorlabs stock no. VG100 for \$87.98 in 2018), 3" stainless-steel post (Edmund Optics stock no. 59-754 for \$10.25 in 2018), 3" post holder (Edmund Optics stock no. 58-979 for \$13.25 in 2018), and a 2"x3" slotted base plate (Edmund Optics stock no. 03-655 for \$15.00 in 2018) for the UV-NIR silicon photodetector.

Figure 8.1 shows a schematic of experiment 8.1.

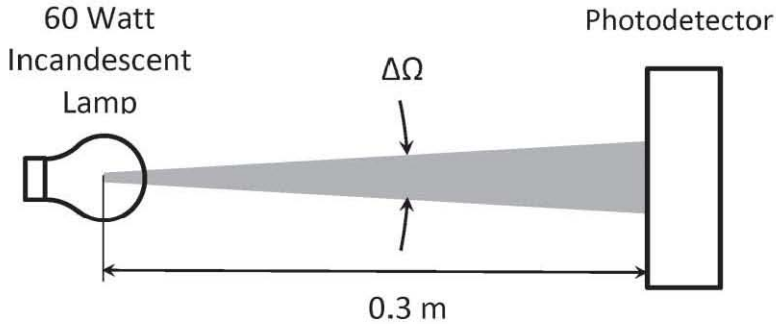


Figure 8.1 Schematic of experiment 8.1.

The schematic of experiment 8.1 is achieved through the following procedure:

1. Set up the 60-W incandescent tungsten lamp at a height of 6.5" above the 36"x12" breadboard.
2. The UV-NIR silicon power photodetector is attached to the 36"x12" breadboard at a distance of 30 cm from the 60-W incandescent lamp using the adjustable-height V-clamp, 3" stainless-steel post, 3" post holder, and 2"x3" slotted base plate.
3. Measure the tungsten lamp power P_L incident upon the UV-NIR silicon power photodetector.
4. Determine the solid angle $\Delta\Omega$ that the 60-W incandescent tungsten lamp subtends at the UV-NIR silicon power photodetector using the relationship $\Delta\Omega = \frac{\pi d^2}{4R^2}$, where $d = 1.0$ cm is the diameter of the UV-NIR silicon power photodetector and $R = 30$ cm is the distance between the 60-W incandescent tungsten lamp and the UV-NIR photodetector.
5. Determine the total power emitted by the 60-W incandescent tungsten lamp in the UV-NIR spectral region using the relationship $P_{UV-NIR} = \frac{4\pi}{\Delta\Omega} P_L$.

6. The efficiency η of the 60-W incandescent tungsten lamp in the UV-NIR region is obtained using the relationship $\eta = \frac{P_{UV-NIR(W)}}{60(W)}$.

8.2 Light-emitting diode (LED) lamps

LED lamps have a much higher efficiency level in the visible region than incandescent tungsten lamps. The output in the visible region for a 10-W LED lamp is the same as that of a 60-W incandescent tungsten lamp.

Experiment 8.2: Measure the UV-NIR efficiency of a 10-W LED lamp using a UV-NIR silicon power photodetector placed at a distance of 0.30 m from the LED lamp.

The optical components for this experiment are the following:

1. 10-W LED lamp.
2. UV-NIR silicon power photodetector (Edmund Optics stock no. 89-310 for \$795.00 in 2018).

The optomechanical and other components for this experiment include the following:

1. Power meter (Edmund Optics stock no. 89-305 for \$850.00 in 2018), adjustable-height V-clamp (Thorlabs stock no. VG100 for \$87.98 in 2018), 3" stainless-steel post (Edmund Optics stock no. 59-754 for \$10.25 in 2018), 3" post holder (Edmund Optics stock no. 58-979 for \$13.25 in 2018), and a 2"x3" slotted base plate (Edmund Optics stock no. 03-655 for \$15.00 in 2018) for the UV-NIR silicon power photodetector.

Figure 8.2 shows a schematic of experiment 8.2.

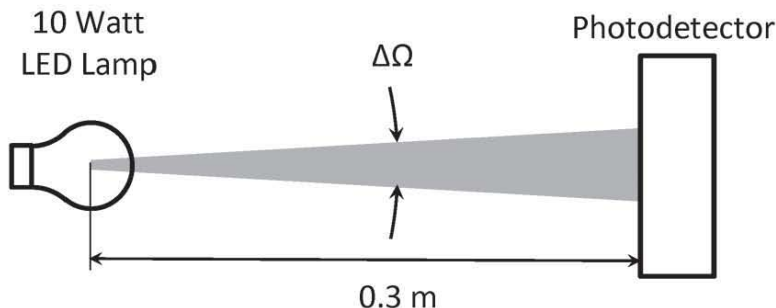


Figure 8.2 Schematic of experiment 8.2.

The schematic of experiment 8.2 is achieved through the following procedure:

1. Set up the 10-W LED lamp at a height of 6.5" above the 36"x12" breadboard.
2. The UV-NIR photodetector is attached to the 36"x12" breadboard at a distance of 30 cm from the 10-W LED lamp using the adjustable-height V-clamp, 3" stainless-steel post, 3" post holder, and 2"x3" slotted base plate.
3. Measure the LED lamp power P_L incident upon the UV-NIR silicon power photodetector.
4. Determine the solid angle $\Delta\Omega$ that the 10-W LED lamp subtends at the UV-NIR silicon power photodetector using the relationship $\Delta\Omega = \frac{\pi d^2}{4R^2}$, where $d = 1.0$ cm is the diameter of the UV-NIR photodetector and $R = 30$ cm is the distance between the 10-W LED lamp and the UV-NIR silicon power photodetector.
5. Determine the total power emitted by the 10-W LED lamp in the UV-NIR spectral region using the relationship $P_{UV-NIR} = \frac{4\pi}{\Delta\Omega} P_L$.
6. The efficiency η of the 10-W LED lamp in the UV-NIR region is obtained using the relationship $\eta = \frac{P_{UV-NIR}(W)}{10(W)}$.

8.3 Lasers

The word *laser* is an acronym for *light amplification by stimulated emission of radiation*. In 1960, T. H. Maiman at the Hughes Research Laboratories discovered the first (Ruby) laser at 694.3 nm. Lasers are now found not only in research laboratories but also in many production plants and even on construction sites.

Experiment 8.3: Measure the wall plug efficiency of a 0.9-mW 532-nm laser using a multimeter for an AC ammeter and an AC voltmeter, assuming no phase difference between the current and voltage for the laser power supply.

The optical components for this experiment are the following:

1. 0.9-mW 532-nm laser (Thorlabs stock no. CPS532-C2 for \$162.18 in 2018).
2. UV-NIR silicon power photodetector (Edmund Optics stock no. 89-310 for \$795.00 in 2018).

The optomechanical and other components for this experiment are the following:

1. 5VDC regulated power supply (Thorlabs stock no. LDS5 for \$86.96 in 2018), 11-mm kinematic mount (Thorlabs stock no. MK11F for \$90.00 in 2018), 3" stainless-steel post (Edmund Optics stock no. 59-754 for \$10.25 in 2018), 3" post holder (Edmund Optics stock no. 58-979 for \$13.25 in 2018), 1/2" translation stage (Thorlabs stock no. MT1 for \$297.94 in 2018), and a base plate for the 1/2" translation stage (Thorlabs stock no. MT401 for \$23.66 in 2018) for the 0.9-mW 532-nm laser.
2. Power meter (Edmund Optics stock no. 89-305 for \$850.00 in 2018), adjustable-height V-clamp (Thorlabs stock no. VG100 for \$87.98 in 2018), 3" stainless-steel post (Edmund Optics stock no. 59-754 for \$10.25 in 2018), 3" post holder (Edmund Optics stock no. 58-979 for \$13.25 in 2018), and a 2"x3" slotted base plate (Edmund Optics stock no. 03-655 for \$15.00 in 2018) for the power meter.
3. Multimeter (Fluke stock no. 8808A for \$850.00 in 2018).

Figure 8.3 shows a schematic of experiment 8.3.

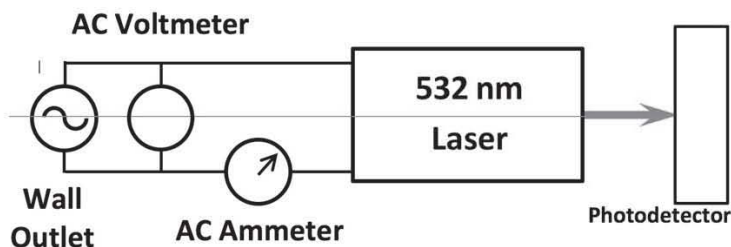


Figure 8.3 Schematic of experiment 8.3.

The schematic of experiment 8.3 is achieved through the following procedure:

1. The 0.9-mW 532-nm laser is attached to the 36"x12" breadboard using the 11-mm kinematic mount, 3" stainless-steel post, 3" post holder, ½" translation stage, and the base plate for the ½" translation stage.
2. The 0.9-mW 532.0-nm laser is set at a height of 6.5" above the 36"x12" breadboard.
3. The 0.9-mW 532.0-nm laser beam is adjusted to propagate along the long edge of the 36"x12" breadboard.
4. The UV-NIR silicon power photodetector is attached to the 36"x12" breadboard using the adjustable-height V-clamp, 3" stainless-steel post, 3" post holder, and 2"x3" slotted base plate.
5. The UV-NIR silicon power photodetector is adjusted so that the 0.9-mW 532-nm laser beam is incident upon the center of the UV-NIR silicon power photodetector.
6. Measure the power of the 0.9-mW 532.0-nm laser beam incident upon the UV-NIR silicon power photodetector.
7. Measure the power used for the excitation of the 0.9-mW 532.0-nm laser supplied by the wall plug using the product of the current measured by the AC ammeter and the voltage measured by the AC voltmeter.

8. The wall plug efficiency of the 0.9-mW 532.0-nm laser is given by the power of the 0.9-mW 532.0-nm laser beam measured by the UV-NIR silicon power photodetector in step 6 divided by the wall plug power used for the excitation of the laser in step 7.

Experiment 8.4: Measure the wall plug efficiency of a 0.8-mW 632.8-nm He-Ne laser using a multimeter for an AC ammeter and an AC voltmeter, assuming no phase difference between the current and voltage for the laser power supply.

The optical components for this experiment are the following:

1. 0.8-mW 632.8-nm He-Ne laser (Thorlabs stock no. HNLS008L for \$889.44 in 2018).
2. UV-NIR silicon power photodetector (Edmund Optics stock no. 89-310 for \$795.00 in 2018).

The optomechanical and other components for this experiment are the following:

1. 3" stainless-steel post (Edmund Optics stock no. 59-754 for \$10.25 in 2018), 3" post holder (Edmund Optics stock no. 58-979 for \$13.25 in 2018), ½" translation stage (Thorlabs stock no. MT1 for \$297.84 in 2018), and a base plate for the ½" translation stage (Thorlabs stock no. MT401 for \$23.66 in 2018) for the 0.8-mW 632.8-nm He-Ne laser.
2. Power meter (Edmund Optics stock no. 89-305 for \$850.00 in 2018), adjustable-height V-clamp (Thorlabs stock no. VG100 for \$87.98 in 2018), 3" stainless-steel post (Edmund Optics stock no. 59-754 for \$10.25 in 2018), 3" post holder (Edmund Optics stock no. 58-979 for \$13.25 in 2018), and a 2"x3" slotted base plate (Edmund Optics stock no. 03-655 for \$15.00 in 2018) for the power meter.
3. Multimeter (Fluke stock no. 8808A for \$850.00 in 2018).

Figure 8.4 shows a schematic of experiment 8.4.

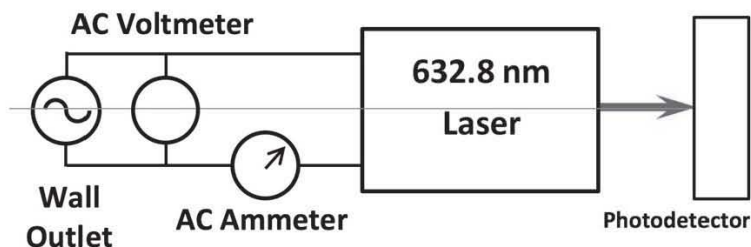


Figure 8.4 Schematic of experiment 8.4.

The schematic of experiment 8.4 is achieved through the following procedure:

1. The 0.8-mW 632.8-nm He-Ne laser is attached to the 36"x12" breadboard using the 3" stainless-steel post, 3" post holder, ½" translation stage, and the base plate for the ½" translation stage.
2. The 0.8-mW 632.8-nm He-Ne laser is set at a height of 6.5" above the 36"x12" breadboard.
3. The 0.8-mW 632.8-nm He-Ne laser beam is adjusted to propagate along the long edge of the 36"x12" breadboard.
4. The UV-NIR silicon power photodetector is attached to the 36"x12" breadboard using the adjustable-height V-clamp, 3" stainless-steel post, 3" post holder, and 2"x3" slotted base plate.
5. The UV-NIR silicon power photodetector is adjusted so that the 0.8-mW He-Ne laser beam is incident upon the center of the UV-NIR silicon power photodetector.
6. Measure the power of the 0.8-mW 632.8-nm He-Ne laser beam incident upon the UV-NIR silicon power photodetector.
7. Measure the power used for the excitation of the 632.8-nm He-Ne laser supplied by the wall plug using the product of the current measured by the AC ammeter and the voltage measured by the AC voltmeter.
8. The wall plug efficiency of the 0.8-mW 632.8-nm He-Ne laser is given by the power of the 632.8-nm He-Ne laser beam measured by the UV-NIR silicon power photodiode in step 6 divided by the

wall plug power used for the excitation of the 0.8-mW 632.8-nm He-Ne laser in step 7.

CHAPTER 9

LIGHT DETECTORS

9.1 Photomultiplier tubes

The invention of the photomultiplier tube (PMT) is based on the discovery of two phenomena: (1) the photoelectric effect, which is the emission of an electron from the surface of a photocathode by a photon, and (2) the secondary emission of electrons by an energetic electron striking an electrode. A PMT is a vacuum photoemissive detector, which contains a photocathode and a number of secondary emitting stages called dynodes. The multiplication factor for a single electron emitted by the photocathode in the PMT with 10 dynode stages may be of the order of 1×10^6 .

Experiment 9.1: Measure the power of a 0.9-mW 532-nm laser using a 532-nm OD 4 notch filter and a PMT.

The optical components for this experiment consist of the following:

1. 0.9-mW 532-nm laser (Thorlabs stock no. CPS532-C2 for \$162.18 in 2018).
2. 25.0-mm diameter, 532.0-nm OD 4 notch filter (Edmund Optics stock no. 67-119 for \$329.00 in 2018).
3. 8-mm voltage output type Hamamatsu PMT (Edmund Optics stock no. 83-898 for \$1175.00 in 2018).

The optomechanical and other components for this experiment are the following:

1. 5VDC regulated power supply (Thorlabs stock no. LDS5 for \$86.96 in 2018), 11-mm kinematic mount (Thorlabs stock no. MK11F for \$90.00 in 2018), 3" stainless-steel post (Edmund Optics stock no. 59-754 for \$10.25 in 2018), 3" post holder (Edmund Optics stock no. 58-979 for \$13.25 in 2018), 1/2" translation stage (Thorlabs stock no. MT1 for \$297.94 in 2018),

and a base plate for the $\frac{1}{2}$ " translation stage (Thorlabs stock no. MT401 for \$23.66 in 2018) for the 0.9-mW 532-nm laser.

Figure 9.1 shows a schematic of experiment 9.1.

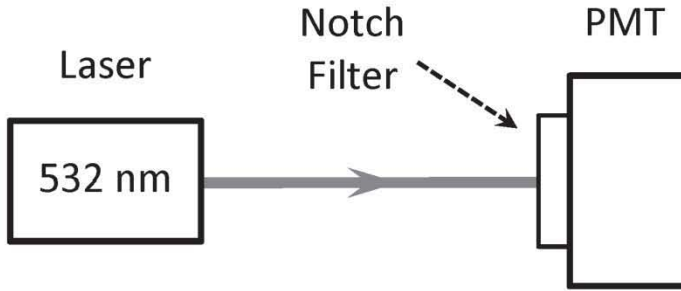


Figure 9.1 Schematic of experiment 9.1.

The schematic of experiment 9.1 is achieved through the following procedure:

1. The 0.9-mW 532.0-nm laser is attached to the 36"x12" breadboard using the 11-mm kinematic mount, 3" stainless-steel post, 3" post holder, $\frac{1}{2}$ " translation stage, and the base plate for the $\frac{1}{2}$ " translation stage.
2. The 0.9-mW 532.0-nm laser is set at a height of 6.5" above the 36"x12" breadboard.
3. The 0.9-mW 532.0-nm laser beam is adjusted to propagate along the long edge of the 36"x12" breadboard.
4. The 532.0-nm notch filter is taped to the input window of the Hamamatsu PMT.
5. The Hamamatsu PMT is attached to the 36"x12" breadboard with the center of the input window of the PMT at a height of 6.5" above the 36"x12" breadboard.
6. The Hamamatsu PMT is adjusted so that the 0.9-mW 532.0-nm laser beam is incident upon the 532.0-nm notch filter at a 0° angle of incidence and centered upon the input window of the PMT.
7. Measure the power P_{PMT} of the 0.9-mW 532.0-nm laser beam by the Hamamatsu PMT.

8. The power of the 532.0-nm green laser beam is equal to P_{PMT} divided by the transmittance of the 532.0-nm notch filter.

Experiment 9.2: Measure the power of a 0.5-mW 632.8-nm He-Ne laser using a 632.8-nm OD 4 notch filter and a PMT.

The optical components for this experiment consist of the following:

1. 0.8-mW 632.8-nm He-Ne laser (Thorlabs stock no. HNLS008L for \$889.44 in 2018).
2. 25.0-mm diameter, 632.8-nm OD 4 notch filter (Edmund Optics stock no. 67-120 for \$329.00 in 2018).
3. 8-mm voltage output type Hamamatsu PMT (Edmund Optics stock no. 83-898 for \$1175.00 in 2018).

The optomechanical components for this experiment consist of the following:

1. 3" stainless-steel post (Edmund Optics stock no. 59-754 for \$10.25 in 2018), 3" post holder (Edmund Optics stock no. 58-979 for \$13.25 in 2018), $\frac{1}{2}$ " translation stage (Thorlabs stock no. MT1 for \$297.84 in 2018), and a base plate for the $\frac{1}{2}$ " translation stage (Thorlabs stock no. MT401 for \$23.66 in 2018) for the 0.8-mW 632.8-nm He-Ne laser.

Figure 9.2 shows a schematic of experiment 9.2.

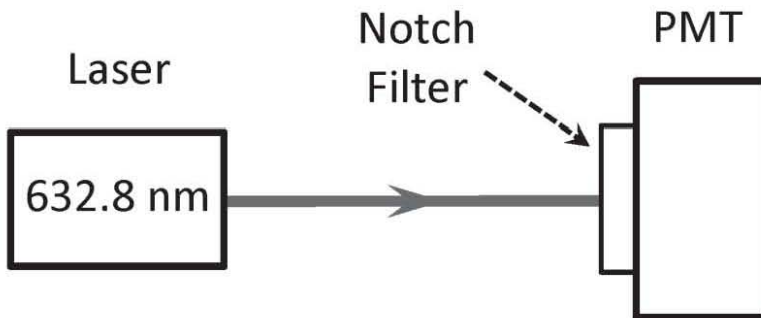


Figure 9.2 Schematic of experiment 9.2.

The schematic of experiment 9.2 is achieved through the following procedure:

1. The 0.8-mW 632.8-He-Ne laser is attached to the 36"x12" breadboard using the 3" stainless-steel post, 3" post holder, 1/2" translation stage, and the base plate for the 1/2" translation stage.
2. The 0.8-mW 632.8-nm He-Ne laser is set at a height of 6.5" above the 36"x12" breadboard.
3. The 0.8-mW 632.8-nm He-Ne laser beam is adjusted to propagate along the long edge of the 36"x12" breadboard.
4. The 632.8-nm notch filter is taped to the input window of the Hamamatsu PMT.
5. The Hamamatsu PMT is attached to the 36"x12" breadboard with the center of the input window of the PMT at a height of 6.5" above the 36"x12" breadboard.
6. The Hamamatsu PMT is adjusted so that the 632.8-nm He-Ne laser beam is incident upon the 632.8-nm notch filter at a 0° angle of incidence and centered upon the input window of the PMT.
7. Measure the power P_{PMT} of the 0.8-mW 632.8-nm He-Ne laser beam using the Hamamatsu PMT.
8. The power of the 632.8-nm He-Ne laser beam is equal to P_{PMT} divided by the transmittance of the 632.8-nm notch filter at 632.8 nm.

9.2 Silicon photodiodes

Silicon photodiodes are based on the photovoltaic effect, which measures the voltage produced by the separation of electrons and holes in a semiconductor p-n junction.

Experiment 9.3: Measure the power of a 0.9-mW 532-nm laser using a 532-nm OD 4 notch filter and a silicon photodiode.

The optical components for this experiment are the following:

1. 0.9-mW 532-nm laser (Thorlabs stock no. CPS532-C2 for \$162.18 in 2018).
2. 25.0-mm diameter, 532-nm OD 4 notch filter (Edmund Optics stock no. 67-119 for \$329.00 in 2018).

3. 2.5-mm diameter silicon photodiode receiver module (Edmund Optics stock no. 57-623 for \$425.00 in 2018).

The optomechanical and other components for this experiment are the following:

1. 5VDC regulated power supply (Thorlabs stock no. LDS5 for \$86.96 in 2018), 11-mm kinematic mount (Thorlabs stock no. MK11F for \$90.00 in 2018), 3" stainless-steel post (Edmund Optics stock no. 59-754 for \$10.25 in 2018), 3" post holder (Edmund Optics stock no. 58-979 for \$13.25 in 2018), 1/2" translation stage (Thorlabs stock no. MT1 for \$297.94 in 2018), and a base plate for the 1/2" translation stage (Thorlabs stock no. MT401 for \$23.66 in 2018) for the 0.9-mW 532-nm laser.
2. 110V/220V 1-channel power supply (Edmund Optics stock no. 57-629 for \$550.00 in 2018) for the silicon photodiode.

Figure 9.3 shows a schematic of experiment 9.3.

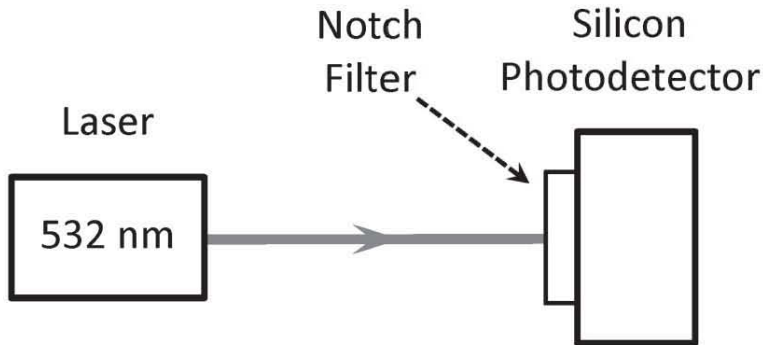


Figure 9.3 Schematic of experiment 9.3.

The schematic of experiment 9.3 is achieved through the following procedure:

1. The 0.9-mW 532.0-nm laser is attached to the 36"x12" breadboard using the 11-mm kinematic mount, 3" stainless-steel post, 3" post holder, 1/2" translation stage, and the base plate for the 1/2" translation stage.
2. The 0.9-mW 532.0-nm laser is set at a height of 6.5" above the 36"x12" breadboard.

3. The 0.9-mW 532.0-nm laser beam is adjusted to propagate along the long edge of the 36"x12" breadboard.
4. The 532.0-nm notch filter is taped to the input window of the silicon photodiode.
5. The silicon photodiode is attached to the 36"x12" breadboard with the center of the input window of the silicon photodiode at a height of 6.5" above the 36"x12" breadboard.
6. The silicon photodiode is adjusted so that the 0.9-mW 532.0-nm laser beam is incident upon the 532.0-nm notch filter at a 0° angle of incidence and centered upon the input window of the silicon photodiode.
7. Measure the power P_{PMT} of the 0.9-mW 532.0-nm laser beam using the silicon photodiode.
8. The measured power of the 0.9-mW 532.0-nm laser is equal to P_{PMT} divided by the transmittance of the 532.0-nm notch filter at 532.0 nm.
9. The actual power of the 0.9-mW 532-nm laser is 2.0x the measured power because the diameter of the 532-nm laser beam is 3.5 mm compared to the 2.5-mm diameter of the silicon photodiode.

Experiment 9.4: Measure the power of a 0.8-mW 632.8-nm He-Ne laser using a 632.8-nm OD 4 notch filter and a silicon photodiode.

The optical components for this experiment are the following:

1. 0.8-mW 632.8-nm He-Ne laser (Thorlabs stock no. HNLS008L for \$889.44 in 2018).
2. 25.0-mm diameter, 632.8-nm OD 4 notch filter (Edmund Optics stock no. 67-120 for \$329.00 in 2018).
3. 2.5-mm diameter silicon photodiode receiver module (Edmund Optics stock no. 57-623 for \$425.00 in 2018).

The optomechanical and other components for this experiment consist of the following:

1. 3" stainless-steel post (Edmund Optics stock no. 59-754 for \$10.25 in 2018), 3" post holder (Edmund Optics stock no. 58-979 for \$13.25 in 2018), $\frac{1}{2}$ " translation stage (Thorlabs stock no. MT1 for \$297.84 in 2018), and a base plate for the $\frac{1}{2}$ " translation stage (Thorlabs stock no. MT401 for \$23.66 in 2018) for the 0.8-mW 632.8-nm He-Ne laser.
2. 110V/220V 1-channel power supply (Edmund Optics stock no. 57-629 for \$550.00 in 2018) for the silicon photodiode.

Figure 9.4 shows a schematic of experiment 9.4.

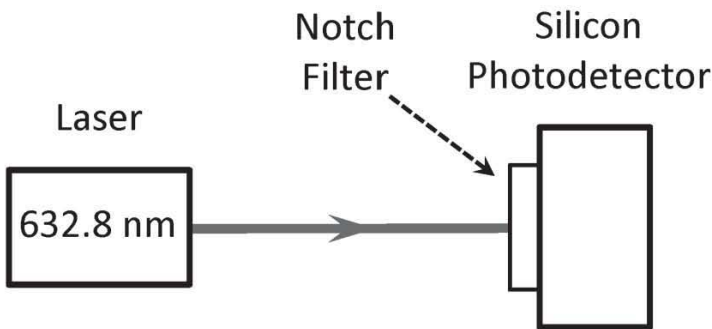


Figure 9.4 Schematic of experiment 9.4.

The schematic of experiment 9.4 is achieved through the following procedure:

1. The 0.8-mW 632.8-nm He-Ne laser is attached to the 36"x12" breadboard using the 3" stainless-steel post, 3" post holder, $\frac{1}{2}$ " translation stage, and the base plate for the $\frac{1}{2}$ " translation stage.
2. The 0.8-mW 632.8-nm He-Ne laser is set at a height of 6.5" above the 36"x12" breadboard.
3. The 0.8-mW 632.8-nm He-Ne laser beam is adjusted to propagate along the long edge of the 36"x12" breadboard.
4. The 632.8-nm notch filter is taped to the input window of the silicon photodiode.
5. The silicon photodiode is attached to the 36"x12" breadboard with the center of the input window of the silicon photodiode at a height of 6.5" above the 36"x12" breadboard.

6. The silicon photodiode is adjusted so that the 632.8-nm He-Ne laser beam is incident upon the 632.8-nm notch filter at a 0° angle of incidence and centered upon the input window of the silicon photodiode.
7. Measure the power P_{PMT} of the 632.8-nm He-Ne laser beam using the silicon photodiode.

The measured power of the 632.8-nm He-Ne laser beam is equal to P_{PMT} divided by the transmittance of the 632.8-nm notch filter at 632.8 nm.

APPENDIX

OPTICAL AND OPTOMECHANICAL COMPONENTS

A.1 Optical components

Figure A1.1 shows a photo of the 0.9-mW 532.0-nm laser (Thorlabs stock no. CPS532-C2).



Figure A1.1 Photo of the 0.9-mW 532-nm laser. (Courtesy of Thorlabs)

Figure A1.2 shows a photo of the 0.8-mW 632.8-nm He-Ne laser (Thorlabs stock no. HNLS008L).



Figure A1.2 Photo of the 0.8-mW 632.8-nm He-Ne laser. (Courtesy of Thorlabs)

Figure A1.3 shows the schematic of a plano-convex lens.

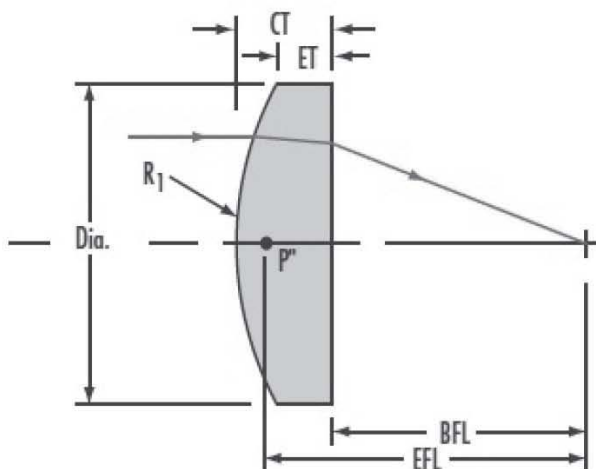


Figure A1.3 Schematic of a plano-convex lens. (Courtesy of Edmund Optics)

Specifications of the plano-convex lenses required for the experiments in this book are given in Table A1.1.

Table A1.1 Specifications of plano-convex lenses. (Courtesy of Edmund Optics)

Edmund Optics Stock No.	Dia. (mm)	EFL (mm)	BFL (mm)	CT (mm)	ET (mm)	R ₁ (mm)	Glass Type
45-146	25.0	35.0	30.42	7.01	2.00	18.11	N-BK7
32-482	25.0	100.0	97.17	4.30	2.77	51.68	N-BK7
45-098	25.0	25.0	20.22	8.00	2.43	16.82	N-SF5
32-862	25.0	125.0	122.70	3.50	2.28	64.62	N-BK7
32-478	25.0	50.0	46.75	4.90	1.68	25.84	N-BK7
49-854	12.7	12.7	10.46	4.00	1.72	9.97	N-SF11

Figure A1.4 shows the schematic of a double-convex lens.

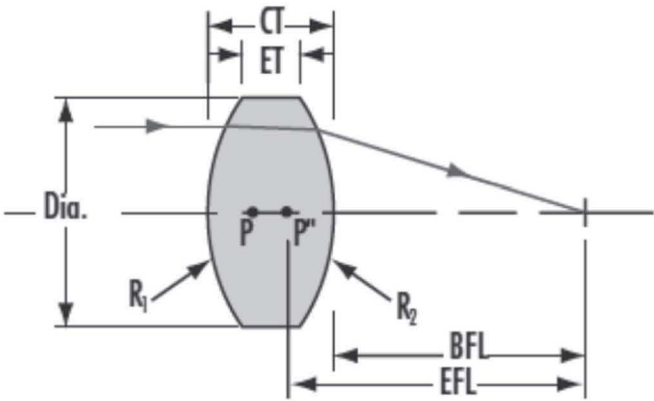


Figure A1.4 Schematic of a double-convex lens. (Courtesy of Edmund Optics)

Specifications of the double-convex lenses required for the experiments in this book are given in Table A1.2.

Table A1.2 Specifications of double-convex lenses. (Courtesy of Edmund Optics)

Edmund Optics Stock No.	Dia. (mm)	EFL (mm)	BFL (mm)	CT (mm)	ET (mm)	R ₁ = - R ₂ (mm)	Glass Type
32-490	25.0	25.0	22.47	8.00	2.90	31.94	N-SF5
32-625	25.0	50.0	48.29	5.00	1.88	50.80	N-BK7

Figure A1.5 shows a photo of the 10-μm diameter ceramic aperture (Edmund Optics stock no. 84-910).



Figure A1.5 Photo of the 10-μm diameter ceramic aperture. (Courtesy of Edmund Optics)

Figure A1.6 shows a photo of the UV-NIR silicon power photodetector (Edmund Optics stock no. 89-310).



Figure A1.6 Photo of the UV-NIR silicon power photodetector. (Courtesy of Edmund Optics)

The specifications of eyepiece reticles are given in Table A1.3.

Table A1.3 Specifications of eyepiece reticles. (Courtesy of Edmund Optics)

Eyepiece Reticle	Edmund Optics Stock No.	Diameter (mm)	Thickness (mm)	Linewidth (mm)
1-mm scale/100Div	54-422	19	1.5	0.0035
10-mm scale/100Div	36-125	19	1.1	0.010

Figure A1.7 shows a photo of the 24-mm diameter 18-mm focal length Olympus PNL 10X microscope objective (Edmund Optics stock no. 86-813).



Figure A1.7 Photo of the 24-mm diameter 18-mm focal length 10x Olympus microscope objective. (Courtesy of Edmund Optics)

Figure A1.8 shows a schematic of the 25.4-mm diameter 25.4-mm focal length enhanced-aluminum spherical mirror (Edmund Optics stock no. 43-335).

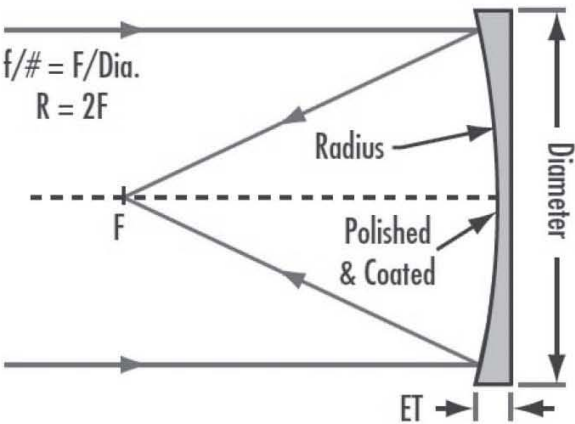


Figure A1.8 Schematic of the 25.4-mm diameter 25.4-mm focal length enhanced-aluminum spherical mirror (Dia.: 25.4 mm; F: 25.4 mm; ET: 6.35 mm). (Courtesy of Edmund Optics)

Figure A1.9 shows a photo of the 10x 632.8-nm He-Ne laser beam expander (Edmund Optics stock no. 55-578).

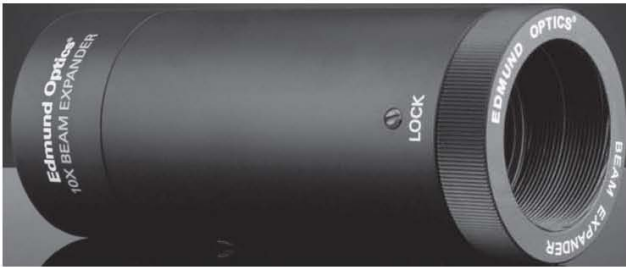


Figure A1.9 Photo of the 10x 632.8-nm He-Ne laser beam expander. (Courtesy of Edmund Optics)

Figure A1.10 shows a photo of the 30° off-axis parabolic mirror (Edmund Optics stock no. 35-490).



Figure A1.10 Photo of the 30° off-axis parabolic mirror. (Courtesy of Edmund Optics)

Figure A1.11 shows a schematic of the 64-mm diameter ellipsoidal mirror (Edmund Optics stock no. 90-968).

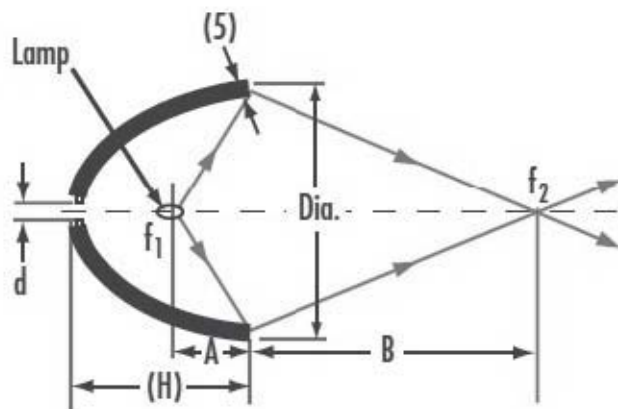


Figure A1.11 Schematic of the 64-mm diameter ellipsoidal mirror (Dia: 64 mm; f_1 : 11 mm; f_2 : 78 mm; A: 31 mm; B: 36 mm; d: 18 mm). (Courtesy of Edmund Optics)

The following three graphs give the efficiency of three different gratings as a function of wavelength:

Figure A1.12 shows the diffraction efficiency of the 1200-grooves/mm 25-mm square transmission grating (Edmund Optics stock no. 49-582).

Figure A1.13 shows the diffraction efficiency of the 1200-grooves/mm 25-mm square 500-nm ruled diffraction grating (Edmund Optics stock no. 43-005).

Figure A1.14 shows the diffraction efficiency of the VIS holographic grating (Edmund Optics stock no. 43-216).

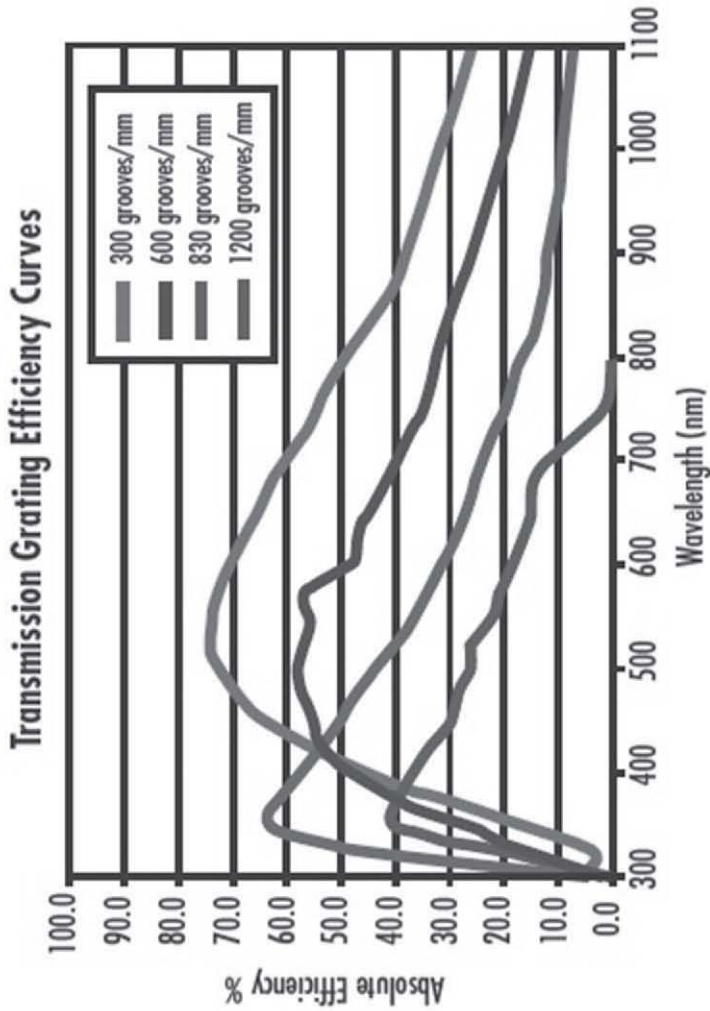


Figure A1.12 Diffraction efficiency of the 1200-grooves/mm 25-mm square transmission grating. (Courtesy of Edmund Optics)

Typical Efficiency Curves for Ruled Gratings Optimized (Blaze) Wavelengths from 500 - 800nm

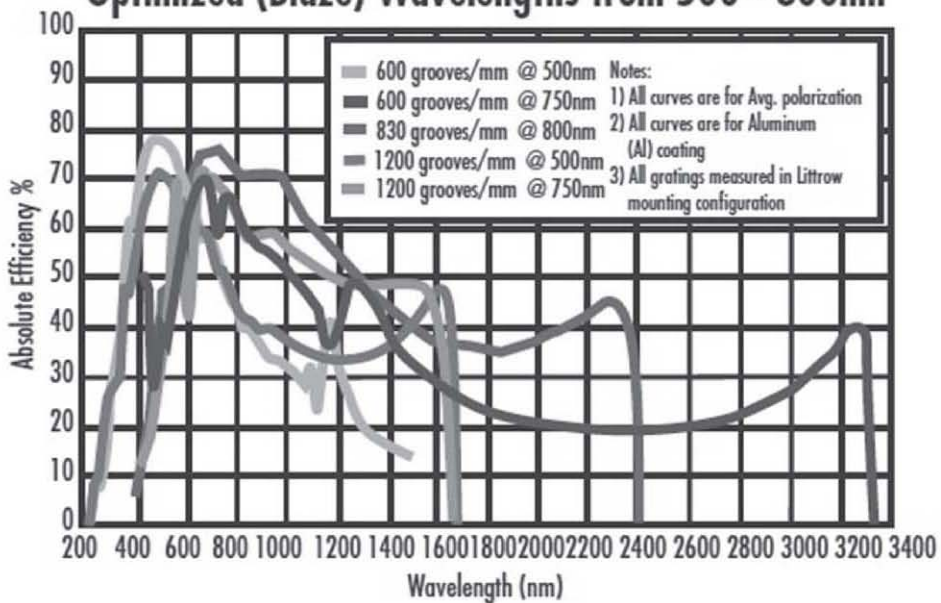


Figure A1.13 Diffraction efficiency of the 1200 grooves/mm 25 mm square 500-nm ruled diffraction grating. (Courtesy of Edmund Optics)

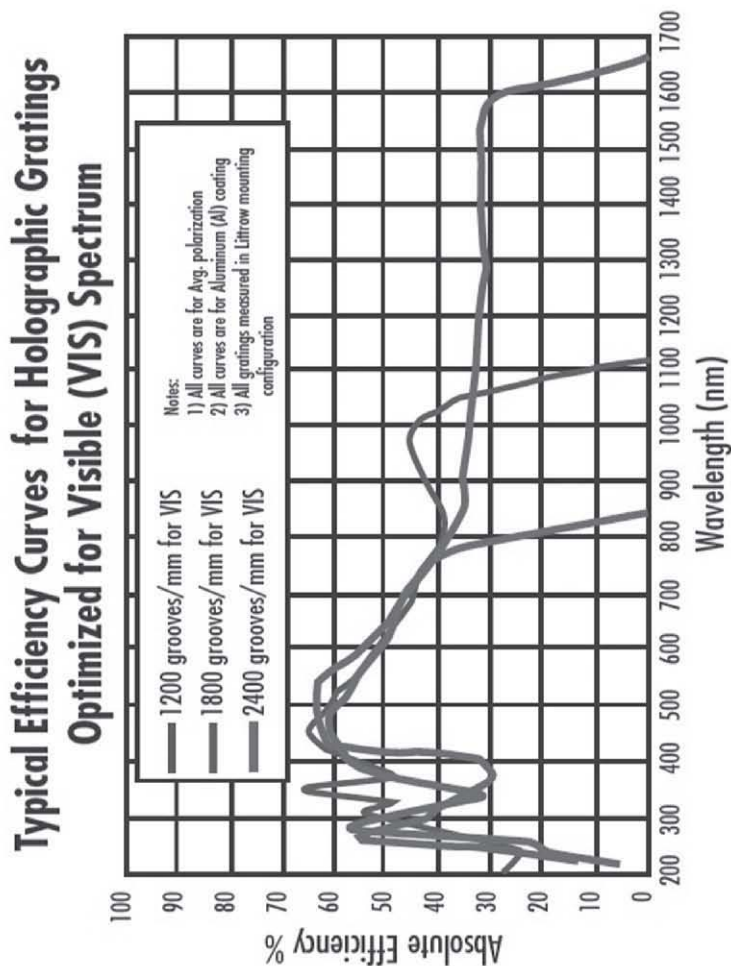


Figure A1.14 Diffraction efficiency of the 1200 grooves/mm VIS holographic grating. (Courtesy of Edmund Optics)

Figure A1.15 shows a photo of the 25.4-mm diameter 532.0-nm quartz zero-order half-wave plate (Edmund Optics stock no. 43-697).



Figure A1.15 Photo of the 25.4-mm diameter 532.0-nm quartz zero-order half-wave plate. (Courtesy of Edmund Optics)

Figure A1.16 shows a technical image of the 632.8-nm quartz zero-order half-wave plate (Edmund Optics stock no. 43-701).

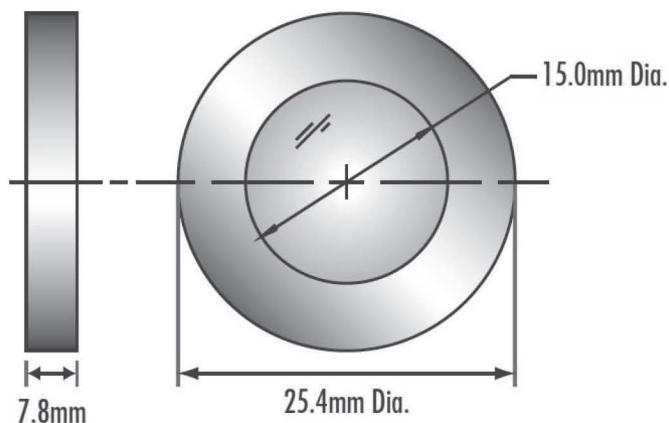


Figure A1.16 Technical image of the 25.4-mm diameter 632.8-nm quartz zero-order half-wave plate. (Courtesy of Edmund Optics)

Figure A1.17 shows the transmission of the 25.0-mm diameter high-contrast glass linear polarizer (Edmund Optics stock no. 47-216).

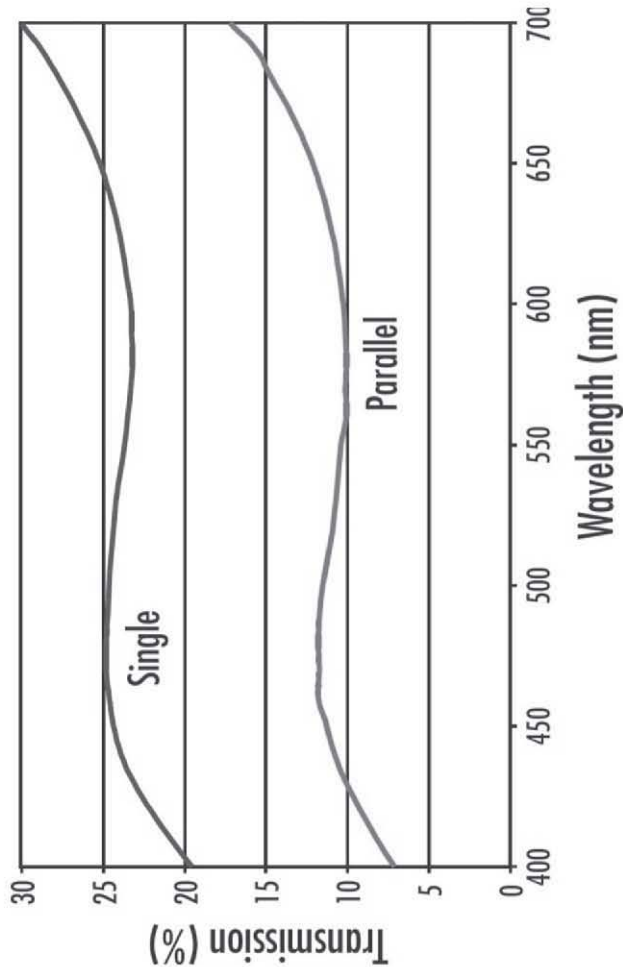


Figure A1.17 Transmission of the 25.0-mm diameter high-contrast glass linear polarizer. (Courtesy of Edmund Optics)

Figure A1.18 shows the separation angle of the calcite Wollaston polarizer (Edmund Optics stock no. 68-821).

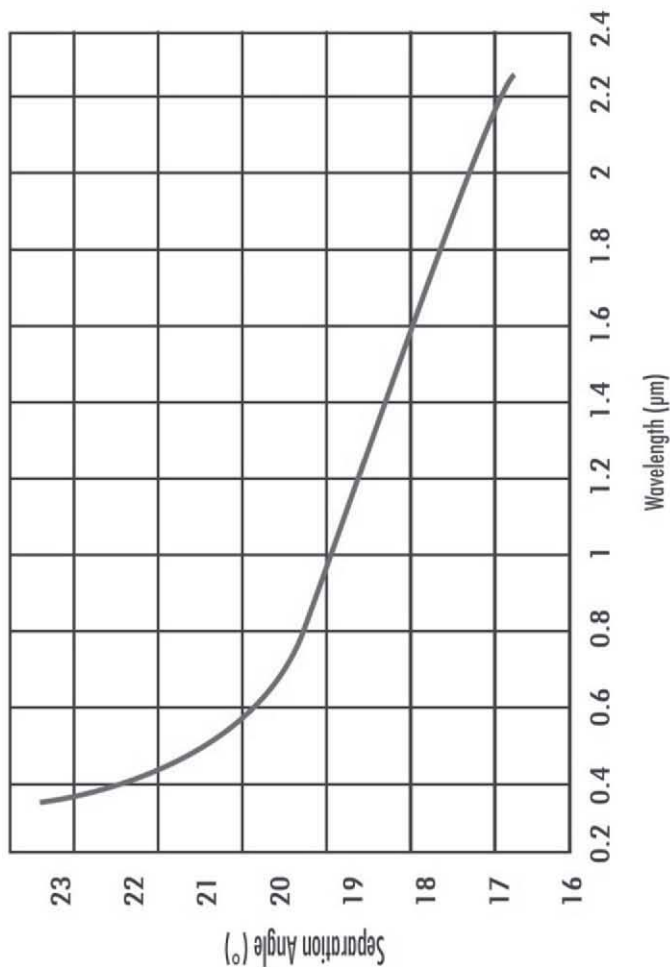


Figure A1.18 Separation angle of the calcite Wollaston polarizer. (Courtesy of Edmund Optics)

Figure A1.19 shows the separation angle of the quartz Rochon polarizer (Edmund Optics stock no. 68-824).

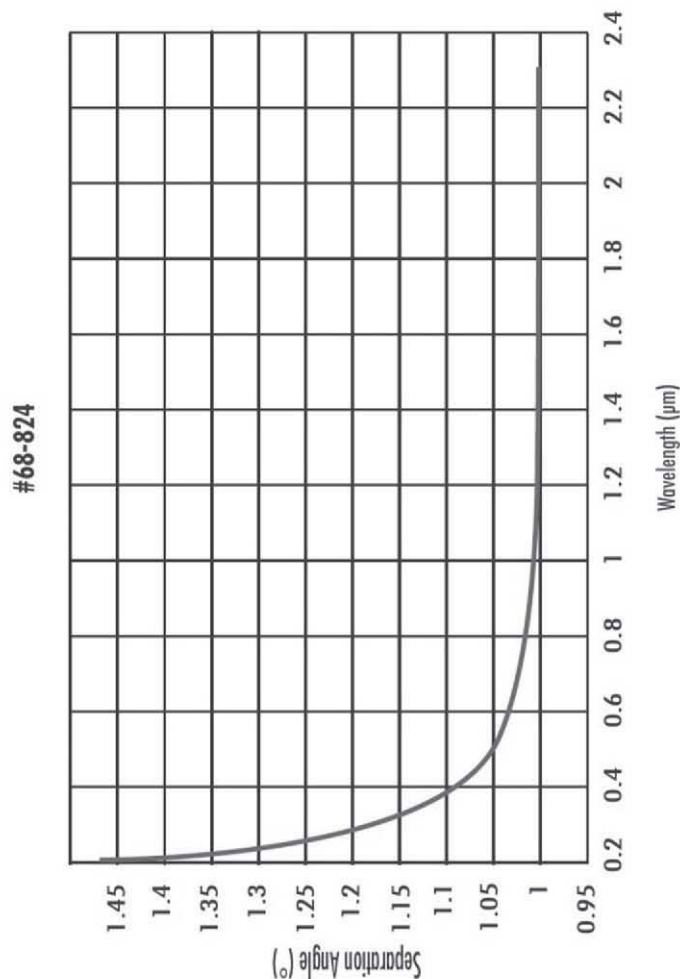


Figure A1.19 Separation angle of the quartz Rochon polarizer. (Courtesy of Edmund Optics)

Figure A1.20 shows a schematic of the fused silica Brewster window (Edmund Optics stock no. 65-825).

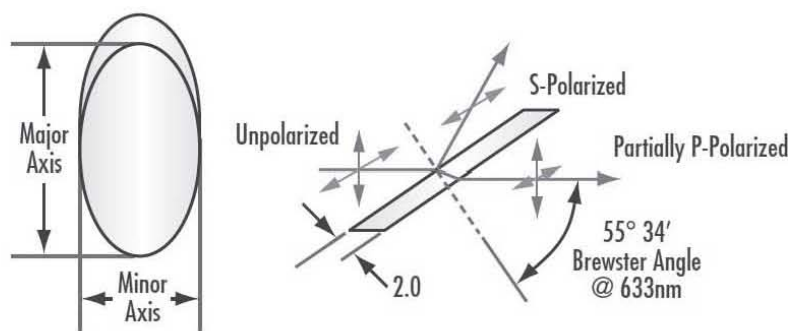


Figure A1.20 Schematic of the fused silica Brewster window (Major Axis: 26.53 mm; Minor Axis: 15.0 mm). (Courtesy of Edmund Optics)

Figure A1.21 shows the transmission and contrast of the linear wire-grid polarizer (Edmund Optics stock no. 34-318).

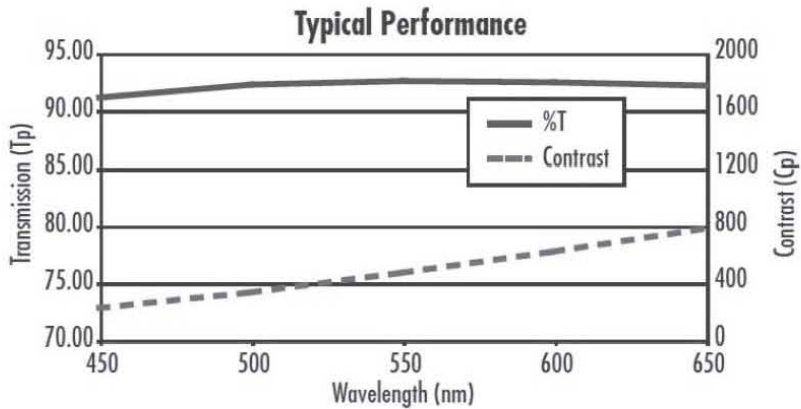


Figure A1.21 Transmission and contrast of the linear wire-grid polarizer. (Courtesy of Edmund Optics)

The values of R measured in experiments 5.1-5.4 may be compared with the calculated values of R using the values of the optical constants n and κ at 532.0 and 632.8 nm for fused silica, germanium, silicon, and zinc selenide listed in Table A1.4.

Table A1.4 Values of n , κ , and R for fused silica, germanium, silicon, and zinc selenide.

Material	Reference	532.0 nm	632.8 nm
		n κ R	n κ R
Fused Silica	I. H. Malitson, <i>J. Opt. Soc. Am.</i> 55 , 1205 (1965)	1.461 0 0.035	1.457 0 0.035
Germanium	D. E. Aspnes and A. A. Studna, <i>Phys. Rev. B</i> 27 , 985 (1983)	4.919 2.361 0.515	5.472 0.816 0.486
Silicon	D. E. Aspnes and A. A. Studna, <i>Phys. Rev. B</i> 27 , 985 (1983)	4.152 0.052 0.374	3.883 0.020 0.348
Zinc Selenide	S. Adachi and T. Taguchi, <i>Phys. Rev. B</i> 43 , 9569 (1991)	2.671 0.075 0.208	2.553 0.057 0.191

Figure A1.22 shows the transmission of the 532-nm longpass Raman filter (Semrock stock no. LP03-532RU-25).

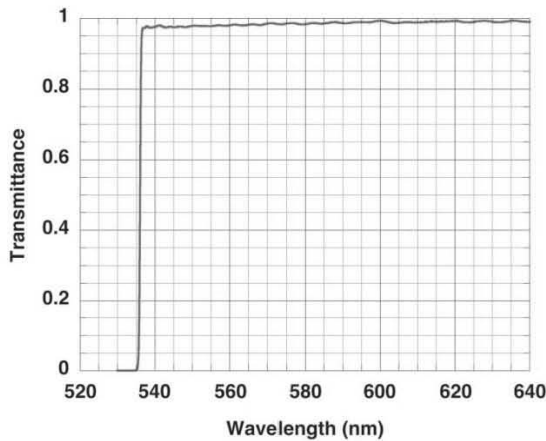
**Figure A1.22** Transmittance of the 532-nm longpass Raman filter. (Data courtesy of Semrock)

Figure A1.23 shows a schematic of the 25.4-mm diameter polka dot beamsplitter (Edmund Optics stock no. 46-458).

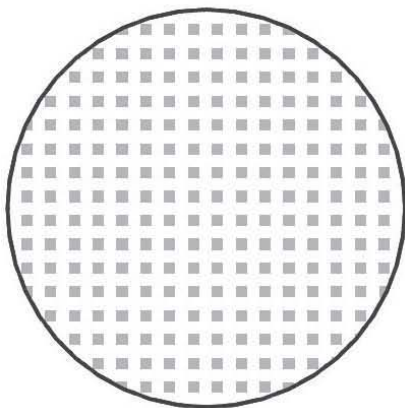


Figure A1.23 Schematic of the polka dot beamsplitter. (Courtesy of Edmund Optics)

Figure A1.24 shows a schematic of the 50/50 pellicle beamsplitter (Edmund Optics stock no. 39-481).

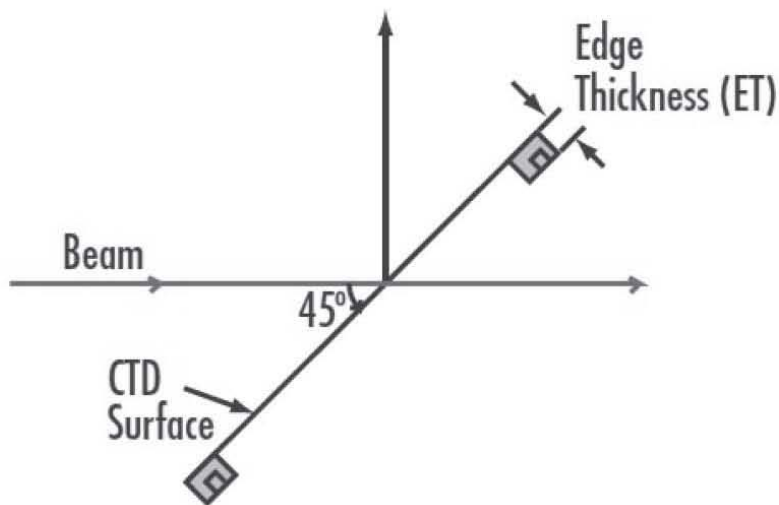


Figure A1.24 Schematic of the 50/50 pellicle beamsplitter. (Courtesy of Edmund Optics)

Figure A1.25 shows a photo of the 25-mm 50/50 cube beamsplitter (Edmund Optics stock no. 47-009).



Figure A1.25 Photo of the 25-mm cube beamsplitter. (Courtesy of Edmund Optics)

Figure A1.26 shows a photo of the 8-mm voltage-output type Hamamatsu PMT (Edmund Optics stock no. 83-898).



Figure A1.26 Photo of the 8-mm voltage-output type Hamamatsu PMT. (Courtesy of Edmund Optics)

A.2 Optomechanical components

Figure A2.1 shows a photo of the 11-mm diameter kinematic mount (Thorlabs stock no. MK11F).



Figure A2.1 Photo of the 11-mm diameter kinematic mount. (Courtesy of Thorlabs)

Figure A2.2 shows a photo of the 3" stainless-steel post (Edmund Optics stock no. 59-754).



Figure A2.2 Photo of the 3" stainless-steel post. (Courtesy of Edmund Optics)

Figure A2.3 shows a photo of the 3" post holder (Edmund Optics stock no. 58-979).



Figure A2.3 Photo of the 3" post holder. (Courtesy of Edmund Optics)

Figure A2.4 shows a photo of the 1/2" translation stage (Thorlabs stock no. MT1).



Figure A2.4 Photo of the 1/2" translation stage. (Courtesy of Thorlabs)

Figure A2.5 shows a photo of the base plate for the $\frac{1}{2}$ " translation stage (Thorlabs stock no. MT401).



Figure A2.5 Photo of the base plate for the $\frac{1}{2}$ " translation stage. (Courtesy of Thorlabs)

Figure A2.6 shows a photo of the 25/25.4-mm diameter kinematic mount (Edmund Optics stock no. 58-854).



Figure A2.6 Photo of the 25/25.4-mm diameter kinematic mount (Courtesy of Edmund Optics)

Figure A2.7 shows a photo of the 2"x3" slotted base plate (Edmund Optics stock no. 03-655).



Figure A2.7 Photo of the 2"x3" slotted base plate. (Courtesy of Edmund Optics)

Figure A2.8 shows a photo of the lens mount for 10-mm optics (Thorlabs stock no. LMR10).



Figure A2.8 Photo of the lens mount for 10-mm optics. (Courtesy of Thorlabs)

Figure A2.9 shows a photo of the adjustable-height V-clamp (Thorlabs stock no. VG100).



Figure A2.9 Photo of the adjustable-height V-clamp. (Courtesy of Thorlabs)

Figure A2.10 shows a photo of the 3-screw adjustable ring mount (Edmund Optics stock no. 36-605) for the 64-mm diameter ellipsoidal mirror.



Figure A2.10 Photo of the 3-screw adjustable ring mount. (Courtesy of Edmund Optics)

Figure A2.11 shows a photo of the mounting adaptor for 19-mm diameter optics (Thorlabs stock no. SM1AD19).



Figure A2.11 Photo of the mounting adaptor for 19-mm diameter optics. (Courtesy of Thorlabs)

Figure A2.12 shows a photo of the 360° high-precision rotation mount (Thorlabs stock no. PR01).



Figure A2.12 Photo of the 360° high-precision rotation mount. (Courtesy of Thorlabs)

Figure A2.13 shows a photo of the adaptor plate for the 360° high-precision rotation mount (Thorlabs stock no. PR01A).



Figure A2.13 Photo of the adaptor plate for the 360° high-precision rotation mount. (Courtesy of Thorlabs)

Figure A2.14 shows a photo of the mounting plate for the 25.4-mm diameter 30° off-axis parabolic mirror (Edmund Optics stock no. 47-111).



Figure A2.14 Photo of the mounting plate for the 25.4-mm diameter off-axis parabolic mirror. (Courtesy of Edmund Optics)

Figure A2.15 shows a photo of the 25.0/25.4-mm square kinematic mount (Edmund Optics stock no. 58-857).



Figure A2.15 Photo of the 25.0/25.4-mm square kinematic mount. (Courtesy of Edmund Optics)

Figure A2.16 shows a photo of the 25.4-mm diameter polarizer mount (Edmund Optics stock no. 55-010).



Figure A2.16 Photo of the 25.4-mm diameter polarizer mount. (Courtesy of Edmund Optics)

A3. Stock numbers and prices of optical, optomechanical, and other components

Component	Stock Number	2018 Price
36"x12" breadboard	Edmund Optics 03-643	\$495.00
2"x3" slotted base plate	Edmund Optics 03-655	\$15.00
3" post holder	Edmund Optics 58-979	\$13.25
3" stainless-steel post	Edmund Optics 59-754	\$10.25
3" spring-type caliper and divider	Starrett 274-3	\$68.00
0.9-mW 532-nm laser	Thorlabs CPS532-C2	\$162.18
5V DC power supply for the 0.9-mW 532.0-nm laser	Thorlabs LDS5	\$86.96
11-mm diameter kinematic mount for the 0.9-mW 532.0-nm laser	Thorlabs MK11F	\$90.00
½" translation stage	Thorlabs MT1	\$297.94
Base plate for the ½" translation stage	Thorlabs MT401	\$23.66
25.0-mm diameter, 35.0-mm effective focal length MgF ₂ -coated N-BK7 plano-convex lens	Edmund Optics 45-146	\$32.50
25/25.4-mm kinematic mount	Edmund Optics 58-854	\$109.00
10-μm ceramic aperture	Edmund Optics 84-910	\$107.00
Mount for 10-mm optics for the 10-μm ceramic aperture	Thorlabs LMR10	\$20.81
UV-NIR silicon power photodetector	Edmund Optics 89-310	\$795.00
Power meter for the UV-NIR silicon power photodetector	Edmund Optics 89-305	\$850.00
Adjustable-height V-clamp	Thorlabs VG100	\$87.98

25.0-mm diameter, 25.0-mm effective focal length MgF ₂ -coated N-SF5 double-convex lens	Edmund Optics 32-490	\$31.50
25.0-mm diameter, 50.0-mm effective focal length MgF ₂ -coated N-BK7 double-convex lens	Edmund Optics 32-625	\$31.50
0.8-mW 632.8-nm He-Ne laser	Thorlabs HNLS008L	\$889.44
25.0-mm diameter, 100.0-mm effective focal length MgF ₂ -coated N-BK7 plano-convex lens	Edmund Optics 32-482	\$31.50
25.0-mm diameter, 25.0-mm effective focal length MgF ₂ -coated N-SF5 plano-convex lens	Edmund Optics 45-098	\$32.50
25.0-mm diameter, 125.0-mm effective focal length MgF ₂ -coated N-BK7 plano-convex lens	Edmund Optics 32-862	\$31.50
25.0-mm diameter, 50.0-mm effective focal length MgF ₂ -coated N-BK7 plano-convex lens	Edmund Optics 32-478	\$31.50
37-mm maximum aperture mounted iris diaphragm	Edmund Optics 53-916	\$99.00
19-mm diameter 1-mm scale/100Div eyepiece reticle	Edmund Optics 54-422	\$150.00
Mount for the 19-mm optics	Thorlabs SM1AD19	\$22.66
24-mm diameter, 18-mm effective focal length Olympus 10X microscope objective	Edmund Optics 86-813	\$315.00
19-mm diameter, 10-mm scale/100Div eyepiece reticle	Edmund Optics 36-125	\$150.00
25.0-mm diameter first-surface plane mirror	Edmund Optics 87-371	\$80.00
360° high-precision rotation mount	Thorlabs PR01	\$331.50
Adaptor plate for the rotation mount	Thorlabs PR01A	\$29.33
1" diameter, 1" focal length enhanced aluminum spherical mirror	Edmund Optics 43-536	\$105.00
25.4-mm diameter, 50.8-mm focal length 30° off-axis parabolic mirror	Edmund Optics 35-490	\$205.00
Mounting plate for the 25.4-mm diameter off-axis mirror	Edmund Optics 47-111	\$95.00

12.7-mm diameter, 12.7-mm effective focal length MgF ₂ -coated N-SF11 plano-convex lens	Edmund Optics 49-854	\$30.50
12.7-mm optic component mount	Edmund Optics 64-556	\$39.00
64-mm diameter aluminum-coated ellipsoidal mirror with 11-mm and 78-mm focal lengths	Edmund Optics 90-968	\$195.00
Adjustable ring mount for the ellipsoidal mirror	Edmund Optics 36-605	\$55.00
1200-grooves/mm 25-mm square transmission diffraction grating	Edmund Optics 49-582	\$105.00
25.0/25.4-mm square kinematic mount	Edmund Optics 58-857	\$105.00
25.4-mm diameter, 532.0-nm quartz zero-order half-wave plate	Edmund Optics 43-697	\$430.00
1200-grooves/mm 25-mm square 500-nm ruled diffraction grating	Edmund Optics 43-005	\$107.50
1200-grooves/mm 25-mm square VIS holographic grating	Edmund Optics 43-216	\$140.00
25.4-mm diameter, 632.8-nm zero-order half-wave plate	Edmund Optics 43-701	\$430.00
25.0-mm diameter high-contrast glass linear polarizer	Edmund Optics 47-216	\$160.00
Calcite Wollaston polarizer	Edmund Optics 68-821	\$570.00
25.4-mm diameter polarizer mount	Edmund Optics 55-010	\$165.00
Quartz Rochon polarizer	Edmund Optics 68-824	\$685.00
25-mm diameter, 2.0-mm thick fused silica Brewster window	Edmund Optics 65-825	\$125.00
25-mm diameter mounted wire-grid linear polarizer	Edmund Optics 34-318	\$499.00
25.0-mm diameter, 3.0-mm thick uncoated UV grade fused silica window	Edmund Optics 47-195	\$105.00
25.0-mm diameter, 3.0-mm thick uncoated germanium window	Edmund Optics 68-737	\$175.00
25.0-mm diameter, 3.0-mm thick uncoated silicon window	Edmund Optics 68-527	\$125.00

25.0-mm diameter, 2.0-mm thick uncoated zinc selenide window	Edmund Optics 68-508	\$249.00
25.0-mm diameter, 525-nm bandpass filter	Edmund Optics 87-789	\$195.00
25.0-mm diameter, 625-nm bandpass filter	Edmund Optics 87-791	\$195.00
25.0-mm diameter, 500-nm cut-on wavelength longpass filter	Edmund Optics 47-616	\$125.00
25-mm diameter, 532-nm longpass Raman filter	Semrock LP03-532RU-25	\$695.00
25-mm diameter, 1.0-mm thick 50/50 glass plate beamsplitter	Edmund Optics 43-736	\$40.00
25.4-mm diameter 50/50 UV grade fused silica polka dot beamsplitter	Edmund Optics 46-458	\$155.00
25.4-mm diameter 50/50 pellicle beamsplitter	Edmund Optics 39-481	\$170.00
25.0-mm diameter 50/50 cube beamsplitter	Edmund Optics 47-009	\$220.00
25.0-mm diameter 45° dichroic longpass beamsplitter with 600-nm cut-on wavelength	Edmund Optics 69-890	\$119.00
Multimeter	Fluke 8808	\$850.00
25.0-mm diameter, 532.0-nm OD 4 notch filter	Edmund Optics 67-119	\$329.00
8-mm voltage-output type Hamamatsu PMT module	Edmund Optics 83-898	\$1,175.00
25.0-mm diameter, 632.8-nm OD 4 notch filter	Edmund Optics 67-120	\$329.00
2.5-mm diameter silicon photodiode receiver module	Edmund Optics 57-623	\$425.00
110V/220V 1-channel power supply	Edmund Optics 57-629	\$550.00

INDEX

- 5V DC power supply, 2, 154
- 11-mm diameter kinematic mount, 2, 154
- 12.7-mm EFL plano-convex lens, 35, 129, 156
- 12.7-mm optic component mount, 35, 156
- 19-mm diameter 1-mm scale/100Div eyepiece reticle, 22, 131, 155
- 19-mm diameter 10-mm scale/100Div eyepiece reticle, 23, 131, 155
- 25-mm diameter first-surface plane mirror, 25, 155
- 25.0-mm EFL double-convex lens, 6, 130, 155
- 25.0-mm EFL plano-convex lens, 17, 129, 155
- 37-mm maximum aperture mounted iris diaphragm, 20, 155
- 50.0-mm EFL double-convex lens, 6, 130, 155
- 50.0-mm EFL plano-convex lens, 129, 155
- 100.0-mm EFL plano-convex lens, 14, 129, 155
- 110V/220V 1-channel power supply, 123, 157
- 125.0-mm EFL plano-convex lens, 17, 129, 155
- 360° High-precision rotation mount, 25, 151, 155
- 500-nm cut-on wavelength longpass filter, 87, 157
- 525-nm bandpass filter, 83, 157
- 532.0-nm half-wave plate, 50, 156
- 532-nm laser, 2, 127, 154
- 532-nm longpass Raman filter, 90, 143, 157
- 532-nm OD 4 notch filter, 119, 157
- 600-nm cut-on wavelength dichroic longpass beamsplitter, 105, 157
- 625-nm bandpass filter, 85, 157
- 632.8-nm half-wave plate, 61, 156
- 632.8-nm He-Ne laser, 11, 128, 155
- 632.8-nm OD 4 notch filter, 124, 157
- Adaptor plate for the 360° rotation mount, 25, 152, 155
- Adjustable-height V clamp, 3, 150, 154
- Adjustable ring mount, 36, 150, 156
- Base plate for the ½"-translation stage, 2, 148, 154
- Breadboard, 3, 154
- Brewster window polarizer, 66, 142, 156
- Ceramic aperture, 2, 130, 154
- Cube beamsplitter, 102, 145, 157
- Double-convex lens, 6, 130, 155
- Elliptical mirror, 34, 134, 156
- Experiment 1.1, 1
 - Optical components, 2
 - Optomechanical and other components, 2
 - Schematic, 3
- Experiment 1.2, 6
 - Optical components, 6
 - Optomechanical and other components, 6
 - Schematic, 8

- Experiment 1.3, 11
 - Optical components, 11
 - Optomechanical components, 11
 - Schematic, 12
- Experiment 1.4, 14
 - Optical components, 14
 - Optomechanical components, 14
 - Schematic, 15
- Experiment 1.5, 17
 - Optical components, 17
 - Optomechanical components, 17
 - Schematic, 18
- Experiment 1.6, 20
 - Optical components, 20
 - Optomechanical components, 20
 - Schematic, 21
- Experiment 1.7, 22
 - Optical components, 22
 - Schematic, 23
- Experiment 2.1, 25
 - Optical components, 25
 - Optomechanical components, 25
 - Schematic, 26
- Experiment 2.2, 27
 - Optical components, 27
 - Optomechanical components, 27
 - Schematic, 28
- Experiment 2.3, 29
 - Optical components, 29
 - Optomechanical components, 29
 - Schematic, 30
- Experiment 2.4, 32
 - Optical components, 32
 - Optomechanical components, 32
 - Schematic, 33
- Experiment 2.5, 35
 - Optical components, 35
 - Optomechanical components, 35
 - Schematic, 36
- Experiment 3.1, 39
 - Optical components, 39
 - Optomechanical components, 39
 - Schematic, 40
- Experiment 3.2, 41
 - Optical components, 41
 - Optomechanical and other components, 41
 - Schematic, 42
- Experiment 3.3, 43
 - Optical components, 43
 - Optomechanical components, 43
 - Schematic, 45
- Experiment 3.4, 46
 - Optical components, 47
 - Optomechanical components, 47
 - Schematic, 48
- Experiment 3.5, 50
 - Optical components, 50
 - Optomechanical components, 50
 - Schematic, 52
- Experiment 3.6, 53
 - Optical components, 53
 - Optomechanical and other components, 54
 - Schematic, 55
- Experiment 4.1, 59
 - Optical components, 59
 - Optomechanical and other components, 59
 - Schematic, 60
- Experiment 4.2, 61
 - Optical components, 61
 - Optomechanical components, 62
 - Schematic, 62

- Experiment 4.3, 64
 - Optical components, 64
 - Optomechanical components, 64
 - Schematic, 65
- Experiment 4.4, 66
 - Optical components, 66
 - Optomechanical and other components, 66
 - Schematic, 67
- Experiment 4.5, 69
 - Optical components, 69
 - Optomechanical and other components, 69
 - Schematic, 70
- Experiment 5.1, 73
 - Optical components, 73
 - Optomechanical and other components, 73
 - Schematic, 74
- Experiment 5.2, 75
 - Optical components, 75
 - Optomechanical and other components, 76
 - Schematic, 77
- Experiment 5.3, 78
 - Optical components, 78
 - Optomechanical and other components, 78
 - Schematic, 79
- Experiment 5.4, 80
 - Optical components, 80
 - Optomechanical and other components, 80
 - Schematic, 81
- Experiment 6.1, 83
 - Optical components, 83
 - Optomechanical and other components, 83
 - Schematic, 84
- Experiment 6.2, 85
 - Optical components, 85
 - Optomechanical components, 85
 - Schematic, 86
- Experiment 6.3, 87
 - Optical components, 87
 - Optomechanical and other components, 88
 - Schematic, 88
- Experiment 6.4, 90
 - Optical components, 90
 - Optomechanical and other components, 90
 - Schematic, 91
- Experiment 6.5, 92
 - Optical components, 92
 - Optomechanical and other components, 92
 - Schematic, 93
- Experiment 7.1, 95
 - Optical components, 95
 - Optomechanical components, 95
 - Schematic, 96
- Experiment 7.2, 97
 - Optical components, 97
 - Optomechanical and other components, 97
 - Schematic, 98
- Experiment 7.3, 99
 - Optical components, 99
 - Optomechanical and other components, 100
 - Schematic, 101
- Experiment 7.4, 102
 - Optical components, 102
 - Optomechanical and other components, 102
 - Schematic, 103
- Experiment 7.5, 104
 - Optical components, 104
 - Optomechanical and other components, 105
 - Schematic, 106
- Experiment 8.1, 109
 - Optical components, 109
 - Optomechanical and other components, 109
 - Schematic, 110

- Experiment 8.2, 111
 - Optical components, 111
 - Optomechanical and other components, 111
 - Schematic, 112
- Experiment 8.3, 113
 - Optical components, 113
 - Optomechanical and other components, 113
 - Schematic, 114
- Experiment 8.4, 115
 - Optical components, 115
 - Optomechanical and other components, 115
 - Schematic, 116
- Experiment 9.1, 119
 - Optical components, 119
 - Optomechanical and other components, 119
 - Schematic, 120
- Experiment 9.2, 121
 - Optical components, 121
 - Optomechanical components, 121
 - Schematic, 121
- Experiment 9.3, 122
 - Optical components, 122
 - Optomechanical and other components, 123
 - Schematic, 123
- Experiment 9.4, 124
 - Optical components, 124
 - Optomechanical and other components, 124
 - Schematic, 125
- Fused silica window, 73, 143, 156
- Germanium window, 75, 143, 156
- Glass plate beamsplitter, 95, 157
- He-Ne laser beam expander, 133
- Holographic grating, 50, 137, 156
- Kinematic mount, 2, 146, 154
- Lens mount for 10-mm optics, 2, 154
- Linear polarizer, 59, 139, 156
- Microscope objective, 22, 132, 155
- Multimeter, 113, 157
- Mount for the 19-mm diameter optics, 23, 151, 155
- Mounting plate for the off-axis parabolic mirror, 32, 152, 155
- Off-axis parabolic mirror, 32, 133, 155
- Pellicle beamsplitter, 99, 144, 157
- Plano-convex lens, 1, 128, 129, 155
- Polarizer mount, 60, 153, 156
- Polka dot beamsplitter, 97, 144, 157
- PMT (photomultiplier tube), 119, 157
- Post holder, 2, 147, 154
- Power meter, 3, 154
- Rochon polarizer, 63, 141, 156
- Ruled diffraction grating, 43, 136, 156
- Silicon photodiode, 122, 157
- Silicon window, 78, 143, 156
- Slotted base plate, 2, 149, 154
- Spherical mirror, 29, 132, 155
- Square kinematic mount, 39, 153, 156
- Stainless-steel post, 2, 146, 154
- Translation stage, 2, 147, 154
- Transmission diffraction grating, 39, 135, 156
- UV-NIR silicon power photodetector, 2, 131, 154
- Wire-grid polarizer, 69, 142, 156
- Wollaston polarizer, 61, 140, 156
- Zinc selenide window, 80, 143, 157